Technische Universiteit
Eindhoven
University of Technology

A MONITORING SYSTEM FOR BICYCLE PAVEMENT CONDITIONS USING CYCLISTS' SMARTPHONES

A first look at the capabilities of measuring bicycle vibrations using smartphone sensors

MASTER'S THESIS

Author : S.P. (Stefan) Werner
Student ID : 0783896
Final presentation data : 06-02-2017
E-mail : s.p.werner93@gmail.com

INSTITUTION

University : Eindhoven University of Technology (TU/e)
Faculty : Faculty of the Built Environment
Master Track : Construction Management & Engineering

IN COLLABORATION WITH

Company : Royal HaskoningDHV

GRADUATION COMMITTEE

Chairman (TU/e) : prof.dr.ir. B. (Bauke) de Vries
Graduation supervisor (TU/e) : dr. ing. P.J.H.J. (Peter) van der Waerden
Graduation supervisor (TU/e) : ir. A.W.J, (Aloys) Borgers
External supervisor (RHDHV) : ir. P. (Peter) Morsink

PREFACE

After 8 to 9 months of hard work, frequent meetings with my graduation committee and hours of work as an graduate intern at Royal HaskoningDHV, I present with great pleasure my official thesis as the result of my graduation project. This thesis represents the end of my master Construction Management and Engineering at the Eindhoven University of Technology. In my time at the university, I started my education within the bachelor of Architecture, Urbanism and Building Sciences, continued with my Master in the field of Urban Development and Innovation Sciences, and now (nearly) graduated in the field of Smart Mobility.

By conducting research in the fields of smart mobility, bicycle asset management and smartphone sensor technologies, I had chosen a challenging topic due to the fact that I did not yet know that much about these topics and because smart mobility has always had my interest. Therefore, I took the opportunity of this graduation project to develop myself in the field of smart mobility, from which I will definitely profit in my further career.

During the execution of this research, I have received help, guidance and knowledge from a number of people without which this research would not have been possible. First of all, I would like to extend my gratitude towards Peter van der Waerden and Aloys Borgers for their very personal support, and the time they have made to share their knowledge and guide me during the meetings. Throughout the entire graduation period they continued to challenge me to get a deeper understanding on the subject.

Next, I would also like to thank Peter Morsink for the opportunity to graduate at Royal HaskoningDHV. The enthusiasm of the team on my subject inspired me to make the best of my graduation research possible. They were always available when I got stuck and searched someone to spar with. Especially, Peter supported me with his knowledge on smart mobility, his experience with bicycle projects, and his network to put me in touch with the right persons, but his enthusiasm and energy for the research helped me the most. Furthermore, I would like to thank all the people at Royal HaskongDHV who shared their experiences with me and provide recommendations to help me further with my project.

Furthermore, I also want to thank my former colleagues Robert Haverkort and Bas Bruins Slot for supporting me in the early stages of the graduation project, and I would like to extend my gratitude towards Ron van Leeuwen for making the environmental test laboratory of Thales Cryogenics available for my research. The ability of making use of the electrodynamic shaker for testing definitely boosted the quality of the research specifically towards the smartphone sensors.

Last but not least, I would like to thank all my friends and family for their support. Especially my parents Chris and Lily, and my girlfriend Lindsay for their empathy and support in the stressful periods throughout not only my graduation project, but also throughout my entire study. I hope that every reader will enjoy reading and learning from this thesis report as much as this graduation project was to me.

Stefan Werner
Eindhoven, 2018

SP Werner

SUMMARY

For several years now, there has been a growing interest in accomplishing higher levels of cycling in cities, since a lot of cities struggle with severe problems of air pollution, noise, congestions and parking problems as a result of high, and sometimes even growing levels, of motorized traffic. Cities are more and more recognizing what cycling brings to a city besides the fact that it is an effective way of addressing the major issues behind the high level of dependency on private cars. Many cities are working on making their urban environments more bicycle-friendly to encourage their residents to cycle. Recent literature has illustrated that the focus of all efforts concerning the promotion of cycling must be the improvement of cyclists perceived safety and comfort levels.

One aspect in particular appears to strongly influence these levels, namely the pavement surface conditions. Cyclist perceive the pavement surface conditions by way of bicycle vibrations that are transmitted from the surface. Besides the vibrations directly associated with the pavement surface structure, the vibrations are typically caused by two different types of pavement issues, namely by cracked roads and coarse roads. The former refers to one or multiple successive impacts due to cracks, potholes or tree root damages. The latter refers to a continuous random vibrations due to worn pavement surfaces.

Currently, these pavement conditions are assessed through visual inspections, which is a resource inefficient manner, as these inspections are costly, time consuming and labor-intensive. Moreover, it is a subjective approach, making it dependable on the knowledge and experience of the inspectors. Thus, given the growing interest of making the bicycle a competitive transportation mode and that governmental authorities only have limited funds for the operations and maintenance of the bicycle infrastructure, a more resource efficient manner is needed for obtaining objective asset conditions data regarding bicycle pavement surfaces in order to stimulate people to start using the bicycle.

This research therefore introduces a new system for collecting this bicycle asset condition data and is called ‘Bicycle Infrastructure Monitoring System’ (BIMS). BIMS will collect the asset condition data on the basis that pavement surface condition can be manifested in terms of vibrations transmitted to the cyclist. The system aims to objectively assess the pavement surface conditions by measuring these vibraitons with the sophisticated sensors embedded in modern day smartphones. By collecting this vibration data in combination with location data from cyclists’ smartphones, BIMS will be able to continuously monitor the asset condition data regarding bicycle pavement surfaces. The valuable information resulting from BIMS will help road managers to make more efficient use of their limited resources in relation to operation and maintenance, renewal and auditing of the bicycle environment.

This research first presents a strong foundation for BIMS by elaborating on all the sub-processes involved and what these sub-processes entail, based on the knowledge acquired from the literature review. Basically for BIMS five sub-processes can be distinguished: ‘Input’, ‘Pre-Process’, ‘Process’, ‘Evaluation’, and ‘Output’. These sub-processes are depicted in a process flow diagram which provides a better comprehensive understanding of the general flow of information and the actions involved of each sub-processes.

This research further focuses particularly on the feasibility of BIMS assessment component. For the assessment, BIMS intends to use an already existing method of dynamic comfort mapping introduced by Bíl et al. (2015) for converting the vibration measurement's outcome into a dynamic comfort index (DCI). The functionality and feasibility of this method is already proven in the study of Bíl et al. (2015). However, since this research differs in using data from smartphones located in cyclist's trousers instead of an accelerometer mounted to the front fork of a bicycle to assess the bicycle pavement surface conditions, the original formula for the computation of the DCI is altered and is referred to as DCI_{sum}. Furthermore, based on the insights of both the study of Bíl et al. (2015) and the literature, several other aspects are discussed in how they should be dealt with as they concern the methodology's outcome, namely cyclist's weight, bicycle characteristics, data collection from multiple cyclists, and pedaling movement of the cyclist. This study then researches this assessment component on the basis of two studies.

First, a case study is conducted which examines if the current sensor quality is sufficient in order to provide reliable data for BIMS. This case study specifically tested only the sensors relevant for the data collection of BIMS, namely the accelerometer for the vibration data and the GPS receiver for the location data. These sensors are tested on their accuracy, sensitivity and consistency. This evaluation is based on five tests, where three tests focus on the smartphones' accelerometer and two tests on the smartphones' GPS receiver. In total the sensors of three smartphones of different brands and ages are tested in order to provide a general impression of the overall smartphone sensor quality. The test results show that smartphones' accelerometers are capable of measuring accelerations with high level of precision, as for the accelerometers considerable low sensitivities and accuracies are observed with high consistencies. In addition, the test results show that smartphones' GPS receiver can provide GPS data with an acceptable level of accuracy.

Next, a field experiment is undertaken in order to prove the feasibility of assessing the pavement surface conditions based on smartphone data. In addition, since the original method of dynamic comfort mapping is altered, the field experiment re-examines the functionality and feasibility of this method based on smartphone-data. Based on vibration data collected from three test riders, the field experiment applies the altered method to four road segments in the city center of Eindhoven, the Netherlands. In order to evaluate the performance of the dynamic comfort mapping method based on smartphone data, it is compared to DCI-values derived in the study of Bíl et al. (2015). From this comparison, it seems that the smartphone-based method does not performs similarly as the original method, since in general the DCI_{sum} values are observed to be 0.2 to 0.3 lower than the comparative DCI values. However, even though smartphone-based method performs worse in comparison with the original method, the results of the field experiment show that it is possible to distinguish different pavement surfaces, and of different qualities based on vibrations data collected from smartphones. In addition, based on the strong correlations found between the data sets of the test riders, the experiment achieves to illustrate the workability of combining data gathered from multiple cyclists. Regarding the method of dynamic comfort mapping, more detailed research is necessary in order for BIMS to adopt this method. This study may be seen as a first step towards more objective and sophisticated methods to collect asset condition data regarding the bicycle environment.

SAMENVATTING

Sinds enkele jaren is er een groeiende interesse in het bereiken van hogere niveaus van fietsen in steden, aangezien veel steden worstelen met ernstige problemen van luchtverontreiniging, lawaai, verkeersopstoppingen en parkeer problemen als gevolg van de hoge, soms zelfs groeiende niveaus van gemotoriseerd verkeer. Steden erkennen steeds meer wat fietsen voor een stad kan betekenen, naast het feit dat het een effectieve manier is om de belangrijkste problemen aan te pakken die te maken hebben met de hoge afhankelijkheid van personenauto's. Veel steden werken eraan hun stadsomgeving fietsvriendelijker te maken om hun inwoners aan te moedigen om te gaan fietsen. Recente literatuur heeft aangetoond dat de focus van alle inspanningen met betrekking tot het aanmoedigen van fietsgedrag moet liggen op het verbeteren van de veiligheid- en comfort-niveaus van fietsers.

Éen aspect in het bijzonder blijkt deze niveaus sterk te beïnvloeden, namelijk de condities van het wegdekoppervlak. De fietser ervaart namelijk de condities van het wegdek aan de hand van de fietstrillingen die worden overgebracht vanuit het wegoppervlak. Naast de trillingen die direct verband houden met de oppervlaktestructuur van de verharding, worden de trillingen meestal veroorzaakt door twee typische soorten wegdekschades, namelijk door beschadigde wegen en ruwe wegen. De eerste verwijst naar een of meerdere opeenvolgende klappen (of trillingen) als gevolg van scheuren, kuilen of boomwortelbeschadigingen. De laatste verwijst naar de continue willekeurige trillingen als gevolg van versleten wegdekken.

Op dit moment worden de wegdek condities beoordeeld aan de hand van visuele inspecties wat een inefficiënte strategie is, aangezien deze inspecties duur, tijdrovend en arbeidsintensief zijn. Daarbij is het een subjectieve methodiek die afhankelijk is van de kennis en ervaring van de inspecteurs. Dus gezien de groeiende interesse om de fiets een competitieve transportmodus te maken en dat overheidsinstanties slechts beperkte middelen hebben voor het beheer en onderhoud van fietsinfrastructuur, is er een efficiëntere manier nodig om objectieve data te verzamelen met betrekking tot de oppervlakken van de fietsverhardingen om mensen te stimuleren om de fiets te gaan gebruiken.

Dit onderzoek introduceert daarom een nieuw system voor het verzamelen van deze asset conditie data genaamd 'Bicycle Infrastructure Monitoring System' (BIMS). Het systeem doelt erop om objectief de conditie van verhardingsoppervlakken te beoordelen door de trillingen te meten die je ervaart tijdens het fietsen met de geavanceerde sensoren die zijn geïntegreerd in huidige smartphones. Door deze trillingsdata te verzamelen in combinatie met GPS-data van smartphones van alledaagse fietsers, kan BIMS continu data verzamelen en monitoren met betrekking tot de condities van de verhardingsoppervlakken van fietspadden. De waardevolle informatie die voortvloeit uit BIMS zal wegbeheerders helpen om hun beperkte middelen efficiënter te gebruiken met betrekking tot het beheer en onderhoud, vernieuwing en auditing van de fietsomgeving.

Dit onderzoek presenteert eerst een sterke basis voor BIMS door alle betrokken sub-processen te beschrijven en aan te duiden wat ze inhouden. In principe zijn er voor BIMS vijf sub-processen te onderscheiden: 'Input', 'Pre-Process', 'Process', 'Evaluation', en 'Output'. Deze sub-processen worden afgebeeld in een processtroomdiagram wat een goed overzicht biedt van de algemene informatiestroom en de betrokken acties van elke sub-proces.

Dit onderzoek richt zich verder in het bijzonder op de haalbaarheid van BIMS beoordelingscomponent. BIMS zal hiervoor gebruik maken van een bestaande methode genaamd 'dynamic comfort mapping' geïntroduceerd door Bíl et al. (2015). Deze methode zal gebruikt worden om de resultaten van de trillingsmeeting om te zetten in een 'dynamic comfort index' (DCI). De functionaliteit en haalbaarheid van deze methode is al aangetoond in de studie van Bíl et al. (2015). Aangezien dit onderzoek verschilt in het gebruiken van data verzamelt met een smartphone vanuit de broek, in plaats van een accelerometer die op de voorvork van een fiets is bevestigd, om de condities van de fietsverhardingen te beoordelen, is de originele formule voor het berekenen van de DCI gewijzigd en wordt DCI_{sum} genoemd. Verder, gebaseerd op de inzichten van zowel de studie van Bíl et al. (2015) en de literatuur, worden er ook verschillende aspecten besproken in hoe ze moeten worden aangepakt aangezien ze betrekking hebben op de uitkomst van de methode, namelijk het gewicht van de fietsers, de fietskenmerken, data verzameling van meerdere fietsers en trapbeweging van de fietser. Deze studie onderzoekt de beoordelingscomponent op basis van twee studies.

Als eerste wordt een case study uitgevoerd die onderzoekt of de huidige sensorkwaliteit voldoende is om BIMS te voorzien met betrouwbare data. Deze case studie testte specifiek alleen de sensoren die relevant zijn voor de data verzameling van BIMS, namelijk de accelerometer voor de trillingsdata en de GPS-ontvanger voor de locatie-data. Deze sensoren worden geëvalueerd op nauwkeurigheid, gevoeligheid en consistentie. Deze evaluatie is gebaseerd op vijf testen, waarbij drie testen gericht zijn op de accelerometer en twee testen op de GPS-ontvanger van de smartphones. In totaal worden de sensoren van drie smartphones getest om een algemene indruk te geven van de smartphonesensor kwaliteit. De testresultaten tonen aan dat de accelerometers van smartphones in staat zijn om versnellingen te meten met een hoge mate van nauwkeurigheid, aangezien aanzienlijke lage gevoeligheden en nauwkeurigheden worden waargenomen met hoge consistenties voor de accelerometers. Daarnaast laten de testresultaten van de GPS-ontvanger zien dat smartphones GPS data kunnen aanleveren met acceptabele nauwkeurigheden.

Vervolgens wordt een veldexperiment uitgevoerd om de haalbaarheid aan te tonen dat de condities van verhardingen kan worden beoordeeld aan de hand van smartphone-data. Daarbij aangezien de oorspronkelijke methode van 'dynamic comfort mapping' is gewijzigd, heronderzoekt het veldexperiment de functionaliteit en haalbaarheid van deze methode. Op basis van trillingsdata verzameld van drie testrijders past het veldexperiment de gewijzigde methode toe op vier wegsegmenten in het stadcentrum van Eindhoven. Om de prestaties van de methode op basis van de smartphone data te evalueren, wordt deze vergeleken met DCI-waarden berekend in de studie van Bíl et al. (2015). Uit deze vergelijking blijkt dat de smartphone gebaseerde methode niet op dezelfde manier functioneert als de oorspronkelijke methode, aangezien de DCI_{sum} waardes over het algemeen 0,2 tot 0,3 lager zijn dan de vergelijkbare DCI-waardes. Hoewel de op smartphone gebaseerde methode slechter presteert in vergelijking met de originele methode, tonen de resultaten van het veldexperiment aan dat het mogelijk is om verschillende types en kwaliteiten verhardingen te onderscheiden op basis van trillingsdata verzameld met de smartphones. Daarbij toont het veld experiment aan dat de data van meerdere fietsers gecombineerd kan worden aangezien sterke correlaties gevonden worden tussen de datasets van de testrijders. Met betrekking tot de methode is meer gedetailleerd onderzoek nodig voordat het kan worden toegepast door BIMS. Deze studie kan worden gezien als een eerste stap in de richting van meer objectieve en geavanceerde methoden voor het verzamelen van data over condities van de fiets omgeving.

ABSTRACT

There has been a growing interest in making cycling a competitive mode of transport, as it is a healthy, environmental friendly alternative and cities are coping with severe problems resulting from the high levels of motorized traffic. In the process of bicycle facility planning, tackling issues regarding cyclist' comfort and safety levels is of utmost importance in order to stimulate and promote cycling as a transportation mode. Especially poor pavement surface conditions appears to strongly affect these levels. The pavement surface conditions are currently assessed through visual inspections, which is an subjective and outdated approach that does not tackle maintenance issues in a resource efficient manner. Since the condition of bicycle surfaces can be manifested in terms of bicycle vibrations, a Bicycle Infrastructure Monitoring System (BIMS) is proposed, which intends to objectively assess the bicycle pavement surface conditions by measuring these bicycle vibrations with the sophisticated sensors embedded in modern day smartphones. By collecting this vibration data in combination with location data from cyclists' smartphones, BIMS will be able to continuously monitor the asset condition data regarding bicycle pavement surfaces. The valuable information resulting from BIMS will help road managers to make more efficient use of their limited resources in relation to operation and maintenance, renewal and auditing of the bicycle environment. This study presents a strong foundation for BIMS by describing all the processes involved and what they entail. This study has further focused particularly on the feasibility of BIMS assessment component, by first conducting a case study which examined if the current sensor quality is sufficient in order to provide reliable data for BIMS. Based on five tests, this case study has shown that smartphones' motion sensors are capable measuring accelerations with a high level of precision and that the location sensors provide GPS data with an acceptable level of accuracy. Next, a field experiment was undertaken in order to prove the feasibility of assessing the pavement surface conditions based on smartphone data, and to examine if an already existing method of dynamic comfort mapping can be used for converting the vibration measurement's outcome into a dynamic comfort index (DCI). The field experiment has demonstrated that it is possible to distinguish different pavement surfaces, and of different qualities based on vibrations data collected from smartphones. Regarding the method of dynamic comfort mapping, more detailed research is necessary in order for BIMS to adopt this method. This study may be seen as a first step towards more objective and sophisticated methods to collect asset condition data regarding the bicycle environment.

TABLE OF CONTENTS

LIST OF FIGURES

LIST OF TABLES

1 INTRODUCTION

Governmental agencies and researchers emphasizes the necessity to shift more towards a sustainable urban mobility (European Commision, 2017; Ministry of Infrastructure and the Environment, 2016; Neirotti et al., 2014; Wefering et al., 2013). The negative effects of high levels of CO_2 emissions, noise emissions, and poor air quality have to be regulated and minimized. The major issue behind these problems is the high level of dependency on the use of private cars. One way to approach this manner is to encourage alternative transport modes such as alternative fuel vehicles, carpooling, and cycling (Accenture, 2014). Cycling is, in contrast to the other transport modes, a healthy, environmentally friendly alternative, which also contributes towards improving citizens' quality of life and urban livability, and it strengthens the economy (Accenture, 2014; European Commision, 2017; Fishman, 2016; Gössling, 2016; Hull & O'Holleran, 2014). It is an efficient way for urban areas to use expensive and scarce space in urban areas (Fishman, 2016). Cities are embracing cycling for its potential to what it brings to a city and many of them are actively working on integrating cycling and making the urban environment more bicycle-friendly.

However, these promised benefits are unlikely to persuade the society to start cycling. One important factor, which deems to influence the mode-choice is the perceived level of safety and comfort of the bicycle in traffic (Heinen et al., 2010; Van Overdijk et al., 2017). A lot of people are concerned about the safety risks associated with cycling. Götschi et al. (2016) mention that these risks "play a greater role for the individual, as they affect crash victims immediately, and deter potential cyclists from riding". The perceived level of safety and comfort is mainly determined by the bicycle infrastructure offered to cyclists (Ayachi et al., 2015; DiGioia et al., 2017; Fishman, 2016; Schaap et al., 2015; Wegman et al., 2012). Thus, providing a bicycle-friendly environment, which accommodates safe and comfort bicycling, can and will increase the attractivness of using bicycles as a significant mode of transport (Joo & Oh, 2013; Schepers et al., 2017).

From a recent study conducted by Van Overdijk (2016), one aspect in particular of the bicycle infrastructure seems to be one of the most influential factors of the perceived level of cycling comfort and safety, namely the pavement surface condition of the bicycle infrastructure. The pavement surface condition strongly influences the bicycle route-comfort, and thus the perceived level of safety, as there is an indirect connection between the perceived level of comfort and safety (Van Overdijk, 2016). Cyclist perceive the pavement surface conditions by way of bicycle vibrations that are transmitted from the surface. Irregularities and unevenness due to edges of tiles or cobllestones, tree root damages, sagging, or uneven joints are the main cause of these bicycle vibrations (Champoux et al., 2007; KOAC WMD, 2002). Thus, a poor pavement surface conditions manifests itself in terms of vibrations induced to the cyclist.

1.1 PROBLEM DEFINITION

One of the fundamentals for providing bicycle-friendly environments, that accommodates safe and comfort cycling, is to assess the current network. This in order to determine where maintenance and/or improvements are necessary (Joo & Oh, 2013). Since pavement surface conditions is identified to strongly influence route-comfort, assessing the current bicycle network on these conditions is crucial in order to stimulate people to use the bicycle. Currently, the basis of assessing the bicycle pavement conditions in order to determine if

maintenance is necessary, is through visual inspections. Unfortunately, the literature does not provide adequate information regarding the details of this type of inspection. Therefore, three interviews were conducted with experts in the domain of road management of bicycle infrastructure. The interviews provided extra information regarding the policy and frequency of these inspections, and the decision-making procedure of planning maintenance. The design structure of the interview can be found in appendix I.

1.1.1 EXPERT INTERVIEWS

The visual inspections are mostly conducted by foot or car driving at crawl speed, and sometimes even with high definition video footage. The latter is favorable in the case of busy roads, where the normal inspection approach would lead to obstruction or congestion of passing traffic. During these inspections, all the road sections (cycle path, footpath, car lane etc.) of a particular segment are inspected simultaneously. Only with isolated bicycle paths a focused inspection is conducted. The visual inspections evaluate each road segment on surface defects (e.g. cracks, raveling, potholes, sagging, tree root damages) by means of severity and dimensions for each 100 meters. Next, based on the severity and dimension of a particular damage, a particular maintenance measure is advised.

These inspections however, are not the triggering attribute on the decision if maintenance is necessary. The final call is made by a road manager. He/she performs a 'measure assessment' in which he/she assesses each advised maintenance measure resulting out of the visual inspections and decides whether or not maintenance measures will be executed. Ideally, each measure would be executed. However, due to governmental authorities only having limited funds, priorities must be made about which road has to be maintained first. The reasons for these priorities can differ per governmental authority. It can for instance that an authority simply governs that first the main roads with the busiest traffic flows are maintained. It also can be based on future spatial plans. Thus, overall the visual inspections can be seen as a first round evaluation indicating which roads need maintenance and what kind of maintenance, where after the road managers makes a second round evaluation based on his/her limited funds, priorities and vision.

Furthermore, governmental authorities conduct on average the visual inspection for closed pavements (asphalt and concrete) once a year and for open pavements (tiles and cobblestones) once every two or three years. The higher inspection frequency of the closed pavements is because when there is a damage and it is not intervened at the right moment, it will result in heavier and more costly maintenance measures, which is less the case with open pavements.

1.1.2 DETAILED PROBLEM DEFINITION

From the previous section, it can be noticed that the current practice of visual inspections is a resource inefficient approach for assessing the bicycle pavement surface. These inspections are costly, as they are conducted at crawl speed, making them are very time consuming and labor-intensive. In addition, the visual inspection is dependable on the knowledge and experience of the inspectors, as it is a subjective approach for assessing the pavement surface conditions. Thus, given the growing interest of using bicycle as a transportation mode, a more resource efficient manner for obtaining objective asset condition data regarding bicycle pavement surfaces is needed to be able to maintain and improve the current quality of the bicycle environment with the limited funds of governmental authorities. This in order to stimulate people to start using the bicycle.

The current study therefore proposes a new system for collecting bicycle asset condition data and is reffered to as 'Bicycle Infrastructure Monitoring System' (BIMS). BIMS will collect the asset condition data on the basis that pavement surface conditions can be manifested in terms of vibrations transmitted to the cyclist. More specific, the system intends to measure the bicycle vibrations in order to objectively assess the surface pavement conditions. This approach is not new, as several researchers already have measured these vibrations to objectively describe the properties of pavement surfaces (Bíl et al., 2015; Hölzel et al., 2012; Olieman et al., 2012). However, they all measured the level of vibrations using Instrumented Probe Bicycle (IPB), which is a bicycle equipped with multiple sensors that in particular measures both bicycle position and acceleration. This systems concept aims at using a more recent fast emerging technique for measuring the vibrations experienced while cycling, namely the sensors present in modern-day smartphones. Smartphone are currently a symphony of different sensors capable of measuring valuable data from the physical world and its intersection with human behavior (Johnston & Robinson, 2015). More and more researchers are acknowledging the opportunities that arise from using the smartphone sensors for collectively sensing the urban environment (Allmendinger et al., 2017; Azzoug & Kaewunruen, 2017; Novakova & Pavlis, 2017).

Furthermore, the system intends to collect the smartphone data from every-day cyclists using crowdsourcing techniques. Based on the data generated by these cyclists, BIMS will continuously monitor the bicycle pavement surface conditions. This enables road managers to schedule maintenance more efficiently and reduce the costs of it, since they will be able to faster spot poor pavement surface conditions, and act more rapidly on abrupt damages. In addition, the system uses an objective approach to assess the pavement surface conditions, which will ensure consistency in the assessment. Moreover, the system also provides opportunities to obtain more valuable information then only about the pavement surface, like intensity of traffic flows, sections speeds, or origin-destination information. In the long run this system will improve cyclists' perceived comfort and safety levels, as the quality of the bicycle pavement surfaces will be maintained and even improved. In comparison with the other similar methods, a great advantage of this system over the other similar methods is that it uses already available sources to generate the data, which makes it easy transferable in contrast to acquiring an IPB.

1.2 BICYCLE INFRASTRUCTURE MONITORING SYSTEM

Since this study is a component of a larger concept, this section will provide a more comprehensive understanding of the total concept of the 'Bicycle Infrastructure Monitoring System' (BIMS). BIMS concept proposed in this study will continuously collect and monitor asset condition data regarding the bicycle infrastructure's pavement surface conditions based on vibration data collected by cyclists' smartphones using crowdsourcing techniques, for the benefit of improving cyclists' comfort and safety levels on the road. The system is mainly designed to aid road managers in operations and maintenance of their bicycle infrastructure with its output. Road managers only have to provide the bicycle network and corresponding quality condition threshold values as input for the system, and it will provide the road managers with up to date information about the pavement surface conditions of the bicycle network based on the data collected by cyclists. In addition, the system will indicate which segments exceed the defined quality condition threshold values. A schematic process flowchart of the suggested BIMS concept is depicted in figure 1.1.

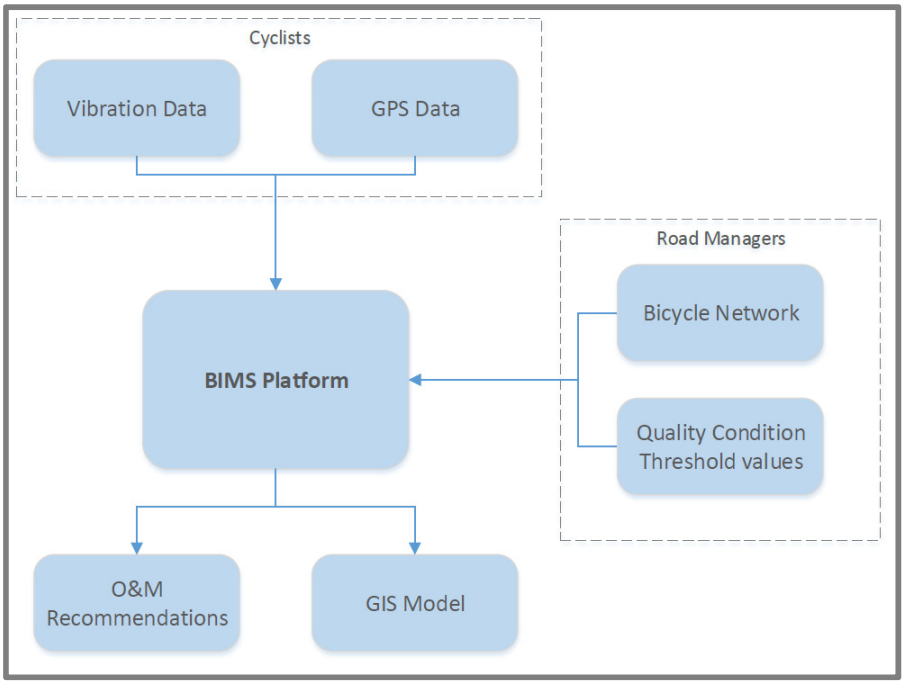

Figure 1.1: Schematic process flow diagram BIMS Concept

Fundamental for this system is the manner of how the asset condition of the bicycle infrastructure is assessed, namely by measuring the transmitted vibrations experienced while cycling with the cyclist's smartphones. The vibration data will be collected using a an application installed on a mobile phone. Using crowdsourcing techniques the data from all the cyclists participating will be collected. This data is then processed and converted into an index, indicating the pavement surface condition. In addition, the derived indexes will be linked to cyclist's GPS positioning.

The system's output will not only be valuable for road managers, but also for cyclists. From the study of Van Overdijk (2016), cyclists appear to rate route-comfort as an important deterrent of using the bicycle as a transportation mode. Since cyclist perceive route-comfort primarily by the means of transmitted vibrations and the GPS position is linked to the vibration data, the system's output can be used to map comfort levels of cycling routes. This will enable cyclists to pro-actively plan the most comfortable route to their destinations.

Besides that the system will preserve the high quality of the bicycle environment. It will also contribute to several other aspects. From an economic perspective, the system will reduce the cost of operations and maintenance, as it could partly replace the visual inspection of the bicycle pavement surfaces, and aid road managers to plan their maintenance operations more efficiently. In addition, instead of developing new expensive resources, BIMS solely uses already existing resources.

Out of a social perspective, BIMS will promote public participation, as it relies on every-day cyclist to be the target group for collecting the data. From an environmental perspective, the system will indirectly contribute to a more sustainable environment. It enhances the bicycle infrastructure offered to the society which will stimulate them of using the bicycle as a

sustainable transportation mode. Moreover, if the system would accomplish to replace the visual inspection, no more vehicular traffic will be necessary for monitoring the bicycle pavement surface conditions.

1.3 RESEARCH OBJECTIVE

The objective of this study is to create a foundation for BIMS, that is capable of collecting, analyzing and monitoring asset condition data regarding the bicycle environment's pavement surface conditions. In general, the system intends to address the issues related to operations and maintenance of the bicycle pavement surfaces, which will become more important given the growing interest of the bicycle as a sustainable transportation mode inside a city. Road managers will gain the most of a system like BIMS, since it will monitor the bicycle pavement surface conditions and will help them to faster spot poor surface qualities, to schedule maintenance more efficiently, and to act more rapidly on abrupt damages to road surfaces.

The main objective of this research is to demonstrate the technical feasibility of the assessment of pavement surface conditions based on vibration data collected via cyclists' smartphones for BIMS. This report therefore first evaluates the current quality of modern-day smartphone sensors in order to ensure that the current quality is sufficient for BIMS, and since few is known about the accuracy, sensitivity and consistency of smartphone sensors. Next, this study proposes a method for the assessment and proves its feasibility. Furthermore, this study aims to present of what can be achieved using big data of available resources and the opportunities that arise with it, instead of continuously developing new resources.

1.3.1 RESEARCH QUESTIONS

Out of the problem definition and research objectives resulted the following main research question:

"Can the pavement quality be indicated with a set of individual vibration measurements using internal smartphone sensors, and is it possible to convert these measurements into a surface quality index, for the benefit of collecting asset condition data regarding the bicycle pavement quality?"

In order to support the main research question, the following sub-questions have been defined:

1. How is pavement and its condition related to cyclists' level of comfort and safety according to literature?
2. Which factors influence the vibrations transmitted from the pavement surface to the cyclist?
3. What is the current practice for assessing the bicycle environments' pavement surface condition?
4. What are state-of-the art bicycle monitoring technologies for collecting asset condition data regarding the bicycle environments?
5. How reliable is the smartphone as a data collection tool for BIMS?

6. What are the benefits and drawbacks of the smartphone-based vibration measurement for determining the pavement surface condition compared to the current practices?
7. How can the results of this research be implemented in operations and maintenance plans of road managers?

1.3.2 LIMITATIONS

The scope of the BIMS introduced in this research is limited to assess and monitor the bicycle environment on pavement surface conditions. If the assessment of the pavement surface conditions is combined with other aspects concerning the perceived levels of comfort and safety of bicycle infrastructure (e.g. traffic volumes, driving directions, presence of median barriers, etc.), a proper and total assessment can be conducted of the bicycle environment.

Furthermore, this study particularly is limited to only investigating the assessment component of BIMS. In addition, this study is limited to the assumption of cyclists' smartphones being located in their trousers. In practice this location might differ per cyclist, or even per trip.

1.4 RESEARCH DESIGN & THESIS OUTLINE

The literature study that is conducted in order to gain knowledge about the research subject and associated aspects is described in Chapter 2. A clear overview of the outcomes of previous studies and experiments will be provided. This review will serve as an inception report prior to the further development of this study and it will be used to answer the first, second, third and fourth sub-research question.

In chapter 3 the research approach of this report is discussed. The aspects, as a result of the literature review concerning bicycle monitoring technologies, are used to design a more detailed process flow diagram for BIMS than the diagram depicted in figure 1.1 of section 1.2. This diagram will provide a more comprehensive understanding of the systems' underlying concept by addressing all the sub-processes involved in the system. The research approach will discuss the cycling comfort assessment method, which is intended to be employed by BIMS. The method is based on the dynamic comfort mapping method introduced by Bíl et al. (2015). Due to one principal difference of data to be collected via smartphones located in cyclists' trousers instead of an accelerometer mounted to the bicycle, the method needs to be adjusted on multiple aspects. These aspects are covered in the research approach. Furthermore, this chapter discusses how the method of dynamic comfort mapping is researched and tested, as the new aspects affect its outcome in some sort. This study researches BIMS assessment component on the basis of two studies.

First a case study is conducted to examine if the current sensor quality of smartphones is sufficient to be used as data collection tool for the cycling comfort assessment method. The total design, execution and results of the case study will be discussed in Chapter 4 of this study. The outcome of the case study is used to answer the fifth sub-research questions. Next, a field experiment is conducted in order to prove the feasibility of using the dynamic comfort mapping method based on data collect via smartphones. In chapter 5 of this report the elaboration of this field experiment is described. The experience gained from this experiment together with the acquired knowledge of the literature review are used to answer the sixth and seventh sub-research question.

Chapter 6 presents the conclusion, discussion and recommendations of this study. In the conclusion the main and sub research questions are answered based on the findings of this study. Next, the discussion critically evaluates the cycling comfort assessment method on multiple aspects. In addition, the case study as well as the field experiment are evaluated on elements which could have been done better or differently. Finally and foremost, this report presents the recommendations regarding future research topics as well as recommended future practical developments concerning BIMS.

The stages presented in this report provide an excellent workflow of handling and processing information for this report, and the overall outcome provides a strong foundation for further development of the proposed BIMS concept.

2 LITERATURE REVIEW

2.1 INTRODUCTION

For several years now, there has been a growing interest of making urban environments more bicycle-friendly to encourage their residents to cycle (Fishman, 2016), as a lot of cities are struggling with severe problems resulting from the high levels of motorized traffic (Docherty, 2003; Fishman, 2016; Gössling, 2016; Lyons, 2016; Pucher et al., 2010). As a logical result, this will lead to an increase in topics concerning bicycle asset management (Calvey et al., 2015). One major part of this is the maintenance and operations of bicycle pavement surfaces. As a strong knowledge bases for this research as well as for future research, this chapter provides a review of the current literature concerning the collection of asset condition data of bicycle tracks' pavement surfaces and related aspects. First, relevant studies are reviewed with regard to the influence of pavement on cyclists' comfort and safety levels, followed by studies with regard to the vibrations experienced as a cyclist. Next, an overview is provided of recent bicycle monitoring technologies for the benefit bicycle asset management. This chapter will end with a general conclusion of the findings in the literature review.

2.2 PAVEMENT CONDITIONS

This section will narrow down the scope from comfort and safety aspects of bicycle infrastructure to the importance of pavement conditions on not only safety and comfort aspects of cycling, but also on route choice behavior. First, a brief explanation will be presented on the factors influencing the choice of pavement type by road managers.

2.2.1 ASPECTS INFLUENCING PAVEMENT CHOICE

As is well known, asphalt and concrete are the most comfortable pavements to cycle on, it provides the smoothest ride. So why aren't all bicycle paths finished with an asphalt or concrete pavement? A study by Kiwa KOAC, a Dutch testing and consultancy company in the field of mobility infrastructure and former KOAC WMD (2002), presented the factors influencing the pavement choice by road managers. According to this study, a road designer/manager determines his/her choice of pavement type on more aspects than the user-preference, or in this case the cyclist. The costs associated with the construction, management and maintenance play an important role in the decision process, which is mainly affected by the load bearing capacity and sediment sensitivity of the subsurface, and the traffic load. Moreover, road managers should also take maintenance vehicles, emergency services and crossing heavy traffic into account. Furthermore, the pavement choice must fit within the sustainable policies of the Netherlands, the risk of damage caused by tree roots should be considered, and the possible presence of underground systems, such as sewers, cables and/or pipelines. Finally, the aesthetic aspects might also be of influence, for example in the case of historic centers. In this case, more traditional pavements (e.g. cobblestones) are preferred as they better fit in the environment.

2.2.2 PAVEMENT IN RELATION TO COMFORT

Hölzel et al. (2012) mention in their research on cycling comfort on different road surfaces that bicycle infrastructure must offer comfortable cycling, which requires smooth rolling at the lowest possible energy input. They state that the roll smoothness of a bikeway is related to the rolling resistance which is strongly influenced by the pavement surface type and in

which condition it is. For instance, a brick road is much rougher than an asphalt road, and thus will have a higher rolling resistance, which stands for higher energy inputs. The higher energy inputs will have a negative influence on comfort levels. A simple example, cyclists in general do not like to ascend a slope due to the high energy input it requires. Hötze et al. (2012) investigated the effects of four different road surfaces (asphalt, concrete slabs, cobblestones, self-binding gravel) on cycling comfort. They included hardly used surfaces, and worn surfaces which really needed maintenance. Some main conclusions of their research are that asphalt is the most comfortable surface to cycle and concrete slabs is a good alternative. Another conclusion was that the riding quality or comfort is negatively linear dependent from increasing velocities, meaning that with increasing velocities the ride quality decreases. Similar results are observed in the Studies of KOAC WPM (2002), Niska and Sjörgen (2014), and Ayachi et al. (2015). However, the study by Niska and Sjörgen (2014) revealed that cyclists found a gravel surface more comfortable than concrete slabs, even if the gravel surface was more uneven. Cyclists indicated that the persistent rhythmic vibrations due to the concrete slab joints were experienced as uncomfortable.

A recent study by Blauw (2016) commissioned by the ANWB on recreational biking in the Netherlands examined how recreational cyclists experience their trip(s) in the Netherlands. This research presents several improvements for the bikeways in Utrecht in the field of safety and comfort. 49% of the participating cyclists indicated the comfort of the bikeways as a point of improvement. This involves in particular bumps, tree roots, holes and pits in the road surface. Note that this only include the recreational cyclists and their trips account for 21% of all trips made by bike (Schaap et al., 2015). Utilitarian cyclists might evaluate comfort less important, because the bicycle is mainly used as a transport mode to ride from A to B, and where recreational cycling is more about the comfort, ease and environment of cycling. Kang & Fricker (2013) acknowledge this statement by indicating in their literature review that bicyclist's preferences for their bike trip differ according to their purpose (e.g., recreation vs. commuting), riding skill (e.g., experienced vs. inexperienced) and sex.

Calvey et al. (2015) conducted a research on cyclists' perceptions of satisfaction and comfort. They state that comfort is a subjective term as individuals evaluate what comfortable is or not based on their own opinion. The personal comfort is in relation to cycling infrastructure directly affected by how important they rate particular variables. For instance, if an individual considers the pavement condition to be extremely important when they cycle, then ultimately the bikeway quality will affect how comfortable they feel when cycling. One crucial finding out of the research of Calvey et al. (2015) on user importance and comfort perception in relation to cycling infrastructure was that the two most important variables ('Path is free from debris' and 'Path is free from surface defects') are both maintenance issues and thus related to pavement conditions.

Where Calvey et al. (2015) describe comfort level more as a subjective term, KOAC WPM (2002) describe it more as an 'intrinsic' property of the pavement type. They support this statement by indicating that the same ranking of the pavement types is observed when considering damages to the surface as when considering no damages to the surface. Although, the differences between the open and closed pavements slightly decreases, meaning that the comfort level of closed pavements proportionally deteriorate more due to damages than open pavements.

2.2.3 PAVEMENT IN RELATION TO SAFETY

Pavement conditions is at first sight associated with cyclists' comfort due to the transmitted vibrations. However, it could also play an important role on cyclists' safety as the organization Bicycle Network (2017) indicates on an article on their webpage about surface smoothness. When riders are exposed to extreme vibrations due to undulations, bumps and/or rough surfaces, it can get hazardous for cyclists directly. For instance, riders can lose control of their bike due to these extreme vibrations and crash, or they could be forced to ride elsewhere on a less safe (and less comfortable) bikeway. Another consequence of poor pavement conditions is that riders sometimes avoid these paths by cycling on the road instead of the designated bike-part (in mixed traffic situations), which increases the risk of being hit by a motorized vehicle.

According to Ormel and Schepers (2009) 74% of all bicycle accidents are single-bicycle accidents, which are accidents where no other road user is involved (e.g. falling off a bicycle, hitting a pothole or leaving the road). Almost half of these single-bicycle accidents is partly caused by infrastructure (e.g. collisions with sidewalk, slippery surfaces, gutters, slots, poles and pits) (Schepers, 2008). In addition, a research conducted by the Dutch organization VeiligheidNL (2012) on bicycle accidents in the Netherlands in which they try to get more insight in the nature, size, underlying causes and the consequences of bicycle accidents, they found that approximately 30% of the accidents is partly caused by the road conditions. Moreover, the proportion of accidents caused by road conditions due to poor road conditions is 22%.

Another interesting finding was recently made by Baetslé and Poorter (2015) at the University of Gent. They researched the influence of pavement quality on the viewing habbits of kids and adults. According to this research, it appears that cyclists cycling on a poor quality bikeway look on average 63% of the time at the surface, which is more than twice as much than a bikeway of good quality. Although paying attention to the road sounds good at first sight, it also means that cyclists pay much less attention to other road users. This can lead to hazardous situation to be noticed later, or even too late, by cyclists.

2.2.4 PAVEMENT IN RELATION TO BICYCLE USE

Some studies investigated the deterrents of using the bicycle as a transportation mode and found some interesting findings on the relation between pavement and bicycle use. A study by Parkin et al. (2008) on bicycle determinants for cycling to work found that pavement quality was negatively correlated with the number of residents in an area cycling to work. The higher the defects of a pavement score, the lower the cycle proportion to work. This confirms the view that poorly maintained roads are a deterrent to cycling. Parkin et al. (2008) uses the same clarification as Hölzel et al. (2012) for this phenomenon, namely that cycling on a poorly road surface is less pleasant and also takes a greater amount of energy to traverse. Another study by Winters et al. (2011) on motivators and deterrents of bicycling found that unsafe surfaces have a strong deterrent effect when deciding to cycle. They also state that cyclists are more likely to use the bicycle due to good road surfaces. Thirdly, a study by Transport for London (2008) on business case on cycling in London found that after resurfacing a bikeway, the number of cyclists doubled. Hence, as Transport for London (2008) also notes, this increase is partly due to the total growing share of cyclists in London.

2.2.5 PAVEMENT IN RELATION TO ROUTE CHOICE BEHAVIOR

At first, it was assumed that cyclists always choose the shortest route, though more recent literature emphasize that comfort aspects regarding cycling should also be taken into account (Heinen et al., 2010). Out of these comfort aspects the effect of pavement conditions have for long be neglected on route choice behavior of cyclists (Heinen et al., 2010; Landis, 1994). However, recent studies have presented evidence of the importance of pavement conditions on cyclist route choice behavior (Landis et al., 1997; Pucher et al., 2010; Van Overdijk, 2016; Van Overdijk et al., 2017). The bad condition of a bikeway is a deterrent for a cyclist to ride on it, because the lack of suitable surface for cycling decrease the sense of security, which forces the cyclists to choose an alternative route (Segadilha & Sanches, 2014).

Van Overdijk (2016) recently conducted a study on the influences of comfort aspects on route- and mode choice decisions of cyclists in the Netherlands. Where many literature articles emphasize that travel time as the most important route-choice aspects (Stinson & Bhat, 2003), illustrates van Overdijk (2016) that several other comfort aspects were found to be more important and influential on route-choice behavior. At first, the presence of a cycling facility was most important, followed by a smooth pavement. Moreover, this research shows that cyclists are prepared to choose a 4 minute longer route on a trip of 15 minutes for a higher quality pavement. Stinson and Bhat (2003) found that travel time to be most important, Although they added that separate paths, smooth pavements and less crossings were preferred.

2.3 VIBRATIONS EXPERIENCED AS A CYCLIST

The pavement conditions also influence the 'ride' or 'trip' quality of a cyclist in terms of transmitted vibrations. Giubilato and Petrone (2012), and Bíl et al. (2015) confirm this by stating that cyclists perceive the pavement conditions by way of bicycle vibrations transmitted from the surface, and that this is among the most important causes of discomfort. As vibrations increases, comfort decreases. The characteristics of the bike (e.g. mass, tire pressure, stiffness and suspension of frame, suspension saddle) determine to which extent the vibrations are transmitted to the cyclist's body due to irregularities in the road (KOAC WMD, 2002).

2.3.1 DYNAMIC COMFORT

Champoux et al. (2007) established two different definitions of road bike comfort to discriminate between two types of comfort, namely 'static comfort' and 'dynamic comfort'. Static comfort is related to a person's perception of the bike at rest, such as the bike size or selection of proper components (e.g. saddle, shape handlebar, etc.). It also refers to positioning and the flexibility of the cyclist, and his or her ability to adapt. On the other hand, dynamic comfort relates to the perceived vibrations transmitted towards the cyclist. Most studies focused on the dynamic comfort since it is related to the transmitted vibrations which can be a significant cause of discomfort (Champoux & Drouet, 2012; Lépine et al., 2014, 2015; Wojtowicki et al., 2001).

However, most of the previous studies were specifically analyzing the influence of design components on the vibration level perceived by the cyclist, and in addition, helping manufactures in designing better bicycles frame materials to improve cyclist's comfort

(Vanwalleghem et al., 2012). Some examples are the insertion of rubber into the frame, application of a frame material with a higher damping capacity, or implementation of flexible zones in the frame. Although it should be noted that most of these design improvements are applied to racing bicycles. These are all attempts to improve shock (vibration) absorption capacity of the bicycle. Other studies tried to develop force transducers (e.g. instrumented pedals, stems and seat posts) or excitation techniques, which are mainly studies that try to understand and measure the vibrations induced to the cyclist (Lépine et al., 2015). In addition, the latter two subjects support the research on bicycle characteristics that could reduce the vibrations induced to the cyclist.

2.3.2 THE ENTITY OF VIBRATIONS

Thus besides an irregular road surface, the bicycle also plays an important role in the entity of the vibration transmitted while cycling. According to Giubilato & Petrone (2012), the transmission of vibrations depends on geometry, mass, inertia and structural characteristics of bicycle components, such as frame, seat post, saddle, fork, stem or handlebar. Hence the large proportion of research regarding the improvement of improve bicycle components on cycling comfort. Vanwalleghem et al. (2012) conducted a study on the evaluation of bicycle dynamics and its relation with cyclist's comfort. They found that out of the three locations a cyclist makes contact with the bicycle (handlebar, saddle and pedals), the most discomfort is experienced near the handlebar and the saddle when riding over a rough surface (Vanwalleghem et al., 2012).

Vibrations are oscillatory motions, which can occur in different forms. Currently there exist 3 different metrics in the literature to quantify the vibration induced to a cyclist: acceleration, transmitted force and adsorbed power (Pelland-Leblanc et al., 2014). All three are adequate to evaluate comfort when cycling, although acceleration is the most frequently used (Giubilato & Petrone, 2012; Olieman et al., 2012). It is also used in the whole-body vibration standards, such as ISO2631, ISO5349 and BS6841. These standards relate comfort to the acceleration level at the contact points between man and machine (bicycle) near the feet, seat-surface and back, only ISO5349 is for hand-arm vibrations. The vibrations are simply evaluated based on the higher the accelerations, the less comfort the human encounters. According to Van den Berg and Groenendijk (2009), the human body is very sensitive to vibration in the range of 3 to 16 Hz. Lower or higher frequencies are more easily tolerated.

2.3.3 ROAD TRANSMITTED VIBRATIONS

As already discussed, the aim of most studies is to define the properties of bicycle components, or to investigate the effect of vibrations on cycling performance. However, studies examining the vibrations that road surfaces transmit towards cyclist is scarce. Section 2.3.1 already discussed the studies of KOAC WPM (2002), Hölzel et al. (2012), and Niska and Sjörgen (2014) in which it was concluded what the most comfortable pavements are. These studies however base their analysis on the vibrations properties of these pavements types, meaning that the pavements are characterized by the amount vibrations they transmit to the cyclist. More specific, these studies measure the amount of vibrations a particular road surface transmit to the cyclist, which subsequently are used to characterize the level of comfort. The more vibrations are transmitted, the less comfort is experienced.

Champoux et al. (2007) defines that there are two typical road pavement issues that cause two different types of excitation (vibration energy transferred to the rider), namely cracked

roads and coarse roads. A cracked road contains cracks, tree roots and/or potholes which are sufficiently spaced to allow the transmitted vibration of the bike to (mostly) vanish between events. The excitation from a cracked road can be considered as a series of successive impacts. A coarse road, on the other hand, transmits a continuous random excitation to the bike. This includes asphalt, concrete or cobblestone roads with a rough but uniform surface structure. Kiwa KOAC, former KOAC WMD (2002), uses a similar approach where the cracked roads are referred to as irregularities and unevenness due to edges of tiles or cobblestones, tree root damages, sagging, uneven connections, traffic threats and so on. And the coarse roads is referred to as the texture or roughness of the pavement type, such as the broom structure of concrete or surface texture of asphalt, cobblestones or concrete tiles. Another road pavement condition can be added based on the study of Niska and Sjörgen (2014). As already discussed in section 2.3.2, a persistent rhythmic vibrations due to slab joints are considered uncomfortable. The excitation of this kind of road characterizes itself as persistent and rhythmic.

2.4 BICYCLE MONITORING TECHNOLOGIES

Closely linked to these pavement issues (cracks, potholes, sagging, roughness etc.) is the operations and maintenance of cycling tracks pavement conditions (Pucher et al., 2010). Calvey et al. (2015) is one of the few which investigated respondents altitude regarding issues related to the cycle path surface in the form of a survey. They found that overall the issues that are directly linked to the pavement surface which could have been prevented with proper maintenance (e.g. roughness, potholes, root damage, broken up surface), appear to be of greater importance for cyclists. Respondents appeared to find general maintenance and upkeep to be important.

The current method of assessing cycle-path pavement condition in order to decide if maintenance is necessary is through direct visual inspections (Calvey et al., 2015; Douangphachanh et al., 2013). These inspections are costly and subjective as they are very time consuming and labor-intensive. Several researchers emphasize the need for more intelligent (smart) manners for the acquisition of asset condition data regarding cycling infrastructure and pavement quality (Bíl et al., 2015; Joo & Oh, 2013; Yamaguchi et al., 2015). Especially since the importance of bicycle transportation is increasing.

There has been a lot of attention paid to the acquisition of asset condition data regarding infrastructure such as motorways, railways and trunk roads, but almost no attention has been paid regarding cycling infrastructure and pavement quality (Calvey et al., 2015; Pucher et al., 2010). For vehicular traffic there exist various traffic monitoring and surveillance technologies, and procedures to collect asset condition data, which provide useful information and data to the governmental agencies for operation and maintenance planning and design purposes (Pearson, 2012). For instance, highway managers established methods, procedures and associated equipment to collect skid resistance, surface roughness and deflection data. Again, such extensive methods for monitoring and collecting asset condition data regarding cycling facilities are either not available, or not at one's disposal due to high costs of such methods or equipment (Mohanty et al., 2014).

2.4.1 SENSOR TECHNOLOGIES FOR INFRASTRUCTURE

One opportunity that arises to respond to this underdeveloped domain is with currently available sensor technologies. The use of sensors and detection technologies in civil infrastructure is a growing subject in recent literature due to rapid transformation of sensors into high-performance measurement devices capable of measuring, gathering, and recording data about the environments in which the devices find themselves (Wang et al., 2014). The availability of powerful new sensors have helped the society with verifying design assumptions, tracking structural performance over a structure's lifecycle, and rapidly identifying unsafe structural conditions originating from damage and deterioration. Wang et al. (2014) describes that the adoption of sensing systems to monitor infrastructural project has undergone three phases: First sensors were used in case studies to assess structure with revolutionary design concepts; Next, sensors were used more widely to monitor structures exposed to extreme loads to determine structural performance; and currently, the sensors are used to generate reliable data to assess the structural health of a system monitored, such as a bridge, road, pipeline, dam, or other vital sources.

The latest advances of sensor technologies are at the beginning of being applied in civil infrastructure, construction, and maintenance. The current strategies of evaluating roadway conditions is through localized visual inspections, which are as discussed time consuming, labor-intensive, and highly subjective, and, in addition, are not performed regularly, require traffic blockage to execute (Mednis et al., 2011; Mohan et al., 2008; Wang & Birken, 2014). These strategies are not suited for the current need and are causing problems in scheduling and implementing maintenance and repair operations. Wang & Birken (2014) describes this need as the critical need to make the right roadway repairs in the right place and at the right time. The advancing sensor technology offers a great opportunity to cost-effectively monitor the roadway condition of a road network system, and, in addition, provide up-to-date information for maintenance activity prioritization. It can be expected that besides the need for cost-effective and efficient monitoring and maintenance techniques for road network systems increases, it will also increase for bicycle network systems, since bicycle transportation is globally increasing.

One technology on which the advancing sensor technology is applied are Instrumented Probe Bicycles (IPB), which are simple bicycles equipped with sensors able to measure and collect data about bicycle-related subjects (Mohanty et al., 2014). The bicycles can be equipped with sensors like bicycle position, acceleration, potentiometer, lateral distance sensor, a laser pointer or a camera (Bíl et al., 2015). The IPB as research tool is an emerging technology in the bicycle-related research, and can be applied on a large variety of research domains. It can be applied to estimate bicycle or cyclists' behavior, to monitor or evaluate bicycle environments or to assist in developing prediction models for bicycle safety, comfort or mobility. The next part of this section will discuss three examples which use the recent sensor technologies and IPB's for their research (see table 2.1).

The first study of Olieman et al. (2012) focused on the vibrations by bicycle, which is also called the dynamic comfort (see section 2.3.1). They measured the level of vibration at four places on the bike (front wheel axel, rear wheel axel, stem and seat post) using accelerometers. These places where strategical chosen to measure both the input and output of the frame and fork, to then establish a transfer function. It seems that the vibrations are distributed in less than 5 milliseconds through the frame. Additionally, it was also investigated to which extent

the vibrations induced to the bicycle where affected by the road surface, speed, wheels and tire pressure. Their research shows that road surface has a significant impact on the vibrations induced to the bicycle, as expected. Asphalt being a smooth surface transmits less vibrations than a rough small cobbles. Furthermore, increasing speeds seems to proportionally increase the transmitted vibrations, thus reducing comfort. Almost the same applies to increasing tire pressures, with the exception that this influence seems to be asymptotical. Different wheelsets did not seemed to affect the entity of the vibration, which is contrary of the general belief.

Table 2.1: Example studies using recent sensor technologies and IPB's

Authors	Sensors Utilized	Application
(Olieman et al., 2012)	Accelerometers	Testing dynamic comfort bicycle
(Joo & Oh, 2013)	GPS receiver, Accelerometer, and Gyro-sensor	Evaluation of bicycle environment in terms of safety and mobility
(Bíl et al., 2015)	GPS receiver and Accelerometer	Objectively describing vibration properties of pavement surfaces

The second study of Joo & Oh (2013) proposed a novel method to monitor the bicycle environment with an instrumented probe bicycle (IPB) equipped with a GPS receiver, accelerometer, and gyro sensor. An IPB is in this study defined as a common bicycle equipped by several technologies which measure both bicycle position and acceleration. Other sensors which are often included are a potentiometer, a lateral distance sensor, a laser pointer and/or a camera (Bíl et al., 2015). Next, the data generated from the IPB is used as input for the method to evaluate the performance of the bicycle environments on safety and mobility, and to translate it to a bicycling monitoring index (BMI). The safety is defined as a cycling stability index (CSI) which is derived from multiple predictors from the IPB data and from the perceived safety data obtained from a questionnaire. The mobility performance is simply expressed in speed and is derived from the GPS receiver. The index from both the safety and mobility is than expressed in a BMI by applying a fault tree analysis (FTA). Finally, the method was applied to demonstrate the feasibility of the implementation. The intention of Joo & Oh (2013) was to incorporate the method/software in public bicycle sharing systems, especially since the most recent bicycle-sharing systems have smart technologies included. In addition, they state that the method is capable of providing more valuable information besides the BMI, such as bicycle counts, section speeds, origin-destination information, hazardous segments and poor segments. However, more extensive analysis and input data is needed to derive more reliable BMI values.

Bíl et al. (2015) conducted a study of a new method of objective bicycle vibration measurements to describe the vibrational properties of different pavement types. This study was a follow up of another study of Bíl et al. (2012) that proposed a method for cycling-track mapping, which has been applied to the Czech cycling trails. The objective of the new method was to contribute to the current cycling-track mapping by adding a robust and objective vibration measurements in the form of dynamic comfort index (DCI), which is able to spot local extremes as well as aggregated values of a segment. The DCI is calculated per second from the measured values of acceleration. These values, or vibration data, are measured with an

accelerometer attached to the front fork of the bicycle. Next, a GPS receiver is used to determine the movement and position of the bicycle so the DCI can be linked to the GPS position. With this geo-referenced data it is possible to map the DCI. Bíl et al. (2015) also researched to which extent the DCI values are dependent on cyclist's speed and bicycle type, and if the DCI values matched the subjective comfort evaluation of cyclists. First, increasing cyclist's speed was found to negatively influence the DCI values and the overall range. They therefore decided to maintain a speed of 15 km/h as standard for the measurements. Secondly, three different bicycles (mountain, racing and touring bicycle) were tested and it did not appeared to significantly influence the DCI values. Lastly, a close relationship was found between the objective DCI and the subjective comfort evaluation of cyclists. A major benefit of this method is that it is effortlessly transferable in contrast to the present-day IPB, which is an advanced piece of technology that can be rather complicated and expensive to reproduce. Another advantage of this kind of approach is that it is objective and therefore does not rely on individuals, as the current visual inspection does.

2.4.2 Crowdsourcing Techniques for Infrastructure

Another opportunity which can easily be combined with the latest sensor technologies is the use of crowdsourcing techniques. Crowdsourcing is a relative new term, being firstly introduced by Jeff Howe (2006) in a Wired magazine Article. Jeff Howe defined crowdsourcing as 'a company or institution taking a function once performed by employees and outsourcing the work through an open call to online communities'. A perfect early example is Treadless, which had the basic idea to put out some defined work to a community and then the community members are able to compete to win the project (Nehls, 2015). There are many more examples in which individuals compete to provide ideas, solutions and/or information to important business, social, policy, scientific and technical challenges (Brabham, 2013).

Over the years crowdsourcing has emerged to be used in multiple applications. One more recent one is using the concept of crowdsourcing for the acquisition of information or input related to infrastructure voluntarily from (local) (road)users (Migue Figliozzi & Blanc, 2015). In many cases smartphone applications are used to 'crowdsource' information about infrastructure maintenance, enforcement requests, and safety issues. The next section will review several recent examples of platforms for crowdsourcing data, and are outlined in table 2.2. Note that the examples will be restricted to crowdsourcing platforms related bicycle infrastructure.

Table 2.2: Example studies using crowdsourcing platforms to acquire data regarding bicycle infrastructure

Name	Year of Introduction	Initial Deployment Location	Source
ORcycle	2014	Oregon	(Miguel Figliozzi, 2015)
Fiets Telweek	2015	The Netherlands	(Scheper et al., 2016)
PING	2017	Brussels	(Bike Citizens & Mobiel 21, 2017)

ORcycle was released in November 2014 and makes use of a crowdsourced platform on which citizens of Oregon can voluntarily provide bicycle-related safety reports about their bicycle infrastructure. The reports contain feedback regarding crashes, safety, or infrastructure issues. The app offers several options to describe the safety problem, such as 'pavement condition', 'narrow bike lane', 'high traffic speed', and 'parked vehicles'. A user may also

upload a photo to clarify the situation. Besides the safety reports, the app will also record and display your bicycle trips. Since its release, ORcycle has collected over 400 safety reports from citizens all over the state of Oregon (Blanc & Figliozzi, 2017). The Oregon Department of Transportation (ODOT) collects and handles these safety reports, and are published in an online mapping application available to all the public on the ORcycle website. Transport planners of Oregon state use this application to better design and upgrade bicycle facilities.

The Fiets Telweek originating from the Netherland had as objective to collect as much data as possible in a week about the bicycle movements in the Netherlands and to visualize the bike network. Since 2015, the Fiets Telweek event has been organized once a year. During this week, people could easily contribute to this project by just downloading the application prior to the week, and to let it record their bicycle trips. This project was (legit) titled as 'The Largest Bicycle Research Ever In The Netherlands' (Scheper et al., 2016). The first week resulted in approximately 38.000 active participants which together cycled almost 400.000 bicycle trips. These trips accounted for more than 1.2 million bicycle-kilometers and were visualized in an online mapping application. The data of these weeks gives governments, for example, the ability to pinpoint bottlenecks in their environment, evaluate the construction of a new bikeways, or to better balance bicycle-related measures that promote bicycle traffic. This project was the first step for the Netherlands to a new level of bicycle monitoring.

PING is a recent introduced crowdsourcing engagement commissioned by Bike Citizens. Bike Citizens is a company founded in 2011, and started business with a simple bike navigation app and smartphone mount. Nowadays, the company focuses more on cycling promotion, app technology, and data analysis for cities. The PING-project is for the first time introduced in Brussels as a pilot-project. The project gives the ability to citizens to directly mark unsafe or unsatisfying traffic situations by pushing their PING button, which is a simple Bluetooth-enabled device that maps the marked spots indicated by the user. When cyclists have reached their destination they can give feedback on their marked PING points in the Bike Citizens app by matching it with different categories, such as road surface, sight, infrastructural design, traffic light etc.. Finally, the marked locations and feedback are reviewed and set to be analyzed. The project started with a pilot of 1,000 citizens of Brussels that all received a PING button.

2.4.3 SMARTPHONE SENSOR TECHNOLOGIES FOR INFRASTRUCTURE

Another emerging and relatively new technique which can easily combines the new sensor technologies and crowdsourcing techniques, is the smartphone. The modern day smartphone includes different sensors capable of measuring valuable data from the physical world and its intersection with human behavior (Johnston & Robinson, 2015). Each new model of smartphone contains more sensors than its older versions raging from barometers to luxometers. Johnston & Robinson (2015) describe in their online article about the opportunity of applying 'sensor repurposing' in smartphones, meaning that sensors are repurposed from their original purpose in a phone. For instance, the battery temperature sensor can be used to measure outdoor ambient temperature when combining data from many devices (Fitchard, 2015). The great advantage for researchers to use sensor repurposing is that it can reduce the capital expenditures drastically, as it allows repurposing of existing sources (sensors) instead of investing and deploying new ones.

Research regarding smartphone sensors is not entirely new. However, the focus has mainly been on activity recognition (Bayat et al., 2014; Botzheim et al., 2013), and not on using these sensors as advanced measuring tool. Yet, researchers do emphasize the great potential of using these sensors to infer information (Akhavian & Behzadan, 2016). Especially since almost all individuals in the modern day world carry a smartphone on a daily basis. This is confirmed by Johnston & Robinson (2015) stating that crowdsourcing techniques allow these scaled networks to be built. Smartphone users will be able to form a part of a social laboratory, acting as surveyors that constantly record data about the environments they find themselves.

Recording data about the conditions of bicycle infrastructure is an example of what is capable with smartphone sensors and crowdsourcing techniques. This section will provide a review of the studies which use the smartphone as an measurement tool to gather and record data related to the condition of bicycle infrastructure, or more specifically the pavement conditions.

The first study is conducted by Kobana et al. (2014). They propose a method to detect road damage by cyclists equipped with a smartphone positioned in their trousers. The purpose of this study was to reduce the cost of maintenance by introducing a new method of detecting road damages. Due to the positioning of the smartphone in a cyclist's trouser, the collected acceleration signal can be categorized in the vibrational signal due to the road condition and the pedaling signal due to the movement of the cyclist. An Independent Component Analysis (ICA) is applied to the raw acceleration data in order to separate the vibration signal from the pedaling signal. Such an analysis is a computational method for estimating source signals from multiple mixed signals. The higher frequency signal from the road can be distinguished from the pedaling signal with this analysis. After the road signal is extracted, the road signal is classified in one of the four road conditions with an algorithm.

The second study is conducted by Niska & Sjögren (2014) for the Swedisch Transport Administration (VTI). Their intention was to use the technology present in smartphones and crowdsourcing techniques to gather data from cyclists using the bicycle network, in order to indicate the smoothness/evenness of the pavement surface. A mobile application developed by the VTI is evaluated in this study focusing on repeatability and practical usefulness, mainly through field studies. One important difference with the study of Kobana et al. (2014) is that in de study of Niska & Sjögren (2014) the phone is attached to the handlebars. Their field studies show different acceleration values varying from one measurements to another however, based on these values, it is possible to distinguish between different pavement types and quality. Another finding from this study is that it is hard to capture local irregularities since the measurements highly depend on the cyclist's lateral positioning on the cycle path. The results of the field studies were also compared to cyclist's subjective comfort in relation to surfacing, and the measurements in general correspond to cyclists opinion. Based on this comparison, an classification was made indicating the level of comfort. Acceleration values above 0.75 are indicated as uncomfortable (red level), values lower than 0.5 as comfortable (green level) and in between as neutral (yellow level). However, the results showed to be affected by speed, phone type, tire pressure and cyclist weight to be influencing the acceleration values.

The third and last study is conducted by Yamaguchi et al. (2015). This study proposed and developed, just like the previous two, a smartphone based system to estimate the road profile by only measuring the vertical acceleration values of a city cycle. The road profile is estimated as the vertical displacement of the tire. Yamaguchi et al. (2015) apply a slightly different approach to their measuring system than Kobana et al. (2014) and Niska & Sjögren (2014). Besides using a smartphone attached to the handlebars, a cyclometer, also known as a bicycle computer, is included that enables them to track and measure a cyclist's performance while cycling. For this study, the cyclometer is used to calculate the running distance with more accuracy and smaller error than distance estimation based on GPS data. The study first examines the vibration characteristics, and state that these characteristics are affected by road path, bicycle structure, smartphone holder, ride speed and tire pressure. For both the bicycle structure and smartphone holder the eigenfrequency is estimated, for the speed a calibration formula is proposed. Next, an algorithm is proposed to eliminate low frequency noise and transform the smartphone measured acceleration to front or rear tire displacement. In addition, a smartphone holder location correction is proposed, since the location is not right above the front tire. Finally, the proposed method was tested and validated by an experiment. The method resulted in a 16% error of the maximum values of the estimated road profiles. In addition, cracks were clearly detected through profile estimation.

2.5 Conclusion

This chapter started with a comprehensive review of current literature on pavement conditions regarding comfort, safety, bicycle use and route-choice of cyclists. By summarizing the findings of sections 2.2, the first sub research question (see section 1.3.1) can be answered. What is striking in the reviewed literature of this section is that the terms 'safety' and 'comfort' are often linked to each other, but it is never substantiated how. Only a few studies make a link between the two terms, stating that these two subjects are 'closely related' or 'go hand in hand'. It seems that 'safety' is used more as an objective term, which can be substantiated. It can be expressed in the risks associated to, in this case, characteristics of the cycling tracks, and cyclist's exposure to these risks. 'comfort', on the other hand, is both a subjective and objective term, as it is related to both cyclists' perceived safety and to the ease of cycling. Cyclists' opinion will differ on what they perceive comfortable or not, and which factors influence these comfort levels. Meanwhile the ease of cycling is a general fact, as some pavement surfaces are scientifically proven to be more convenient to cycle on than others. Based on these findings, the relation between the two terms can therefore be described as such that cycling comfort not only represents the ease of cycling, but also the subjective safety levels of cyclists. Nevertheless, for the remainder of this study, when referring to cyclists' level of comfort, the relation to the ease of cycling is intended. Based on this terminology, a more appropriate answer can be given on the first sub research question.

Next, the chapter provided a compressive review of current literature on the vibrations experienced as a cyclist and the factors affecting these vibrations. The findings (section 2.3) can be used to answer the second sub research question. What can be concluded is that in particular there are two types of vibrations experienced by cyclist due to the pavement surface. First, the vibrations due to the general vibration properties of the surface, and secondly due to surface defects, such as cracks, tree roots, potholes e.g.. Furthermore, the findings of section 2.3 will also be used to identify which factors need to be considered for BIMS.

Further, in order to answer the third and fourth sub question of section 1.3.1, an analysis was conducted on the bicycle monitoring technologies. It can be concluded that there is indeed a growing interest in innovations concerning bicycle asset management, as many discussed technologies have been developed quite recently. Most of them tackle the issue of bicycle maintenance currently being conducted in a resource inefficient manner. The studies discussed in section 2.4.3 use a similar approach as this study to address these issues, namely by using smartphones to assess the pavement surface quality and crowdsourcing technique to collect the relevant data. The findings of these studies showed that, in addition to the aforementioned influencing factors (the bicycle and its characteristics, the cyclist him- or herself, and the road surface) also the pedal movement can influence the smartphone-based vibration measurement when the smartphone is located inside cyclists' trousers.

3 RESEARCH APPROACH

3.1 INTRODUCTION

As already mentioned in section 2.4, research concerning traffic monitoring and surveillance technologies has received a lot of attention in existing literature, as they provide useful information and data to governmental agencies for operation and maintenance planning and design purposes. The focus however of these researchers is mainly on the collection of asset condition data regarding vehicular traffic. Technologies with the focus on bicycle traffic, is still relatively new. Given the growing interest of promoting the bicycle as a sustainable transportation mode inside a city, technologies such as BIMS will become more of interest. Moreover, as mentioned they will improve the perceived safety and comfort levels of cyclist, as the technologies helps governmental agencies (road managers) to maintain or even improve their bicycle environment.

Out of the literature review of chapter 2, a lot of knowledge was acquired regarding research-related topics and associated aspects. Based on this knowledge, a more detailed process flow diagram is designed for the BIMS platform than depicted in figure 1.1 of section 1.2. The diagram provides a better comprehensive understanding of all the sub-processes involved in BIMS.

Next, the cycling comfort assessment method for BIMS will be discussed. BIMS bases its assessment method on a dynamic comfort mapping method introduced by Bíl et al. (2015). The original method is first extensively reviewed, followed by a description of how and why this particular assessment method is employed by BIMS. Additionally, some extra aspects resulting out of the literature review are discussed which should be considered before the method is adopted for BIMS as they affect the method or system in some sort. These elements following out of the literature include the bicycle and cyclist characteristics, data collection from multiple cyclists and pedal movement of the cyclists.

As mentioned in section 1.4, this assessment method is researched and tested based on two studies. First a case study in the form of an explorative study is conducted. The study will elaborately test and analyze the sensor quality of three different smartphones, as the literature relevant to smartphone sensor qualities is minuscule and the data collection via smartphones a crucial component of BIMS is. The main objective of the case study is to examine if the smartphone can be used as a reliable tool for measuring bicycle vibrations and deriving location. Secondly, a field experiment will be conducted in the form of a Proof of Concept (POC). The experiment will demonstrate the feasibility of BIMS fundamental component of using the smartphone as a data collection tool for assessing the pavement surface condition of a bike segment. The research approach will only describe briefly what these studies exactly entail, how and why they are set up, and what they aim to achieve. The complete description of the objectives, execution and analysis of both the case study and field experiment are described separately in chapters 4 and 5 respectively.

As both the case study and the field experiment rely on sensor data from the smartphone and this data needs to be retrieved using a smartphone-app, this research approach will end with the description of the selection process of a data collection app. There are a lot of applications available in the Google Play store capable of reading, logging and analyzing smartphone sensor

data. This section will therefore describe the process for selecting the best suited application for the data collection of this research. At first, several applications will be evaluated against predefined primary and secondary requirements. The app used for the data collection must at least comply with the primary requirements, and the secondary requirements contain elements which are recommended. After this evaluation, the remaining apps will be evaluated on their interface, performance, and usability. The best suited application will be chosen and used for the remainder of the study as data collector.

3.2 PROCESS FLOW DIAGRAM BIMS

The basic concept of BIMS is to collect vibration data via smartphones and crowdsourcing techniques, and convert it to an index to monitor the pavement surface condition of the bicycle network. The system's output is intended to improve cyclists' safety and comfort and aid road managers with planning operations and maintenance of their bicycle infrastructure. The process flow diagram of the BIMS platform is depicted in figure 3.1 related to the sub-processes of the system. Five sub-processes of the system can be distinguished: 'Input', 'Pre-Process', 'Process', 'Evaluation', and 'Output'. Each sub-process is an action which consists of one or multiple activities, and generates a result for the successive sub-processes. As this study merely researches some components of BIMS, this diagram is used to indicate to which components the case study and field experiment of this report contribute.

The first sub-process 'Input' concerns the data collection for BIMS. As discussed, the asset condition of the bicycle pavement surfaces will be determined based on vibration data collected via the sensors of cyclists' smartphones. A tool in the form of a smartphone-application will collect the raw data from the smartphone sensors. The raw data will consist of linear acceleration values - measured from the accelerometer, gyroscope and magnetometer – and GPS coordinates corresponding to these acceleration values. The raw data will be exported, ready to be pre-processed.

After the system's input-data is collected, it will be pre-processed, which basically means that the raw data will be prepared for further processing. The 'Pre-Process' consists of a two basic steps in which the data is transformed to an understandable and desired format. The first step is data cleansing in which the data is cleansed, like resolving the inconsistencies in the data, eliminating outliers, and/or smoothing the noisy data. Next step is the data integration, which will combine and aggregate the data as an incorporated form and structure for further processing. This sub-process results in the refinement of the input-data.

The third sub-process includes the 'Process' of deriving the asset condition data of the bicycle network from the refined data. This concept will represent the asset condition data in the form of a dynamic comfort index (DCI) introduced by Bíl et al. (2015). The DCI is calculated from the measured values of acceleration, and since also GPS data is collected, the DCI can be linked to a GPS position. The DCI will identify the condition of a bicycle segment with a number ranging from zero to one, where an index of one represents a very smooth surface, and an index of zero very irregular surface.

The next sub-process is the 'Evaluation', which logically means evaluating the DCI values. The index values will be categorized into different levels of quality. Each level indicates the pavement surface condition of a particular road segment. The index values will also be

checked against threshold values to make sure it meets established standards. This process of proactively checking data is called data monitoring (Informatica, 2017). A Data Monitoring Tool will support this process. The threshold values of the tool can be created and edited as preferred or needed. If the index values exceed the established standards, an alert can be sent to an administrator. Thus, the categorization together with the Data Monitoring Tool with evaluate the index values, and provide a good overview of the overall quality of the bicycle pavement surfaces.

The final sub-process provides the final 'Output' of the system. This sub-process focusses on the representation of the previous evaluations. For the index values exceeding threshold values, an alert or notification is send to the road manager. The road manager can then perform a measurement test in order to define the appropriate maintenance measures concerning that particular segment. Ideally this follows out of the index values. However this can be rather difficult, since the index values do not make a distinction between different defects and each defect is handled differently as was discussed in the interview findings of section 1.1.1. Further, the categorized levels will be mapped in a GIS (Geographical Information Systems) environment based on the GPS position linked to the data. This will give a direct overview of the bicycle network's surface conditions. The different levels of quality can, for instance, be mapped in different colors, where a color corresponds to a certain level. This will not only indicate which pavement surface conditions are poor, but also which surfaces might need attention in the future.

A great advantage of this system over the current approach of visual inspections, is that the surface quality of the bicycle network will be monitored continuously by every-day cyclists instead of yearly. It is a more resource efficient manner of tackling the maintenance issues, which were found to be important by cyclists in the study of Calvey et al. (2015) discussed in section 2.4. The continuous information provided by the system will aid road managers to faster spot poor surface qualities, to schedule maintenance more efficiently, and to act more rapidly on abrupt damages to road surfaces.

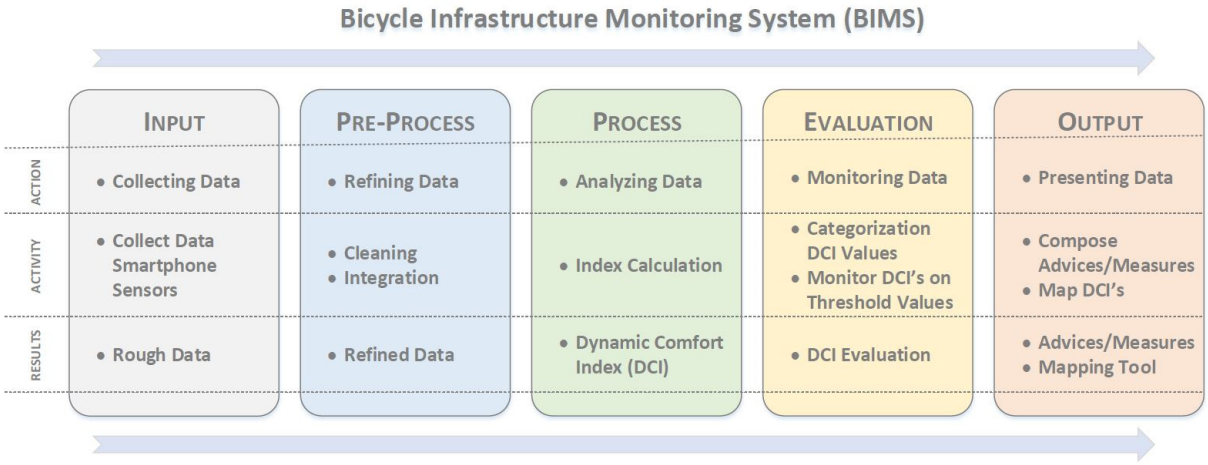

Figure 3.1: BIMS Process flow diagram

3.3 CYCLING COMFORT ASSESSMENT METHOD

As mentioned, this study mainly researches the assessment component of BIMS. When put into context with BIMS process flow diagram of figure 3.1, this component mainly concerns the 'Input', 'Pre-Process', and 'Process' of BIMS. The fundamental method of BIMS for assessing bike segments on pavement surface will be based on the dynamic comfort mapping method of Bíl et al. (2015), since their study is in a lot of aspects similar to BIMS assessment component. Both, for instance, intend to use the bicycle to assess the pavement surface condition based on a vibration measurement. This section will therefore elaborately review the dynamic comfort mapping method of Bíl et al. (2015). First, since the method was briefly described in section 2.4.1, it is elaborated upon, followed by what lessons can be learned from their study, and finally based on the literature findings there will be described what aspects need to be considered and how they are dealt with regarding the method before it can be implemented for BIMS.

3.3.1 DYNAMIC COMFORT INDEX

For the computation of the vibration data to a particular index, BIMS intends to use the dynamic comfort mapping method introduced by Bíl et al. (2015) as a basis. The method was first introduced in the Czech Republic as an objective (quantitative) way of cycling track mapping. It is capable of objectively describing the vibration properties of pavement surface on a particular bicycle segment. These properties are then used to indicate the cycling comfort in the form of a 'Dynamic Comfort Index' (DCI). The DCI represent the inverse value of the energy contained in the signal of acceleration, and is calculated using the following formula:

$$DCI = \left(\sqrt{\frac{1}{n}\sum_{i=1}^{n}(a_i^2)}\right)^{-1} \qquad where\ i = 1,2,\dots,n \tag{1}$$

Where a_i is the measured acceleration value of measurement i and n is the number of measurements during a specific time period. Bíl et al. (2015) calculated the DCI for every single second, however it can also be calculated over a longer time period. The DCI value ranges between zero and one, and is indirectly related to the power of acceleration (or vibrations). Thus, high DCI's identify more comfortable bike segments with less and smaller, and low DCI's represent less comfortable bike segment with large vibrations. By linking GPS data to each corresponding index value, the data can be easily visualized on a map.

The development of the dynamic comfort mapping method was not merely a theoretical study. It has already been applied to the historical center of the city of Olomouc, Czech Republic, and therefore proving the functionality and feasibility of this method. The vibration data was collected using an ordinary bicycle mounted with a GPS device and an accelerometer. figure 3.2 depicts an example of how the DCI is visualized on a map. Logically, the DCI values are categorized by color into different levels, where the red segments represent low DCI values and green segments high DCI values. This is also an possibility of how it can be represented for BIMS.

Figure 3.2: Representation of Dynamic Comfort Index in the city of Olomouc
Source: Transport Research Centre (CDC) http://www.cyklokomfort.cz/en/ (2017)

Lessons Learned

The study of Bíl et al. (2015) did not only introduce the method of dynamic comfort mapping, but they also researched how some factors relate to the DCI, such as speed, bicycle type and also the subjective comfort evaluation by cyclists. Therefore, the lessons learned from their study relevant to BIMS will be briefly described, so they can be taken into account in the assessment methodology.

Firstly, during testing they examined to what extend the DCI values are influenced by speed. A decrease in the DCI values and the overall DCI range was experienced with increasing speeds. It is natural that on the same segment, cyclists are exposed to less vibrations if they cycle slower. Moreover, the dispersion of the DCI values rose with increasing speeds. The DCI values regarding cycle path with significant steepness should therefore be handled with care or even excluded. Eventually, they decided to maintain a speed of 15 km/h as a standard pace for testing. Partly due to the difficulty to maintain a steady pace at higher velocities and at lower speeds it is unsafe because of instability issues of the bike. In addition, for this study and experiment, lower speeds could be dangerous regarding other cyclists, as one might not expect somebody cycling at low speeds.

Secondly, they tested to what extent the DCI depends on bicycle type by testing three different types on multiple segments. They included a racing, touring and mountain bicycle, and all bikes were cycled by the same rider. No significant difference was found between the derived DCI values from the different bicycle types, which is contradicting of what is found in the literature, as it showed that bicycle characteristics influence how the vibrations are transmitted to the cyclist. Although it should be noted that in the study of Bíl et al. (2015) an accelerometer is mounted to the front fork of the bicycle in order to measure the bicycle vibrations. This location is very near the front wheel were the vibrations are measured first. From these wheels the vibrations are then transmitted through the rest of the bicycle. This most likely explains why no difference was found between bicycle types.

Thirdly, they researched the performance of the DCI method by validating if the derived DCI values represent the subjective comfort evaluation of cyclists. Based on a group of 43 volunteers and 11 sections on which they cycled their bike, a close relationship with a correlation coefficient of -0.93 was observed between the objective DCI values and their subjective perceptions. Therefore, they concluded that the DCI can easily interpreted as the level of vibrations experienced while cycling. Also here, it is important to note that the volunteers mostly consisted out of experienced cyclist, and are therefore most probably also cycling enthusiasts. This might give biased results as they will have a stronger opinion regarding bicycle vibrations and cycling comfort, as the research of Ayachi et al. (2015) shows.

3.3.2 Adaptation assessment method for BIMS

Although there are a lot of similarities between the DCI assessment method of Bíl et al. (2015) and the intended BIMS assessment component, there is one principal difference, unfortunately, which makes it impossible to directly adopt their method to BIMS and justify it. Namely, BIMS will rely on vibration data to be collected from cyclist's smartphones located in their trousers, not from an accelerometer mounted to the front fork of its bicycle. Normally, the DCI computation only includes linear acceleration readings of the z-axis of the accelerometer for the vibration data, since this axis is perpendicular towards the road surface and its orientation remains fixed during the measurements. However, in the case of BIMS, the position of the smartphone can vary per cyclist and per trip. It is rather complicated to estimate how the smartphones of cyclists are positioned while they are cycling. Therefore, this study proposes an alteration to DCI formula to disregard the smartphone's position during the measurement.

It is important to note that the alteration does not change the basic principle of the formula. It should still represent the inverse value of the energy contained in the signal of acceleration after the alternation, so the alteration will only change which acceleration values of the accelerometer will be included in the DCI-formula.

To disregard the orientation of the smartphone, the linear acceleration values of all three axes of the smartphone's accelerometer should be included, as the readings of all three axes represent all acceleration-forces, excluding gravity, applicable to the smartphone. An additional benefit of including the values of all three axes is that also lateral evasive maneuvers will be recorded. Normally, when cyclists encounter damages to the road surface during their trip, they circle around it to avoid it, as the study of Wijlhuizen (2014) revealed. This means that if the method of Bíl et al. (2015) was used, this damage was missed, since only the z-axis of the accelerometer is recorded. When including readings of all three axes, also the sudden lateral movements will be recorded, which will result in lower DCI values indicating that something is wrong at that particular spot.

From the three axes acceleration readings, the resultant acceleration $a_{i,xyz}$ (or vector sum) will be calculated for each measurement i, which stands for a vector quantity (acceleration) which is equivalent to the combined effect of two or more component vectors acting at the same point (Galbis & Maestre, 2012). Moreover, since the axes are seen as vectors and all the vector angels are perpendicular to each other, the resultant linear acceleration $a_{i,xyz}$ is calculated using the Pythagoras' theorem with the following formula:

$$a_{i,xyz} = \sqrt{a_{i,x}^2 + a_{i,y}^2 + a_{i,z}^2} \quad (2)$$

Where $a_{i,x}$ is the acceleration value of the x-axis, $a_{i,y}$ the acceleration value of the y-axis, and $a_{i,z}$ the acceleration value of the z-axis of measurement i. Note that the resultant acceleration $a_{i,xyz}$ is computed per datapoint. For the DCI formula, the acceleration value a_i of formula (1) will be simply replaced with the resultant acceleration $a_{i,xyz}$. The DCI formula therefore looks as follows:

$$DCI_{sum} = \left(\sqrt{\frac{1}{n}\sum_{i=1}^{n}\left(a_{i,xyz}^2\right)}\right)^{-1} \qquad where\ i = 1,2,\dots,n \quad (3)$$

The new DCI formula will be referred to as DCI_{sum} to prevent confusion. This formula will be used in the field experiment of chapter 5, where it will be applied to multiple segments to evaluate its performance. Out of the results of the experiment it will be decided if the DCI method can be adopted in this format.

3.3.3 Additional aspects

Besides the smartphone orientation, there are several additional aspects which should be considered as they concern the outcome of the DCI_{sum} methodology for BIMS: cyclist's weight, bicycle characteristics, data collection from multiple cyclists, and pedaling movement of the cyclist. The next sections will discuss what these elements imply and how they will be dealt with or examined for the system.

Cyclist's weight

Firstly, the weight of cyclists should be taken into account, since the DCI's of a particular segment will be calculated from data sets of multiple cyclists. It can be expected that the weight of the cyclist directly influence the vibration measurement, as the measurement is done out of cyclists' trousers. The weight of the cyclist was already identified in the literature study to slightly affect the entity of vibrations, and therefore the outcome of the vibration measurements, but indirectly. The study of Olieman et al. (2012) namely revealed that tire pressure influences how the vibrations are transferred to the rider and since weight influences tire pressure, it therefore indirectly impacts the entity of the vibration. Yet the impact of weight is also applicable to the vibration measurement with the fixed accelerometer. With the smartphone-based vibration measurement, however the bicycle vibrations are directly transferred by the cyclist's body to the smartphone, since the smartphone measures out of the cyclist's trouser. In contrast, the fixed accelerometer measures the bicycle vibrations directly, since it is fixed to the bicycle.

Even though the weight of the cyclist is likely to influence the entity of the measured vibrations, the derived DCI's can still be useful as for BIMS it is expected that if the population generating the data is large enough, the noise effect of weight will be averaged out. Nevertheless, the influence of cyclist's weight to the smartphone-based vibration measurement is examined during the field experiment of chapter 5 by comparing the data of multiple riders over the same segments.

Bicycle characteristics

Secondly, the characteristic of the bicycle itself must be taken into account, as the literature of section 2.3 showed that the bicycle components influence how the vibrations are transmitted to the cyclists. There exists a lot of different bicycle types with different characteristics which likely all have a slightly different effect on how the vibrations are transmitted through the bicycle. Striking is that in the study of Bíl et al. (2015) it was concluded that bicycle type does not have an significant effect on the measured vibrations. This can however most likely be explained by the fact that in their study the vibrations were measured near the front fork, where the surface vibrations can be noticed first. For BIMS assessment method, on the other hand, the vibrations are measured in cyclists' trousers near the saddle, where the surface vibrations are transmitted through the frame of the bicycle.

Therefore, it is expected that the characteristics of the bicycle affect the recorded vibrations and thus also the calculated DCI's. Just like the cyclist's characteristics, it is expected that if the community generating the data for BIMS is large enough, the influence of the bicycle and its component can be neglected, as their noise effect on the DCI's will be eventually averaged out. Due to the previous stated and the limited time period of this study, the influence of bicycle type is not examined during the field experiment. All the measurements during the experiment will therefore be conducted cycling only one specific bicycle.

Data collection from multiple cyclist

Thirdly, for BIMS the intention is to continuously collect the data from multiple cyclists and their smartphones in order to monitor the bicycle pavement surfaces. This entails that the DCI's of a particular segment will be calculated from data sets of multiple cyclists. It is therefore of great importance that the computation of the DCI's based on these sets are consistent over a specific segment.

In the method of Bíl et al. (2015) this aspect is of less interest since they calculate the DCI's of a particular segment based on one recording. They calculated the DCI's for every second of this recording, regardless of the speed of the rider. Each time when new data is generated these values are simply substituted. In the case of BIMS, the data will be continuously collected making the approach of calculating the DCI for every second inconvenient as the locations linked to this second will vary from cyclist to cyclist.

It is therefore suggested for BIMS to calculate the DCI over fixed distance-intervals. For instance, calculating the DCI values for each road segment of 10 meters. This will better ensure the consistency of the DCI computation, as the vibration data of cyclists can simply be allocated to a distance-interval or section based on the linked GPS data. Thus, instead of including all the acceleration values of a single second for the DCI, the acceleration values over a particular section will be included. An additional benefit of this approach is that it will be easier to refer to a specific section. The field-experiment of chapter 5, will examine multiple scales for these distance intervals to finally select the most suitable scale for the DCI assessment method.

Pedaling movement

Fourthly, it is expected that the pedaling movement of the cyclist will have a slight influence on the measurement outcome, since the smartphone-based measurement will be conducted from the cyclist's trouser pocket. The study of Kobana et al (2014) discussed in section 2.4.3

with the similar approach of using smartphones located in cyclists' trousers for assessing the road surface quality, also acknowledged the pedal movement influences the measured vibration signal. The smartphone will not follow the exact same pedal movement as the cyclists' feet does, but more an up and down movement. This movement is schematically depicted in figure 3.3. Pedaling is a relatively slow movement and since acceleration represents the rate at which the velocity of a movement changes, the acceleration force will also be relatively low. However, the pedaling movement is still a motion produced by a specific acceleration-force, and could therefore influence the vibration outcome. On average, cyclist pedal with a rate of approximately 60 rpm, which means that the smartphone's motion follows the same rate. This motion could be traced back in the cyclist's generated vibration data.

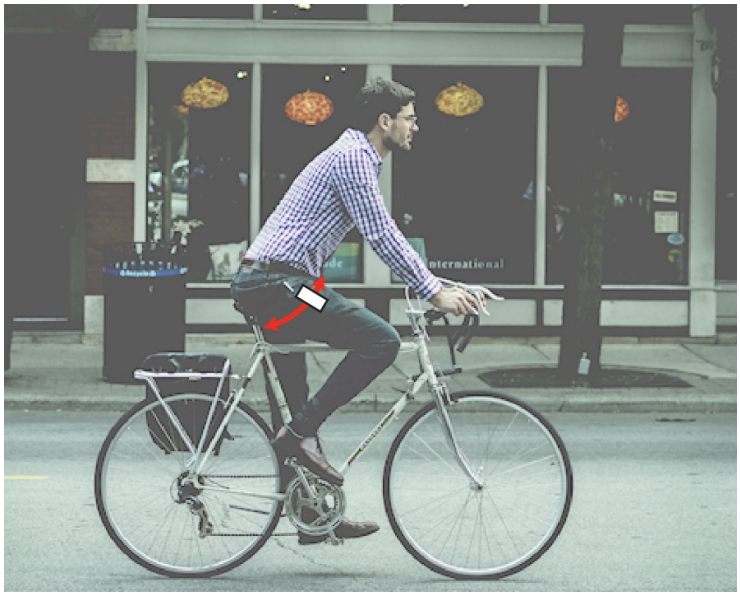

Figure 3.3: Schematic representation of the motion a smartphone makes while cycling

Therefore, this study proposes a variant to the DCI_{sum} formula. Since the pedaling movement as well as the smartphone movement is very slow and acceleration represent the rate at which the movement changes, an alteration to the resultant acceleration formula (2) is proposed. Instead of including on acceleration value of each axis for the resultant acceleration of one data point, the difference in acceleration values of two consecutive points of each axis will be used to calculate the resultant acceleration. If the smartphone movement is slow, than the change in acceleration will also be low, and it will be not or barely noticeable with the new computation of the resultant acceleration. The new computation of the DCI will be referred to as DCI_{diff}, and its formula together with the formula for the new resultant acceleration are as follows:

$$a_{i,xyz} = \sqrt{(a_{i-1,x} - a_{i,x})^2 + (a_{i-1,y} - a_{i,y})^2 + (a_{i-1,z} - a_{i,z})^2} \quad (4)$$

$$DCI_{diff} = \left(\sqrt{\frac{1}{n}\sum_{i=0}^{n}\left(a_{i,xyz}^2\right)}\right)^{-1} \qquad where\ i = 1,2,\dots,n \quad (5)$$

The alteration to the resultant acceleration $a_{i,xyz}$ will not influence the basis of the formula, which is that it represents the inverse value of the energy contained in the signal of acceleration. The difference between formula (2) and (4) is also depicted schematically in figure 3.4. The signal in figure 3.4 represents the acceleration motion of the pedal movement of the smartphone depicted in figure 3.3. The left side of the figure indicates how formula (2) includes the acceleration values for the calculation of the resultant acceleration, and the right side how formula (4) includes these values. As on can see, the pedal movement will be less noticeable when calculated with formula (4) instead of formula (2). Note that this schematic representation is only from one axis.

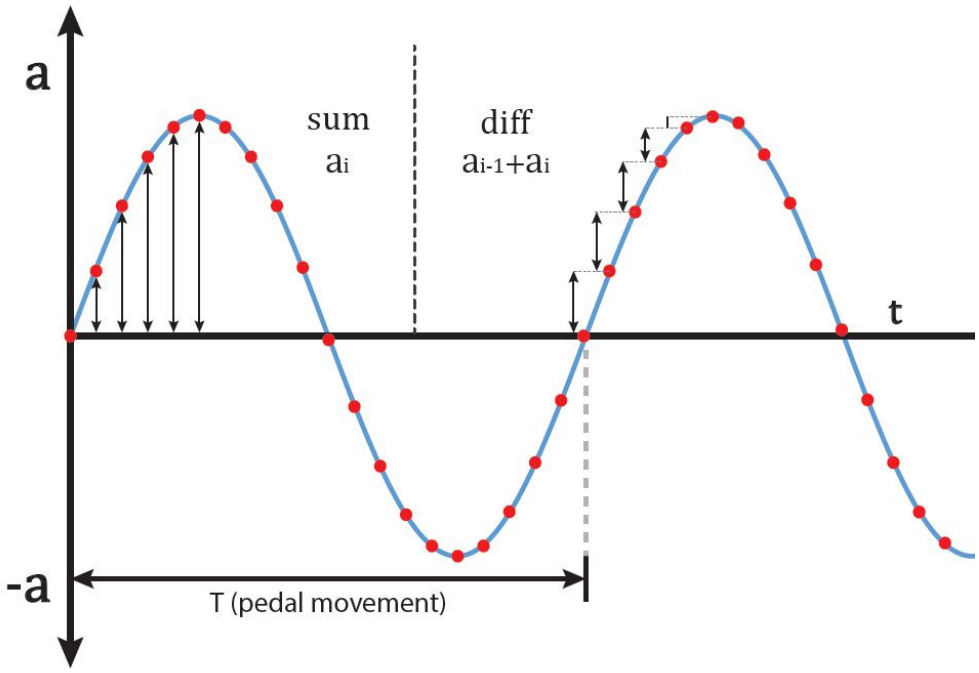

Figure 3.4: Schematic representation of the difference how the resultant acceleration is calculated on the basis of formula (2) and (4)

A possible additional benefit of the DCI_{diff} over formula (3), is that it will represent local extremes more clearly, as the differences in acceleration between two consecutive points are squared. Normally, when a local extreme or shock is recorded it is characterized with a peak (or local maxima) directly followed by a local minima or the other way around. If the two consecutive points are on the local maxima and minima, the resultant acceleration $a_{i,xyz}$ will represent the peak-to-peak value in the case of formula (4). In the case of formula (2), the values of the maxima and minima will be included separately. This phenomenon is depicted schematically in figure 3.5, where on the left it can be seen that the values of the maxima and minima are included separately, and on the right that the resultant acceleration is represented as the peak-to-peak value. The performance of this variant on the DCI_{sum} formula will be tested and evaluated during the field experiment of Chapter 5. It will be compared to the DCI values computed with formula (3).

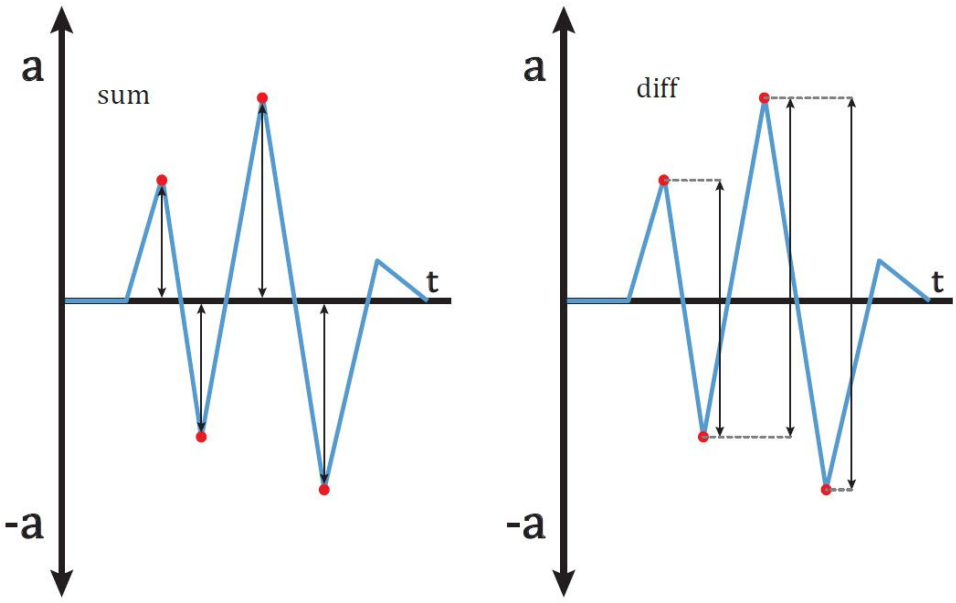

Figure 3.5: Schematic representation of the difference motion a smartphone makes while cycling

3.4 CASE STUDY – SMARTPHONE SENSORS EVALUATION

Although a lot of researchers acknowledge that modern-day smartphones are equipped with advanced sensors (Akhavian & Behzadan, 2016; Ferreira et al., 2017; Johnston & Robinson, 2015; Schirmer & Höpfner, 2013), only a hand full of researchers looked at the full capabilities of these smartphone sensors (Allmendinger et al., 2017; Azzoug & Kaewunruen, 2017; Novakova & Pavlis, 2017), and an even smaller portion really tested them (Amick et al., 2013; Khoo Chee Han et al., 2014; Noury-Desvaux et al., 2011). Since BIMS relies on the data collected from cyclist's smartphone sensors for the assessment of the bicycle pavement surfaces, it is essential to know if the current smartphone sensors are capable of providing this kind of data. In addition, it is important to ensure that the data quality is consistent over different smartphones, since the system will collect data from multiple cyclists with different brands smartphones. Therefore, this case study aims to research if the quality of the current smartphone sensors is sufficient for providing reliable data for BIMS. The case study in the form of an explorative study will test the sensor quality of three smartphones of different brands and ages. This will provide a general overview of what the current quality standard is for smartphone sensors.

The sensors will extensively be tested and analyzed based on five tests. These tests will evaluate sensors' accuracy, sensitivity and consistency. In this research, the accuracy is defined as the degree to which a sensor conforms to the correct value, sensitivity as the smallest amount of change that can be detected by a measurement, and consistency as the way in which sensors are able to produce similar results on the same test.

The case study will only focus on the smartphone sensors that are relevant to the data collection of the system, which are the accelerometer and linear accelerometer for the vibration data and GPS receiver for the location data. The accelerometer and linear

accelerometer of the smartphone should be able to provide reliable data regarding the transmitted vibrations experienced while cycling, and the GPS receiver should link reliable location data to these values. These sensors will be evaluated based on five tests, each test focuses on one particular sensor. Two are focused on the accelerometer, one on the linear accelerometer and two on the GPS receiver. The tests are listed below:

- Test 1 Sensitivity Accelerometer – Accelerometer
- Test 2 Freefall motion – Accelerometer
- Test 3 Controlled Acceleration – Linear Acceleration
- Test 4 GPS Accuracy – GPS Receiver
- Test 5 GPS Distance Accuracy – GPS Receiver

Note that the linear accelerometer measures the same accelerations as the accelerometer, with the exception that the linear accelerometer also uses the gyroscope and the magnetometer to negate the effects of the earths gravitational field (Khoo Chee Han et al., 2014).

3.5 Field experiment–Proof of concept

The prevalence of smartphones is rapidly restructuring the perception of researchers regarding data collection in which individuals can collectively sense the urban environment using smartphone data streams (Allmendinger et al., 2017; Fernee et al., 2012; Matarazzo et al., 2017; Novakova & Pavlis, 2017). BIMS also relies on this technique of crowdsourcing the smartphone data streams in order to collect asset condition data of the bicycle pavement surfaces. The asset condition data is converted out of vibration data collected from multiple cyclists via their smartphones. Previous section discussed a case study examining if the current smartphone sensor quality is at all sufficient for collecting vibration and location data, and whether the sensor quality is equivalent between multiple devices. This field experiment will be a follow up on the case study. It will examine BIMS's fundamental component of using a smartphone-based vibration measurement to indicate the pavement surface quality of a bicycle segment.

The main objective of this field experiment is to serve as Proof-of-Concept (POC) of BIMS assessment component. It will demonstrate that it is feasible to indicate the pavement surface condition with a smartphone-based vibration measurement. The dynamic comfort mapping method of Bíl et al. (2015) will be used for this field experiment. With a small alteration as discussed in section 3.3.2, the method will be applied to multiple segments in the city center of Eindhoven to evaluate its performance.

Furthermore, the experiment will research the elements discussed in section 3.3.3. It will evaluate if the variant on the DCI proposed in formula (4) and (5) is better in distinguishing pavement surface conditions of particular segments, than the original DCI specified in formula (3). Further, the field experiment will examine what the most suitable distance-interval configuration is on which the DCI should be calculated. Finally, the influence of the cyclist's weight will be researched on the DCI outcome by comparing the data generated by three cyclists. The results of the experiment should not only illustrate the feasibility of BIMS but also the best configuration for its assessment method.

3.6 DATA COLLECTION APP

As discussed in section 1.2, BIMS intends to use an application installed on smartphones to collect the relevant data of the motion and location sensor. However, due to the lack of expertise and limited time window of this study, an app offered by the Google Play store is used for reading and collecting the raw sensor data for both the case study and the field experiment. Moreover, as this study is a research study, the app requires some features that can be adapted throughout this study, like for instance sampling speed. The app for BIMS requires these features to be constant in order to ensure that the data is collected consistently.

The Google Play store offers a large variety of apps which are capable of reading, logging and analyzing raw sensor data from smartphones. This section will evaluate multiple apps on a set of predefined requirements, to eventually select the most suitable one for the data collection for the remainder of this study.

3.6.1 SMARTPHONE APP REQUIREMENTS

There exist a large variety of apps capable of reading, logging and/or analyzing data from smartphone sensors. The basis of these apps is much alike. They all use the Android sensor framework to access the sensor platform and acquire raw sensor data (Android Developers, 2017b). The biggest difference between the apps lies in the interface and what kind of options are offered to the user regarding data recording and exporting. The apps will be evaluated based on a set of predefined requirements in order to select the best suitable app for the data collection of this research. These requirements can be categorized into primary and secondary requirements, and are depicted in Table 3.1. An app should at least comply with the primary requirements for it to be used for the data collection.

The primary requirements can be further broken down into sensor, recording, and exporting requirements. The sensor requirements concerns which sensors should be supported by the app. Since, the case study and field experiment require readings from the accelerometer, linear acceleration and GPS receiver, the app must at least support these three sensors. The recording requirements relate to specific recording features. At first the app should support multi-records, which are recordings of multiple sensors simultaneously, since the app should be able to record linear acceleration and GPS simultaneously for the field experiment. Secondly, the sampling frequency should be adjustable and constant over time, since data samples with inconsistent sampling frequencies are not comparable. Thirdly, the recording should include a timestamp of some sort, since some analyses of chapter 4 rely on data in specific time intervals. The last primary requirements are related to the exportation of the raw sensor data. The raw sensors data should be exportable as a csv- or txt-file for further analysis. In addition, the app should save these data files locally and/or be able to export them to an online platform. The secondary requirements include app features which are desirable but not mandatory. These features are the ability to manually alternate the data filename, configure recording time, show device sensor information, and include a keep-screen-on-function.

Table 3.1: App Requirements

Type		Requirement
Primary Requirements	Sensors	Accelerometer
		Linear acceleration
		GPS position
	Recording	Date - time
		Multi-record
		Adjust recording frequency
	Exporting	Format as csv- or txt-file
		Save data-files locally
		Export to e-mail or Google Drive
Secondary Requirements	Additional features	Manually configure filename
		Keep-screen-on function
		Configure recording time
		Device Sensor Info

3.6.2 SELECTION OF SMARTPHONE APP

In total, 11 apps were included in the selection process. These apps were mainly selected from the Google Play store with the exception of the 'FietsComfort' app developed by SGS Intron. This app was obtained directly via the company, and had to be installed manually. The other apps can be downloaded for free in the Google Play store. For some apps a small payment is required to remove advertisements or to enable all the app features, such as export features. Table 3.2 list all the apps included for the evaluation. The table also indicates the app's developer, availability in the Google Play store, and what the associated costs are.

Based on the requirements depicted in Table 3.1, an evaluation matrix was constructed for evaluating the apps listed in table 3.2. The matrix, depicted in table 8.1 of appendix II, simply indicates for each app whether it meets a requirement or not. As mentioned before, if an app does not meet all the primary requirements, it is not suited for the data collection of the remainder of this research. Out of all the apps, only the following apps satisfy the primary requirements: 'AndroSensor', 'Physics toolbox Suite', 'Sensor Record (a)', and 'Sensor Record (b)'. Most of the apps which failed to meet the primary requirements did not include recording or exporting features. The remaining four apps were tested on their interface, performance and usability. From these remaining apps, the 'Sensor Record (a)' app crashed when trying to export a csv-file and the 'Sensor Record (b)' provided an intractable csv-format.

Eventually, the 'AndroSensor' app was chosen instead of the 'Physics toolbox Suite' app based on some legitimate reasons. Firstly, the sampling frequency of the 'Physics toolbox Suite' app could only be adjusted to four fixed sensors rates, and in addition, these were represented textually as can be seen in figure 3.6. For the 'AndroSensor' app, the sampling frequency can be set to any value ranging from 0.001 Hz to 200 Hz. Secondly, the data files retrieved from 'Physics toolbox Suite' app often contained errors when recording multiple sensors.

Table 3.2: Smartphone Sensor Apps

# App	Developer	Available in Google Play store	Costs App
1. AndroSensor	Fiv Asim	✓	€ 0,99 (Optional)
2. FietsComfort	SGS Intron	✗	Free
3. Physics Toolbox Suite	Vieyra Software	✓	Free
4. Raw Sensor Data	AJB Tech	✓	Free
5. Sensor Data	Vipul Lugade	✓	€ 5,49 (Optional)
6. Sensors Record (a)	Martin Golpashin	✓	Free
7. Sensors Record (b)	mrwojtek	✓	Free
8. Sensor Tracker	Bicasoft Technologies	✓	Free
9. Sensors toolbox	EXA Tools	✓	€ 0,69 (Optional)
10. Sensors Multitool	Wered Software	✓	Free
11. Sensors Toolbox	Galaxy Developers	✓	Free

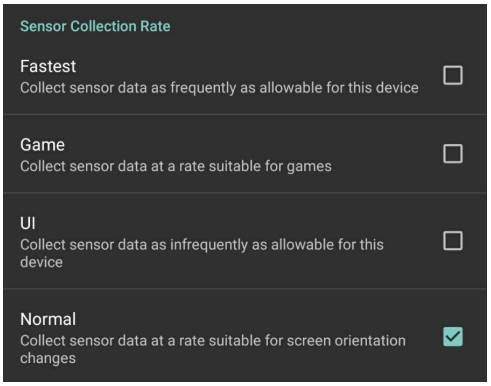

Figure 3.6: Cropped screenshot of 'Physics Tool Suite'

3.7 CONCLUSION

This chapter provided an extensive overview of the steps that will be taken in the research process of this study. At first, the chapter presented an elaboration of the sub-processes involved in the intended BIMS on the basis of the knowledge acquired in the literature review of chapter 2. Based on these sub-processes a process flow diagram was designed indicating the general flow of information and the actions involved of each sub-processes. This diagram can serve as foundation for further development of BIMS. For this study, the diagram is used to indicate to which processes this study contribute, as this study will mainly focus on BIMS assessment component.

Next, the method for the assessing the bicycle pavement surfaces based on smartphone vibrations data is elaborately discussed. This method used the dynamic comfort mapping method introduced by Bíl et al. (2015) as a basis for this assessment. Their method objectively represents the measured bicycle vibrations by computing these vibrations into a dynamic comfort index (DCI). Since the data collection of this study slightly differed from their study,

the original formula for the computation of the DCI needed to be modified. Further, based on the insights of both the study of Bíl et al. (2015) and the literature, several aspects were discussed in how they should be dealt with as they concern the methodology's outcome.

In this study the assessment method will be researched and tested based on two studies. First a cases study will be conducted in which the current quality of smartphones' motion and location sensors will be extensively examined on the basis of five tests. Secondly, a field experiment will be undertaken in which the feasibility of assessing the bicycle pavement surfaces based on smartphone data will be demonstrated.

The chapter ended with describing the selection process of a smartphone application for recording and collecting the sensor data from the smartphones for both the case study and the field experiment. Multiple applications were evaluated based on a set of predefined requirements, and based on their performance and usability. Eventually, the AndroSensor-app was selected to best suit this research needs.

4 CASE STUDY

This section elaborately describes how each of the five tests regarding the smartphone sensors is conducted, analyzed and evaluated. First, the objectives of this case study are defined. Then, since a lot of overlap exist for all test, some general aspects regarding data collection are described. Next, for each test is described which test method is used and what its scope is, followed by a description of the test setup and how the data is collected, and finally a description of how the data is analyzed.

4.1 OBJECTIVES

The main objective of this case study is to evaluate if the smartphone can be used as a reliable measurement tool, and therefore mainly concerns the 'Input' process of the process flow diagram as depicted in figure 4.1. This case study will base this evaluation on five tests which test and analyze the sensor quality of three different smartphone. The tests aim to evaluate the accuracy, sensitivity, and consistency of the sensors relevant for the BIMS, which are the accelerometer, linear accelerometer and the GPS receiver. Further, with the evaluation of three smartphones of different brands and ages, this case study aims at providing a general impression of what the current sensor quality standard is for modern day smartphones and that the qualities do not differ much between devices, in order to illustrate that it is feasible to collect data from multiple smartphones for BIMS.

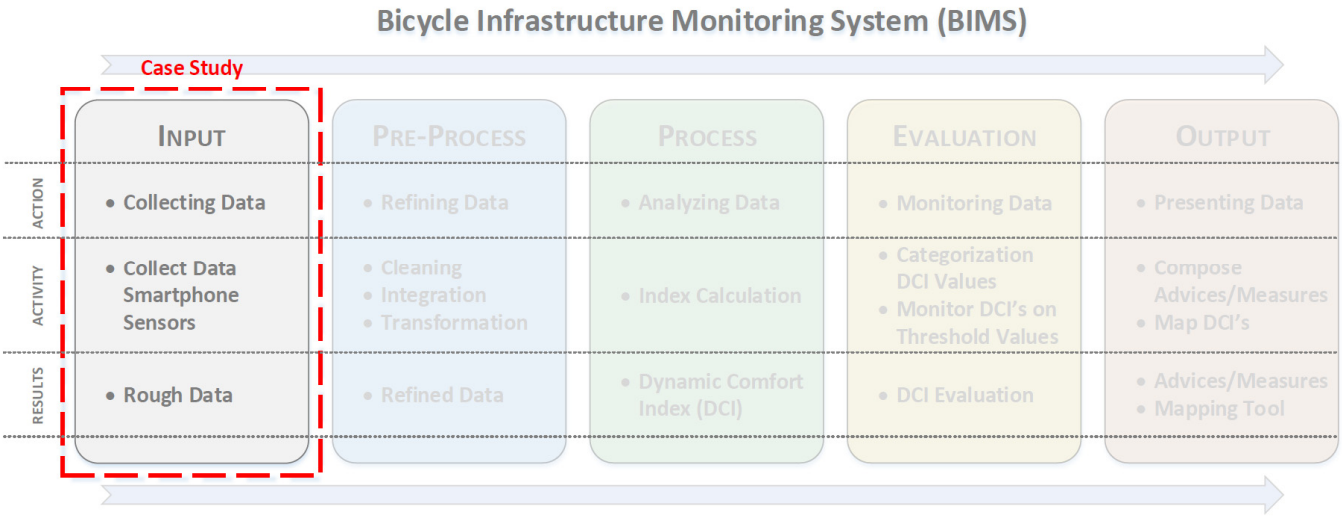

Figure 4.1: Case Study in context with BIMS process flow diagram

4.2 GENERAL ASPECTS DATA COLLECTION

The data for this case study will be collected from three smartphones: Oneplus5, Google Nexus and HTC M9. Table 4.1 contains all the relevant specifications regarding the smartphones and their sensors. The information regarding the smartphone sensors is retrieved using the AndroSensor app, as discussed in section 3.6. It is expected that the OnePlus 5 sensors will be of better quality than the other smartphone sensors, since it is the newest smartphone and therefore used less intensively. Further, it is important to state that at the time of testing only the Google Nexus 6p had the new Android 8 Oreo as mobile operating systems. The OnePlus 5 and HTC M9 still both used the Android 7 as operating system.

Note that the GPS receiver is not included in the table, since no information regarding this sensor could be found. Current smartphones all contain very basic GPS receiver chips (Bauer, 2013). The performance of the GPS receiver logically depends on the chip, but also on which type of smartphone and its operating platform to a considerable extent (Korpilo et al., 2017). Other factors which do not directly affect the performance, but do affect the GPS position accuracy are environmental characteristics (terrain, built structure, tree canopy), (space) weather conditions, and if present the application deriving the GPS position (Bauer, 2013; Korpilo et al., 2017; Noury-Desvaux et al., 2011).

Furthermore, notice that the type of linear accelerometers is not mentioned for the smartphones. The linear accelerometer is a so-called software-based sensor, which means that they derive their data from one or more of the hardware-based sensors. As discussed in the previous section, the linear acceleration derives its data from the accelerometer, gyroscope and the magnetometer, which all are hardware-based sensors. Moreover, since it mainly derives its data from the accelerometer, it has the similar range and resolution as the accelerometer. The GPS receiver, on the other hand is both a hardware- and software-based sensor, since it determines location with its chip and assisting location technologies named Cell ID and Wi-Fi (Korpilo et al., 2017).

Table 4.1: Smartphone Sensor Characteristics

Device	**Oneplus5 (A5000)**	**Google Nexus 6p**	**HTC M9**
Release Date	**June 2017**	**September 2015**	**March 2015**
Operating System	**Android 7**	**Android 8**	**Android 7**
Accelerometer	**BMI160**	**BMI160**	**Accelerometer Sensor**
Vendor	BOSCH	Bosch	hTC Corp.
Range	39.22661 m/s^2	78.4532012939 m/s^2	39.2266 m/s^2
Accuracy/Resolution	0.0023956299 m/s^2	0.0023942017 m/s^2	0.01 m/s^2
Linear Accelerometer	Linear Accelerometer	Linear Acceleration	Linear Acceleration
Vendor	QTI	Google	hTC Corp.
Range	39.22661 m/s^2	78.4532012939 m/s^2	39.2266 m/s^2
Accuracy/Resolution	0.0023956299 m/s^2	0.0023942017 m/s^2	0.01 m/s^2

4.2.1 AndroSensor-app settings

As described in section 3.6, the smartphone sensor data will be collected using the AndroSensor app, which can be downloaded for free in the Google Play store. First, it is important to state that all the recordings done with the AndroSensor app must be started and ended manually, since the app does not offer a feature where recording time can be configured. In addition, the data generated by the app also needs to be retrieved manually from the smartphone. This can be done wireless or by cable. For these test the data was first stored locally on the smartphones and then exported to Google Drive so it could be downloaded for analysis.

Next, the default settings of the app are adjusted in a way that for all the tests, the best and most precise results can be achieved. The most essential setting to ensure precise data quality is the sampling rate (or recording frequency), which is the regular interval at which the software 'asks' the mobile operating system for the particular sensor value and is defined as hertz (Hz). Thus, for example if the sampling rate is 10 Hz, the AndroSensor app will record 10 times a sensor data value in every second. The appropriate sampling rate mainly depends on the signal to be measured. If the sampling rate is too low, information could be lost and the signal will not be represented correctly. If the sampling rate is too high, the measured signal will most probably contain excessive noise (a random fluctuation in the signal) and will generate large data files, which will increase processing time of the data. Therefore, a sample rate of 20 Hz is preset for the recordings of all the tests, with the exception of 'Test 3 Controlled Acceleration'. For this test a higher sampling rate is required of 50 Hz since for this test the recording signals will be analyzed in detail. The sampling rate of 20 Hz for the other test is more than sufficient to ensure precise data quality.

Besides the sampling rate, for each test only data from the relevant sensors will be recorded. Thus, for example, for test 1 only data about the accelerometer will be recorded and for test 4 only data from the GPS receiver. This way no unnecessary data will be recorded and the data analysis process will be more efficient.

Finally, during all the recording the keep-screen-on function is enabled, which will ensure that the smartphone will not lock itself during the recordings. It is of outmost importance that the smartphone is kept 'awake' during the recording, since it is generally known that when a phone falls in 'sleep-mode', the smartphone shut downs parts of the system to save battery power, like sensors or apps running in background. This can be bypassed by alternating the software code, however for this situation an application is used from third parties and so the code cannot be alternated.

4.2.2 Reference device

To better indicate the quality of GPS sensor, a GPS Trip Recorder 747pro will be used as a reference device during 'Test 4' and 'Test 5'. The GPS Trip Recorder 747pro is an advanced GPS logger originating from 2007 and it only logs location data. It records data with a sampling rate of 1 Hz and the data needs to be retrieved manually. The data of the Trip Recorder will be used as a benchmark regarding the GPS data generated by the smartphone. In addition, the GPS Trip Recorders' POI (Point-of-Interest) feature will be used to indicate the exact start and end points for the recordings of test 4 and 5, since for these test the data of all three smartphones is recorded simultaneously, and starting and ending these recordings simultaneously is impossible. Some time will pass between the time the first and last smartphone recording is started or ended if done manually. During this time some biased data might be generated. Thus, to ensure that the data is recorded under the same circumstances and that they are equivalent, POI-feature of the Trip Recorder will be used. By simply pushing a button a POI will be recorded in the data of the Trip Recorder. Next, taken the advantage that all devices work on the basis of precise time measurement, the smartphone data will be filtered based on the POI's timestamps.

Furthermore, no reference device is used to compare the smartphones' accelerometer, since the characteristics of accelerometers installed in smartphones significantly differ from professional accelerometer sensors used in vibration analysis (Feldbusch et al., 2017). The

professional accelerometers are high precision sensors with a resolution up to 10^{-9} g, where smartphones' accelerometer have a resolution up to 10^{-3}. The smartphone sensors are limited in their accuracy since for their technology aspects as miniaturization, robustness, low energy consumption and low price also need to be taken into account.

4.3 TEST 1 - SENSITIVITY ACCELEROMETER

The first test will evaluate the sensitivity and tolerance levels of the smartphone in stationary position. According to Amick et al. (2013), sensitivity describes the gain of the sensor and tolerance levels define the sensitivity range over larger population of sensors. These measurements regarding the sensitivity of accelerometers are sometimes already conducted, however they are conducted by the sensors' manufacturer prior to the accelerometers being installed in smartphones or other mobile multimedia devices. That is why this test is set up to assess the sensitivity of the accelerometers when embedded in smartphones. Thus, this test will determine the sensitivity and tolerance levels of the smartphones listed in table 4.1.

4.3.1 METHOD

The sensitivity and tolerance levels can be determined by applying + 1 g acceleration (or 9.81 m/s^2) to it, noting the output values, rotating the device by 180 degrees so -1 g acceleration is applied to it, and noting the output value again. By subtracting the larger output value from the smaller one, and dividing the result by two, the actual sensitivity of the sensor is determined, and the sensitivity tolerances levels are described as the range of the sensitivities within a smartphone (ST Microelectronics Technical Manual, 2008). The same method is applied in the study of Amick et al. (2013), as they also studied the sensitivity of the accelerometers within mobile consumer electronic devices, or Apple iPod Touch to be more specific.

4.3.2 DATA COLLECTION

The ± 1 g acceleration is applied on the sensor by simply placing the smartphone on a surface with the smartphone screen (z-axis) pointing towards the center of the earth (1 g) or pointing towards the ceiling (-1 g). In both situation a total g-force of 1 is measured due to the downward-pulling gravitational force and the resulting upward reactions force of equal strength (Vieyra et al., 2015). The acceleration values of both situations were recorded for a period of 30 seconds to determine the amount of variation in steady state recording. This protocol was repeated three times for each of the three smartphones.

4.3.3 DATA ANALYSIS

The sensitivity was determined by comparing the mean acceleration across a data recording in the +1 g z-axis position to the mean acceleration of the recording in the -1 g z-axis position. Note that when only noting the z-acceleration value, the surface on which the phone is placed must be exactly leveled, or else some gravitational forces will be absorbed by the x and y acceleration values. This test therefore uses the resultant acceleration value a_{xyz} of the three axes, which can be calculated using the same formula as for the resultant vector principle, as already discussed in section 3.3.3. Formula (2) for the resultant acceleration was applied to the data.

Next, the larger mean acceleration output was subtracted from the smaller mean output, and the result was divided by 2. Further, descriptive statistics, such as mean, standard deviation and coefficient of variation, were generated for the sensitivities within each smartphone. Finally, since the study of Amick et al. (2013) applied the same methodology as discussed in this test and they also researched tri-axial accelerometer's sensitivities, their results will be used as benchmark for this test. In the study of Amick et al. (2013), a mean sensitivity of 0.0165 was measured with a standard deviation of 0.0086 for the tested devices. The tested devices, however, were not smartphones but multiple Apple iPod Touches originating from 2012.

4.3.4 RESULTS

The resulting sensitivities as well as the descriptive statistics for each of the smartphones is presented in table 4.2. For more detailed results see table 8.2 of appendix III, as it indicates the mean observed acceleration values and resulting sensitivities of each trial.

The mean sensitivities, represented in column 'Sensitivity', are 0.151 with standard deviation of 0.0087 for the Oneplus 5, 0.0005 with a deviation of 0.0056 for the Google Nexus, and 0.0125 with a deviation of 0.0023 for the HTC M9. Overall the smartphones score better than the iPods tested in the study of Amick et al. (2013), as one would expect since these smartphone are most probably equipped with more advance technology than the iPods originating from 2012. Furthermore, it can be observed that all three smartphones are very consistent across the three trials given the extremely small standard deviation. All three devices have coefficients of variation smaller than 1%. Although it should be noted that the standard deviation is based on only 3 trials.

Table 4.2: Descriptive statistics of test 1 results

Smartphone	Trials	Sampling Frequency (Hz)	Sensitivity (g)	Std Deviation	Coefficient of Variation
OnePlus 5	3x	20	0.0151	0.0087	0.87%
Google Nexus	3x	20	0.0005	0.0056	0.55%
HTC M9	3x	20	0.0125	0.0022	0.23%

4.4 TEST 2 - FREEFALL MOTION

The second test will test if the accelerometer can detect a freefall motion, which is a type of dynamic acceleration. A freefall motion is an object that is falling under sole influence of gravity (1 g or 9.81 m/s^2) towards the surface of the earth (Khoo Chee Han et al., 2014). Thus, since there is no the resulting upward reaction force of equal strength as in the previous test, all the axes values of the accelerometer should converge to 0 during the freefall. Based on this condition, this test will evaluate how well a smartphone is capable of detecting when it is in freefall motion.

4.4.1 METHOD

A freefall motion can be detected by using the measurements of static acceleration and dynamic acceleration (Clifford, 2006). The change between these values can also be referred to as the dynamic sensitivity (Khoo Chee Han et al., 2014). During the static acceleration only gravity is acting (and a resulting counter force) and the resultant acceleration value should

therefore be equal to 1 g or 9.81 m/s^2, like the previous test. During the dynamic acceleration there is no counter force and the resultant acceleration value should therefore be equal to 0 g or 0 m/s^2. Note that the linear acceleration would be the other way around since it negate the effects of the earth's gravitational field, as discussed in section 3.4.

4.4.2 Data collection

For the actual test, the smartphones where placed against the ceiling of a room with the screen facing upward, and were then dropped towards the ground. This protocol was repeated 5 times for each device. Figure 4.2 provides an abstract representation of the test set-up. The recordings were each started shortly before the fall, and ended after it was dropped. It is of utmost importance that the smartphones fall under a linear motion, meaning that the orientation of the smartphones remains during the fall, otherwise, the acceleration forces due to rotation should be included. If this condition was violated, another trial was conducted.

4.4.3 Data analysis

The data for this test was processed only using MS Excel. The freefall motion is determined by comparing the static acceleration values with the dynamic acceleration values of all three axes. The static resultant acceleration values are derived from a data point right before the drop and the dynamic acceleration values from a data point during the drop. Figure 4.3 depicts how the static (a_1) and dynamic (a_2) acceleration values are obtained. The segment within the dotted line represents the freefall motion, where a_1 is the data point immediately prior to fall and a_2 is the data point after the drop. Note that a_2 should be derived from a data point close after the drop, since air resistance will influence the acceleration values in the later stages. As one may see from the figure, the acceleration value slightly increases after a_2 due to air resistance functioning as counterforce.

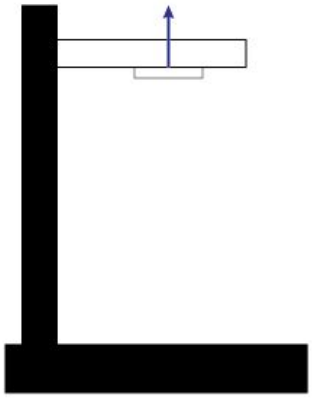

Figure 4.2: Test 2 set-up

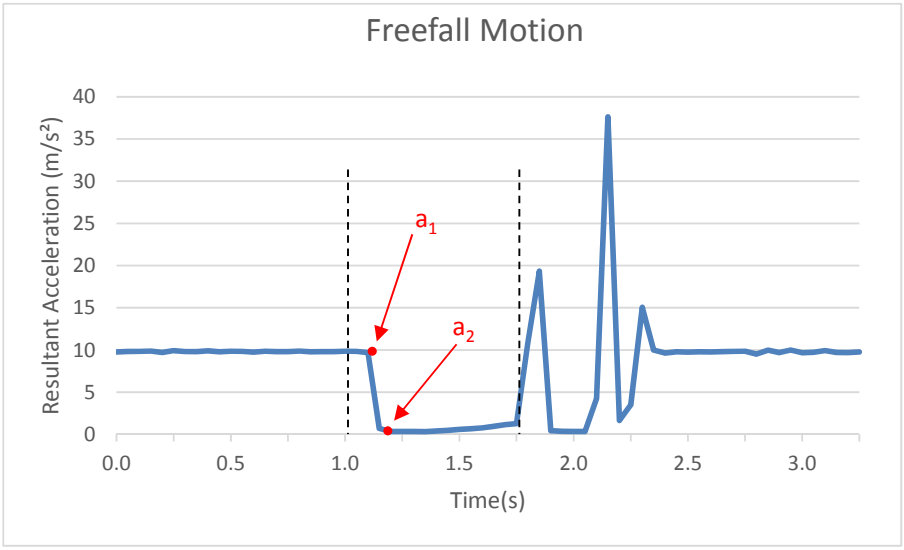

Figure 4.3: Representative Graph from Freefall Motion

After the values of a_1 and a_2 are obtained, the change in acceleration between these two data points is calculated along the x, y and z-axes. Next, the dynamic sensitivity in acceleration is calculated, which is the resultant acceleration value of the change in acceleration. The total formula for calculating the dynamic sensitivity is therefore as follow:

$$dynamic\ sensitivity = \frac{\left(\sqrt{(a_{1,x}-a_{2,x})^2+(a_{1,y}-a_{2,y})^2+(a_{1,z}-a_{2,z})^2}\right)}{9{,}80665} \quad (6)$$

Note that the total resultant acceleration is divided by the force of gravity, as the smartphone' accelerometers provide the data in m/s_2 instead of g. For the dynamic sensitivities of the 5 trials per smartphone, descriptive statistics, such as mean and standard deviation, are generated. Ideally, the dynamic sensitivity should be 1 g (or 9.81 m/s^2), as the values around a_1 should be 1 g and 0 g around a_2. The results will therefore be compared with this established standard of 1 g.

4.4.4 Results

Table 4.3 contains the resulting dynamic sensitivities as well as the descriptive statistics for the five trials of each smartphone combined. In table 8.3 of appendix III more detailed results can be found of each trial separately, including the axis acceleration values of the data points a_1 and a_2.

Table 4.3 shows that the mean dynamic sensitivities of the smartphone are very accurate to one thousandth of 1 g, and, in addition, are very consistent as evidenced by the very small standard deviations ranging from 0.0045 to 0.0064. Although again, it should be noted that these deviation are based on only 5 trials. Furthermore, it can be observed that there is no explicit difference between the three smartphones

Table 4.3: Descriptive statistics of test 2 results

Smartphone	Trials	Sampling frequency (Hz)	Mean dynamic sensitivity (g)	Std Deviation	Coefficient of Variation
OnePlus 5	5x	20	1.0054	0.0045	0.45%
Google Nexus	5x	20	0.9992	0.0064	0.64%
HTC M9	5x	20	0.9962	0.0045	0.46%

4.5 Test 3 - Controlled acceleration

Previous tests examined the smartphone accelerometers in both static and dynamic situations. This third test will examine how accurate the smartphone's linear accelerometers are at detecting the frequency and acceleration-force (or magnitude) of a controlled vibration signal, or a so-called vibratory excitation. The smartphones will be subjected to multiple vibrational signals with predefined magnitudes and frequencies. Based on the data generated by the linear accelerometer, the smartphones should be able to detect the same frequencies and magnitudes as the predefined values. This test will therefore evaluate how accurate the estimated values of the smartphone are compared to the predefined values. Thus, this test basically examines if the smartphone's output corresponds to the input.

4.5.1 Method

An electrodynamic shaker will be used to reproduce the multiple vibrational signals. These shakers are normally used for vibration testing, in the purpose of establishing reliabilities or testing to destruction (De Silva, 2007). This involves applying a controlled amount of vibration

to a test specimen and monitoring the resulting response. In this test, the shaker is only used to subject the smartphones to simple continuous vibration signals of a specific frequency and magnitude. These characteristics of the vibration signal are also referred to as the acceleration profile (De Silva, 2007), here as a test condition. In total, the smartphones were subjected to 10 distinctive test conditions, where each condition defines a vibration signal of a particular frequency and magnitude. The test conditions are listed in table 4.4. The shaker will reproduce the vibration signals in the form of a simple continuous sine wave with the characteristics of one of the test conditions. Thus, the shaker will subject the smartphones to five sine waves with a frequency of 5 Hz with a starting magnitude of 0,2 g raging up to 1 g, and five sine waves with the same magnitudes but then with a frequency of 10 Hz.

Table 4.4: Test Conditions for vibration signal

Condition	Acceleration profile (g-force/Hz)	Condition	Acceleration profile (g-force/Hz)
A-05	0.2g / 5 Hz	A-10	0.2g / 10 Hz
B-05	0.4g / 5 Hz	B-10	0.4g / 10 Hz
C-05	0.6g / 5 Hz	C-10	0.6g / 10 Hz
D-05	0.8g / 5 Hz	D-10	0.8g / 10 Hz
E-05	1.0g / 5 Hz	E-10	1.0g / 10 Hz

4.5.2 DATA COLLECTION

The execution of this experiment occurred at the environmental test laboratory of Thales Cryogenics in Eindhoven, as they are in possession of an ETS MPA406-M232A electrodynamic shaker. For the test set-up, the smartphones were securely attached on the shaker table using fixtures. The smartphones were all mounted with their screens pointing towards the ceiling, since the recordings had to be manually started and ended. Along with the smartphones, an accelerometer was mounted to measure and feedback the input (or control) acceleration a. The data from this accelerometer will be used to define the exact values of the acceleration profiles of each test conditions with an accuracy of 4 decimals. These profiles will be compared to the acceleration profiles detected by the smartphone. The test set up for the electrodynamic shaker is depicted in figures 4.4 and 4.5.

For the recordings, the sampling frequency of the AndroSensor app was increased to 50 Hz, since the data for this test needs to be analyzed in more detail. Furthermore, for each test condition three samples per smartphone were recorded for a period of 30 seconds. Thus, in total 90 data samples were recorded, 30 samples per smartphone. Finally, this test will record the linear acceleration instead of the acceleration, since the force of gravity is automatically excluded from the data. This data structure is much more convenient for the analysis of the signal's magnitudes. In addition, since the smartphone are mounted perpendicular to the excitation movement as depicted in figure 4.5, only the sensor data of smartphones' z-axis needs to be taken into account. The other axes can therefore be neglected.

Figure 4.4: ETS MPA406-M232A Electrodynamic shaker at environmental test laboratory of Thales Cryogenics

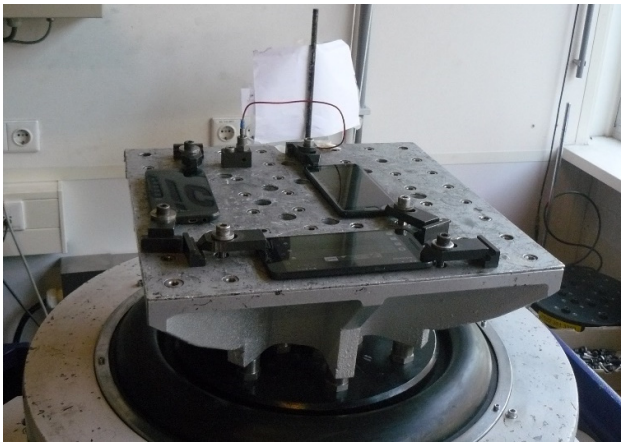

Figure 4.5: Test set-up where all three smartphone are mounted on the shaker table

4.5.3 DATA ANALYSIS

The techniques for analyzing a vibration signal can broadly classified in two groups, in the frequency and time domain (Hanly, 2016). For this test both techniques will be used to analyze the captured signals. The frequency domain will be used to analyze the dominant frequencies of the captured signals, and the time domain to analyze the magnitudes of the signals. After the data is analyzed in both the frequency and time domain, an acceleration profile is defined for each data sample, containing the frequency and magnitude detected by the smartphones. Subsequently, descriptive statistics will be generated for these estimated acceleration profiles. Additionally, the errors of the estimated values will be indicated, which represent the deviation of the estimated values (output) with the true values produced by the shaker (input). The next sections will describe the analysis in the frequency and time domain in more detail.

Frequency domain

By default, the data generated by the smartphone sensors is represented in time domain, since the data consist as a series of data points indexed in time order. For the analysis in the frequency domain, the data first needs to be converted from the time domain to the frequency domain. A fast Fourier transformation (FFT) is therefore applied to the sensor data. FFT is an algorithm for the fast calculation of the discrete Fourier transformation (DFT), which basically decomposes a signal into its frequency components (Hanly, 2016). For this test, the FFT is only applied to the recorded linear acceleration data of the z-axis, since the phones were mounted perpendicular to the excitation direction.

The result after converting the time series data of the captured signal into the frequency domain, is a frequency spectrum from 0 Hz to the half of the selected sampling rate, also known as the Nyquist frequency. The Nyquist frequency is the highest frequency that a captured signal can unambiguously represent, and is thus equal to half the sampling frequency of a particular signal (Hanly, 2016). Note that when a sampling rate of 20 Hz was used like in the other tests, the Nyquist frequency of 10 Hz would have provided some complications. The resulted frequency spectrum represents the distribution of the vibration amplitudes as a function of frequency (Telgarsky, 2013), and enables to perform analysis in

the frequency domain to gain a deeper understanding of the vibration profile. Figures 4.6 to 4.8 provide three frequency spectrums generated from the sensor data of the smartphones. The left figure represents the frequency spectrum of the HTC M9 subjected to test condition C-10, the middle of the Google nexus subjected to test condition E-05, and the right of the OnePlus 5 subjected to test condition A-05. Note that each spectrum is generated out of one data sample, thus in total 90 frequency spectrums were generated.

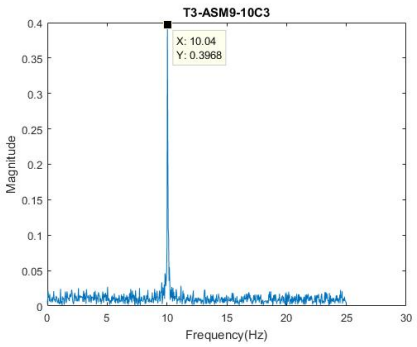

Figure 4.6: Frequency Spectrum from HTC M9 subjected to C-10 (3rd sample)

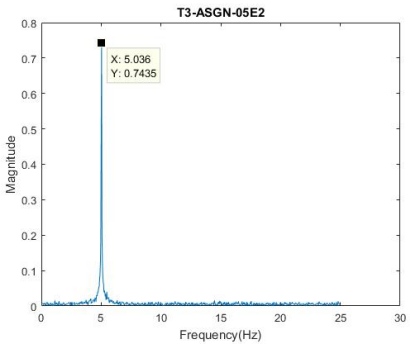

Figure 4.7: Frequency Spectrum from Google Nexus subjected to E-05 (2nd sample)

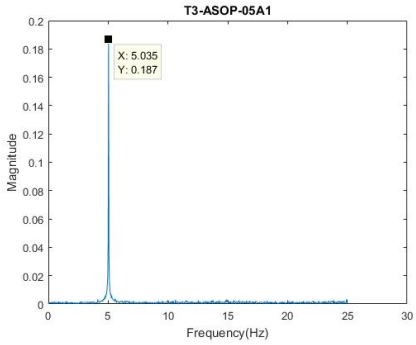

Figure 4.8: Frequency Spectrum from OnePlus 5 subjected to A-05 (1st sample)

For the analysis in this test, the frequency spectrum is used to extract the dominant frequency out of the captured signals, which is the frequency that carries the maximum energy among all frequencies found in the spectrum (Telgarsky, 2013). It will rather be easy to identify these dominant frequency, since the smartphones for this test were only subjected to vibration signals characterized by a single frequency (5 Hz or 10 Hz). As one can see from the figures 4.6 to 4.8, The spectrums will mainly contain the single frequency at which the samples were subjected to and some noise. The conversion to the frequency spectrum and the extraction of the dominant frequency were done using MATLAB. The base of the developed script can be found in appendix IV. This script with small modifications (code data sample, file-name, etc.) was applied to each data sample.

Time domain

Normally, the frequency spectrum is also used to determine the magnitude or acceleration force of each frequency component of a captured signal. For the analysis in this test, an alternative approach is applied to determine the magnitude of the captured signal, since the magnitudes derived from the frequency spectrums will not be representative. These magnitude values will be lower than the actual magnitude reproduced by the shaker, due to a phenomenon called 'aliasing'. Aliasing refers to the distortion that results when the signal reconstructed from samples is different from the original continuous signal (Hanly, 2016). This phenomenon is caused by a too low sampling rate for the recordings. The sampling frequency of 50 Hz is sufficient for identifying the dominant frequency (minimum of 2 times the signal's maximum frequency), however not for determining the magnitude. The phenomenon is best explained visually.

The shaker will produce an excitation or vibration with a particular acceleration-force back and forth, as can be seen in figure 4.9. The excitation is only for a very brief moment on this specified acceleration-force also known as the peak amplitude. The recording will therefore sometimes miss the exact peak amplitude and record a data point right after or before peak,

as can be seen in figure 4.10. This provides a biased representation of the magnitude in the frequency spectrum. To minimize this phenomenon, the recordings' sampling rate could be increased. However, if the sampling frequency is increased, the high quality of the data cannot be guaranteed, as discussed in section 4.2.1.

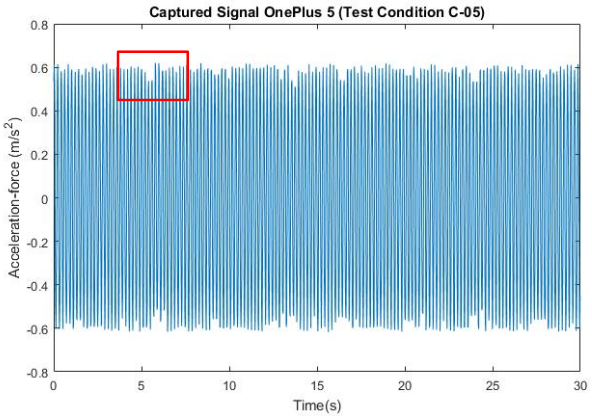

Figure 4.9:5 A sample from the OnePlus 5 of a signal with test condition C-05

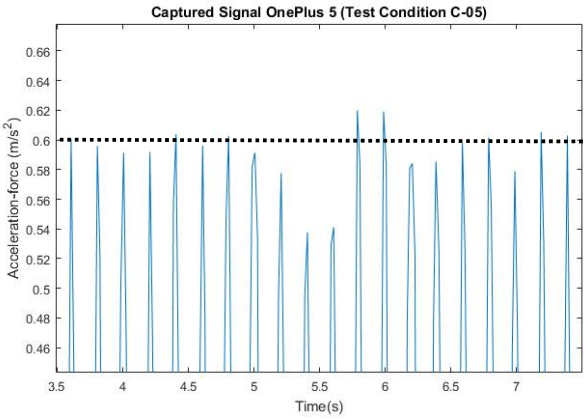

Figure 4.10:5 Magnified segment of the red square in figure 4.9

Therefore, for this test is chosen to use a more simple alternative approach. The approach will determine the signal's magnitude in the time domain instead of the frequency domain. The maximum and minimum amplitudes of the captured signal will be determined over 6 time periods of 5 seconds (recordings are 30 seconds) to identify the peak amplitude of the recorded signal. Next, the absolute mean values of these maxima and minima will be determined. Thus, for each recording a mean magnitude will be determined based on the maxima and minima from 6 consecutive time periods. This should be a good representation of the signal's acceleration force, as it is very unlikely that the recordings 'missed' all the peak amplitudes.

4.5.4 Results

In table 4.5 are the mean errors of the estimated frequencies and magnitudes of the 30 trials of each smartphone presented. The frequency and magnitude error of each trial separately can be found in tables 8.4 and 8.5 respectively of appendix III, including the test conditions and their corresponding input values of the dynamic shaker. The mean errors are represented as the corresponding unit (Hz or g) and as a percentage. Thus, for example, the OnePlus 5 estimated frequencies have a mean error of 0.0119 Hz or 0.17%, and for the estimated magnitude a mean error of 0.0118 g or 2.24%.

Table 4.5: Descriptive statistics test 3 Results

Smartphone	Trials	Sampling frequency (Hz)	Mean error of estimated frequency			Mean error estimated magnitude		
			Hz	%	Std. dev.	g	%	Std. dev.
OnePlus 5	30x	50	0.0119	0.17%	0.0037	0.0118	2.24%	0.0067
Google Nexus	30x	50	0.0127	0.18%	0.0047	0.0214	4.81%	0.0077
HTC M9	30x	50	0.0123	0.17%	0.0043	0.0354	5.45%	0.0169

As one can see from the table, all three smartphone are on average extremely accurate in detecting the frequency of a vibrational signal, as they all estimated the frequency with an mean error smaller than 0.2%. Moreover, when observing table 8.4 of appendix III, it can be acknowledged that all estimated frequency are equal or below an error 0.3%.

For detecting the magnitude, the smartphones appear to be less accurate than for detecting the frequencies, as the mean errors are larger ranging from 2.24% to 5.45%. Additionally, it can be observed that the OnePlus 5 is the most accurate of the three smartphone in estimating the magnitude of a vibration signal. This was already expected since the OnePlus is the newest phone, and is therefore most likely equipped with slightly more advanced sensors.

4.6 TEST 4 - GPS LOCATION ACCURACY

The previous three tests were intended to evaluate the motion sensors of the smartphones. This test, together with test 5, will evaluate the accuracy, reliability and consistency of the smartphones' GPS receivers. This test in particular will evaluate the GPS location accuracy. The GPS location accuracy is in this study referred to as in how accurate a position can be determined by the GPS receiver. Basically, a GPS position is determined by distance measurements from multiple satellites. Essentially, each satellite transmits a unique signal, and GPS receivers measure the distance by the amount of time it takes to receive this signal. With at least four of these independent satellite measurements, the receiver is able to determine a user's position, by using these distance measurements to create the geometries of spheres (Bauer, 2013; Korpilo et al., 2017). This process is also called trilateration and is visualized in figure 4.11.

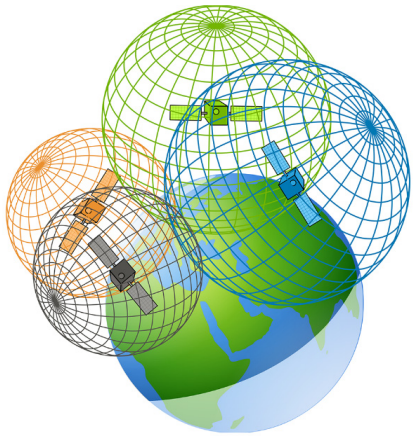

Figure 4.11: GPS trilateration principle

Nowadays, this position can be computed with an accuracy up to 5 to 10 meters, even with low-cost GPS receivers incorporated in todays' smartphones if the circumstances are favorable (Korpilo et al., 2017). This test evaluate if this accuracy can be complied with by the smartphones GPS Receivers by examining their GPS location accuracies of multiple segments with varying environments.

4.6.1 METHOD

The GPS location accuracy of GPS data is affected by a variety of factors. First, as one might expect, the quality of the GPS receiver can greatly affect the accuracy of the recordings (Hess et al., 2012; Ritchie, 2007). For example, the quality can determine the number of channels a GPS receiver can use to track satellites. The more channels it can use, the more accurate it can determine a GPS position. Secondly, the position of satellites at the time the data is recorded (Bauer, 2013; Ritchie, 2007). The more satellites in view, the greater the level of accuracy. The number of satellites naturally fluctuates, as the satellites circle the earth in a precise orbit. Thirdly, the characteristics of the environment in which the data is recorded (Bauer, 2013; Korpilo et al., 2017; Ritchie, 2007). GPS receivers require a direct line of sight to the satellite to determine its position. Objects can block, reflect or weaken the signal between the receiver and a satellite. This is particularly the case in urban environments within valleys and or mountain slopes, where buildings can, for instance, completely block the signal or reflect the

signal on its glass façade. Objects which are less substantial, such as tree covers or car roofs, can weaken the signal. Another factor which particularly affects the accuracy of GPS data generated by smartphones, is the type of smartphone and its operating system (Hess et al., 2012). It does not directly affect the GPS data, however it does affect the performance of the GPS Receiver, as already mentioned in section 4.2.

Taken these factors into account, the test is set up to evaluate the GPS location accuracy of smartphones. The accuracy will be simply determined by the AndroSensor app, as it automatically provides an location accuracy when recording location data. Additionally, the app also indicates the amount of satellites available for that particular phone and to how many it is connected. These aspects will also be incorporated in the evaluation as they influence the location accuracy and therefore could clarify inaccuracies.

However, before the values of the AndroSensor app are blindly adopted for the data analysis, it is important to validate how these values are derived. Unfortunately, the AndroSensor app does not explain these values, although it does indicate that it directly retrieves raw sensor data via the Android Sensor Framework using API's (Application Programming Interface), and that it makes no alternation to the rough data. After some research on the Android developers platform (2017a), it was found that Android defines the (horizontal) GPS accuracy as the radius of 68% confidence. In other words, if a circle is drawn around a derived GPS coordinate with a radius equal to the accuracy, then there is a 68% probability that the true location is inside the circle. Furthermore, the amount of satellites available is derived from the smartphone's satellite list, and the amount of connected satellites from the current state of the GPS engine (Android Developers, 2017a). With this knowledge, these location data characteristics can be properly used for the data analysis and evaluation.

4.6.2 Data collection

Three street segments were chosen on which the GPS location accuracy will be determined for each smartphone. The segments were carefully selected in the city-center of Eindhoven based on the characteristics of their surroundings, as they could affect the GPS data. Figures 4.12 to 4.15 depict the selected segments and their environments. Segment X is characterized by a urban environment with (semi-)high-rise buildings, segment Y by an urban environment with medium-rise buildings, and segment Z by an semi-urban environment with low-rise buildings and a park located next to it. It is expected that the best accuracies are acquired for segment Z, as there are almost no surroundings that can block, reflect or weaken the signal (see figure 4.15), followed by segment Y and segment X.

Each segment was cycled five times with all three smartphones and the GPS Trip Recorder (see section 4.2.2) rigged to the rider. This in order to simultaneously generate the GPS data samples, and thus to ensure that all the data is collected under the same circumstances. During all the recordings the weather circumstances were cloudy, which most probably affect the GPS accuracy badly, as the clouds weaken the signals of the GPS receivers.

Furthermore, as discussed in section 4.2.2, the POI-feature (Point-of-Interest) of the Trip Recorder was used to indicate the exact start and end point of each segment, since it is impossile to start or end all the recordings simultanously. Based on the timestamps of the POI, the rough data sets will be filtered.

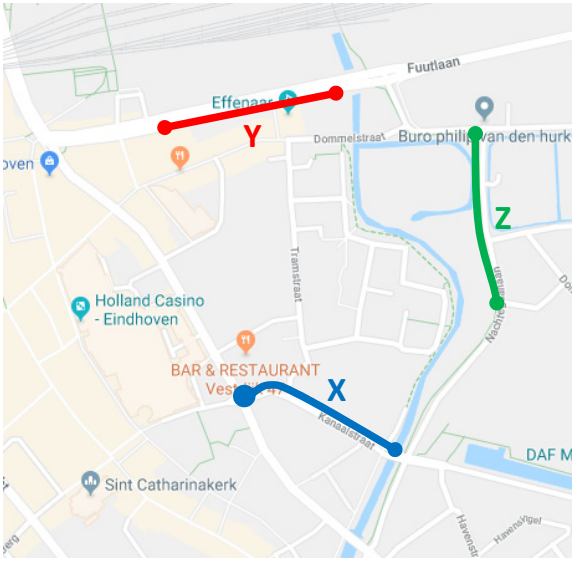

Figure 4.12: Route segments for test 4 - GPS location accuracy

Figure 4.13: Test 4 route segment X

Figure 4.14:6 Test 4 route segment Y

Figure 4.15: Test 4 route segment Z

4.6.3 DATA ANALYSIS

This test, in contrast to the others, does not require an extensive and complicated data analysis, as all the values are already automatically generated by the AndroSensor application. This analysis only requires 3 simple steps. First, the data retrieved from the smartphones needs to be filtered. The data will be filtered based on the POI's determined by the Trip Recorder. These POI's are characterized by timestamps, on which the data will be filtered. All the data outside the start-timestamp and the end-timestamp of a particular segment is seen as redundant and will be excluded.

Next, duplicates in the data samples will be eliminated. The AndroSensor collects the sensor data with a sampling rate of 20 Hz, which is 20 datapoints per second, as discussed in section 4.2.2. However, since GPS is slightly inaccurate on 5 to 10 meters, it cannot derive a new GPS position every 1/20 of a second. The data will therefore sometimes uses the same GPS position for multiple data points. Eliminating the duplicate GPS data points will considerably reduce the size of the data sets. Normally, the data will also contain vibration data and duplicates can therefore not be eliminated. For now the duplicates can be eliminated, since only the GPS data will be analyzed.

Finally, the mean GPS location accuracy, the mean amount of connected satellites, and the mean amount of available satellites will be determined for each data sample, providing 5 results for each smartphone and segment.

Ideally, the data from the smartphone would have been compared to the data of the GPS Trip Recorder. However, since the Trip Recorder's data sets do not automatically provide GPS accuracies of the estimated locations like the AndroSensor app, it is rather complicated to do so. Therefore, the smartphone data will be compared to the established standard of the GPS being accurate up to 10 meters. Although, the Trip Recorder's data will be used to compare the smartphone data visually by plotting both the smartphone and Trip Recorder data using Google Earth. This will provide a general impression of the smartphone GPS receivers accuracy in contrast to the Trip Recorders' accuracy.

4.6.4 Results

The location accuracies, amount of connected satellites and amount of available satellites are presented in table 4.6 of each segment based on the five trials of each phone, and in addition, the mean values over the three segments are indicated per smartphone. The values derived for each trial can be found in table 8.6 of appendix III. Additionally, the plots of all 5 trials per segment and per smartphone can be found in figures 8.1 to 8.3 of appendix III.

Out of table 4.6, it can be observed that none of the three smartphones accomplished to meet the established standard of an accuracy of 10 meters. Only the OnePlus 5 comes near this standard with an average accuracy of 12.37 meters. The general larger accuracies could be explained by the cloudy weather conditions when the data was recorded, as discussed in section 4.6.2.

Table 4.6: Test 4 results GPS location accuracies

Route Segment	OnePlus 5			Google Nexus			HTC M9		
	Accuracy (m)	Connected Satellites	Available Satellites	Accuracy (m)	Connected Satellites	Available Satellites	Accuracy (m)	Connected Satellites	Available Satellites
Segment X	13.18	14.59	32.21	22.31	7.94	24.76	15.04	9.46	21.42
Segment Y	12.28	13.93	31.99	15.91	7.81	24.78	18.75	8.21	21.56
Segment Z	11.66	16.93	32.08	12.42	8.72	24.59	13.81	9.03	21.18
Total	**12.37**	**15.15**	**32.09**	**16.88**	**8.16**	**24.71**	**15.86**	**8.90**	**21.39**

Furthermore, as was discussed in section 4.6.1, it can indeed be noticed that the GPS receiver quality affects the GPS accuracy, since the newest GPS receiver of the OnePlus 5 can connect and find significantly more satellites, which results in the OnePlus 5 to acquire better GPS accuracies than the Google Nexus and HTC M9, as can be observed in table 4.6.

Another factor which was discussed to affect the GPS accuracy were the environmental characteristics. It was therefore expected that the best accuracies would have been found at segment Z, followed by segment Y and X. This assumption can be confirmed, as the best accuracies are observed at segment Z, followed by segment Y and X, only for the HTC M9 a better accuracy is observed for segment Y over X. The justification of the assumption can also

be observed in the plots of each smartphone for each segment depicted in figures 8.1 to 8.3 of appendix III, as for all smartphone the spread of the GPS data points over segment Z is much less than for the other two segments.

When comparing the plots of the Trip Recorder with those of the smartphones depicted in figures 8.1 to 8.3 of appendix III, it can be observed that in general the Trip Recorder is much more consistent in determining the location. It follows a more fluent line in contrast to the smartphone that even sometimes strongly deviate from the cycled path, especially in the more dense areas of segments X and Y. This could be explained by the fact the devices such as the Trip Recorder often have built-in software which pre-process the data to aid in determining the positioning (Bauer, 2013; Korpilo et al., 2017). The data from the smartphones, on the other hand, is not pre-processed, as the AndroSensor app retrieves raw data from the GPS Receiver.

4.7 TEST 5 - GPS DISTANCE ACCURACY

Previous test evaluated the GPS location accuracy of the GPS receivers incorporated in smartphones. This test will focus on another component of the GPS receiver, namely the GPS distance accuracy. For this research, the GPS distance accuracy refers to how accurate the distance travelled can be estimated based on GPS data. It is generally known that distances recorded with a GPS are slightly inaccurate from the true distances travelled by a moving object. This inaccuracy is also referred to as the GPS measurement error in literature (Ranacher et al., 2016). This measurement error depends on the GPS receiver's quality to a considerable extent (Bauer, 2013; Korpilo et al., 2017; Ranacher et al., 2016). This is especially the case with today's smartphones, since they are incorporated with very basic receivers (Korpilo et al., 2017). Therefore, this test aims at examining the GPS distance accuracy of the GPS receivers incorporated in smartphones.

4.7.1 METHOD

For GPS devices, estimating the travelled distance is simply done by "connecting the dots" between GPS coordinates and calculating the distance between them. This distance is calculated using the 'Haversine' formula, which determines the great-circle distance (the shortest path over the earth's surface) between two points on a sphere from their longitudes and latitudes (Cesario et al., 2017). This formula forms the basis for all distance calculation of navigation devices. Normally, this is automatically incorporated in GPS software. However, for this test the distance between two consecutive GPS coordinates will have to be calculated manually based on this formula, since the AndroSensor app only provides raw data. An additional advantage of manually calculating this distance is that the data will not be pre-processed or manipulated by GPS software to adjust the travelled distances, which is often the case nowadays (Bauer, 2013; Korpilo et al., 2017).

Accordingly to the Haversine formula, the distance d willl be calculated with the following formulas:

$$\Delta\sigma = \arccos(\sin\phi_1 * \sin\phi_2 + \cos\phi_1 * \cos\phi_2 * \cos(\Delta\lambda)) \quad (7)$$

$$d = r * \Delta\sigma \quad (8)$$

Were ϕ_1, λ_1 and ϕ_2, λ_2 are the geographical lattitude and longitude coordinates in radians of two consecutive points, $\Delta\lambda$ their absolute difference, $\Delta\sigma$ is the central angel between the two points, and r is the sphere radius or in our case Earth's radius. Figure 4.16 provides an illustration of the central angle $\Delta\sigma$ between two points, P and Q. This test will compare the estimated distance based formulas (7) and (8) and GPS data generated with the smartphone with the exact distance of a particular route. The error between the estimated and the exact distance will be used to define the GPS distance accuracy of the GPS receivers.

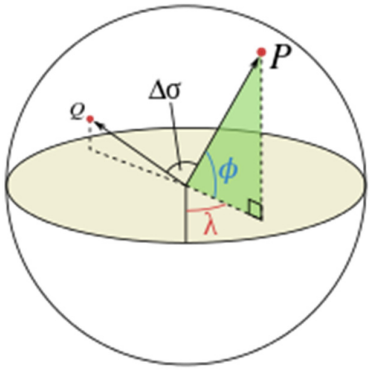

Figure 4.16: Illustration of computing central angle Δσ

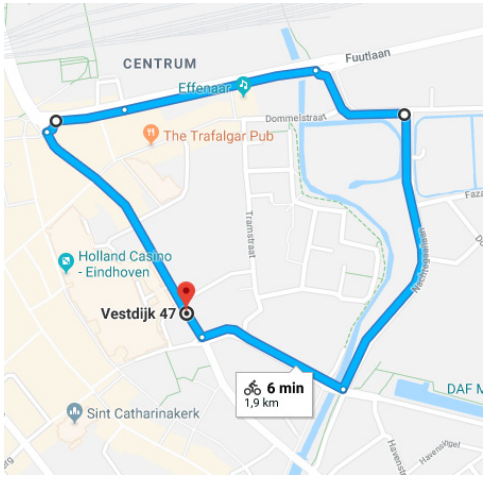

Figure 4.77: Test 5 - Cycling route in Eindhoven

4.7.2 DATA COLLECTION

A route through the city-center of Eindhoven was selected on which the GPS distance accuracies of the GPS receivers will be determined. The route is depicted in figure 4.17. The start and end of the route are at the same point (red point). Note that all the segments of test 4 are included in this route, and therefore the data generated by cycling this route is also used for test 4.

Just like in the previous test, the route was cycled 5 times with all three smartphones rigged to the rider in order to simultaneously generate the GPS data samples under the same conditions. Thus, in total 15 data samples were recorded for the cycled route. For each data sample, the route distance will be calculated. Next, these derived distances will be compared to the exact distance of the cycled route.

The exact distance of this route was determined with a wheel-based cyclocomputer mounted to the bicycle. These devices are capable of measuring the distance to a high level of precision, since the computer derives the travelled distance by simply counting the amount of wheel-revolutions and multiplying it with the wheel's perimeter. The computer will solely be used to determine the exact distance of the cycled route and to demonstrate the GPS distance accuracies of the GPS receivers.

Furthermore, the GPS Trip recorder, introduced in section 4.2.2 will be used as a benchmark to which the performance and quality of the smartphones' GPS receivers will be compared. The recordings for the Trip Recorder were generated simultaneously with the smartphone recordings. This test used, just like for the recordings in test 4, the POI feature of the Trip Recorder to indicate the exact start and end point of the route based on timestamps.

4.7.3 DATA ANALYSIS

For this test, the GPS data of the smartphones as well as the GPS Trip Recorder are analyzed to determine their GPS distance accuracies. These accuracies are represented as the error between estimated distance (based on GPS data) and the exact distance of the cycled route. As already mentioned, the actual distance will be derived using a cyclocomputer. After each time the route is cycled, the distance can simply be read of the device. Estimating the distance based on GPS data, on the other hand, is a more complicated process. MS excel will be mainly used for this process and is conducted in 2 main steps. This process will be applied to each GPS data sample generated by the smartphones and the Trip Recorder.

First, the redundant data of each data sample needs to be eliminated. This concerns excluding the data not relevant to the cycled route and eliminating duplicates in the GPS data. The first is achieved by filtertering the data between the start and end point defined by the POI's of the Trip Recorder. Next, duplicates in the data samples will be eliminated, since only GPS data will be analyzed, just like in the previous test.

Secondly, after the redundant GPS data is removed, formulas (7) and (8) will be implemented in MS Excel in order to calculate the distances between the GPS data points. Subsequently, these distances will be added up, providing the estimated route distance based on GPS data. Finally, the GPS distance accuracies are determined based on the error of the estimated route distance and the true distance.

For the estimated distances, descriptive statistics such as mean and standard deviation will be generated. Addionally, the GPS data will be plotted in order to support the estimated distances. If very deviating distances are found, they could be explained by the visual representations.

4.7.4 RESULTS

In table 4.7 are the results presented of this test. The table contains for each device the mean estimated distance and standard deviations of the five GPS data samples, and the GPS distance accuracies represented as the error over the exact route distance derived from the cyclocomputer. For the cyclocomputer no standard deviation is given, as for all five trials a distance of 1.88 km was measured by the cyclocomputer. This illustrates the high level of precision of the cyclocomputer. The estimated distances of each trial separately with the corresponding distance accuracy can be found in table 8.7 of appendix III. Additionally, the plots of the five trials per device can also be found in figures 8.4 to 8.7 of appendix III.

Table 4.7: Test 5 results of GPS distance accuracies

Device	Trials	Mean distance (km)	Error	Std Deviation	Coefficient of Variation
Cyclocomputer	5x	1.88	-	-	-
Trip Recorder	5x	1.82	3.42%	0.0123	0.68%
OnePlus 5	5x	1.89	2.90%	0.0674	3.56%
Google Nexus	5x	2.00	6.35%	0.1157	5.79%
HTC M9	5x	1.88	1.23%	0.0345	1.84%

Overall it can be observed that all three smartphone overestimate the travelled distance, where the Trip Recorder underestimates the distance. These over- and underestimation can be explained by looking at the GPS data plots of the devices in figures 8.4 to 8.7 of appendix III. It can be seen that the Trip Recorder sometimes cuts of a curve, especially at the upper left corner of figure 8.4. The smartphone, on the other hand, sometimes deviate from the cycled path, resulting in an overestimation of the cycled distance.

When further observing the GPS data plots it can be noticed that especially the Google Nexus sometimes strongly deviates from the travelled path. This can also be observed in table 8.7 of appendix III, as one trial has an distance accuracy of 16.89%. This explains the relatively high mean distance accuracy of 6.35% of the Google Nexus, as it levels the rest of the accuracies. If this trial is excluded, an distance accuracy of 3.72% is achieved. Thus, overall it can be concluded that the distance accuracies of the smartphones are more than acceptable, especially when comparing it to the Trip Recorder.

4.8 Discussion & conclusion

This case study aimed at testing the current sensor technology embedded in smartphones in order to evaluate if smartphones can serve as a reliable data collection tool for BIMS, as the system intends to rely on data to be collected from cyclists' smartphones. In addition, since a lot of literature acknowledges the increasing capabilities of using the smartphone as an advanced measuring tool (Allmendinger et al., 2017; Azzoug & Kaewunruen, 2017; Johnston & Robinson, 2015; Novakova & Pavlis, 2017), but literature supporting this statement with testing of the actual capabilities lags behind.

Based on five tests, the case study examined the accuracy, sensitivity and consistency of the smartphones' sensors. Three tests investigated the smartphones' accelerometer and two tests the smartphones' GPS receiver. In total three smartphones of different brands and ages were tested in order to provide a general impression of the overall smartphone sensor quality. These were the OnePlus5, Google Nexus 6p and HTC M9.

Test 1 and 2 analyzed the smartphones' accelerometer to quantify the stationary and dynamic sensitivities of the acceleration outputs respectively. For the first test, the outputs of the devices demonstrated mean sensitivities ranging from 0.0005g to 0.0125g. Moreover, the sensitivity values were found to be highly consistent across the multiple trials of each smartphone, as evidenced by the low standard deviations and coefficients of variability. These values were evaluated to be very acceptable as all three smartphone performed better than devices test in the study of Amick et al. (2013), which was used as a benchmark. As for the second test, the acceleration outputs indicated mean dynamic sensitivities ranging from 0.9962 to 1.0054, where in an ideal situation a dynamic sensitivity of 1g was obtained. Also here, high consistencies over the derived sensitivities are observed across de trials of each phone, given the small standard deviations and coefficient of variability.

The third test focused its analysis on the linear accelerometer to evaluate the accuracy of the acceleration outputs. All three smartphones appeared to be extremely accurate in detecting the frequency of vibrations signals to which they were subjected to, as on average an accuracy of less than 0.2% was observed for estimating the frequencies. The accuracies for estimating the vibrations signals' magnitudes were slightly less as for both the HTC M9 and Google Nexus

an accuracy of approximately 5% was observed and 2.24% for the OnePlus 5. Higher accuracies could have been acquired for detecting the magnitudes if the maxima and minima used for the analysis were determined over more time periods. The current magnitude accuracies, however, are still acceptable.

Test 4 and 5 examined the smartphones' GPS Receivers to assess the location and distance accuracy of their GPS data respectively. For test 4, the GPS data was observed to have a location accuracy up to 12-17 meters, where the highest accuracies were acquired for the OnePlus 5, as expected, since the OnePlus 5 being the newest phone and therefore being able to find and connect to more satellites. Overall higher accuracies could have been acquired if the weather conditions during the recordings would have been favorable, as the cloudy conditions during the execution of the tests could weaken the GPS signals. Furthermore, the less dense route segments were characterized with better accuracies. As for test 5, the GPS data was used to determine the distance of a cycled route and it was observed that overall the smartphones overestimated the cycled distance by 2-3%, which is more than acceptable as a benchmark GPS device underestimated the distance by 3%.

Thus, overall out of the five tests it can be concluded that all three smartphones are capable of serving as an advanced measuring tool with a high level of precision. It can therefore be stated that in general the overall smartphone sensor quality should be suitable for collecting vibration and GPS data for the BIMS systems. However, it should be noted that all three devices worked with an Android operating systems, the statements above can therefore not be ensured for devices running on other operating systems such as iOS. Although, it is expected that similar qualities will be observed, as the studies of Amick et al. (2013) and Khoo Chee Han et al. (2014) discussed in test 1 and 2 respectively used iPod Touches which operated on iOS and similar results were observed.

5 FIELD EXPERIMENT

This chapter will present a field experiment which will test BIMS assessment method of dynamic comfort mapping discussed in section 3.3 to multiple segments. In addition, the aspects mentioned in section 3.3.3, which are expected to influence the assessment method, will be analyzed in order to examine how these aspects should be handled. This section will first give a short introduction of what this experiment entails, followed by its objectives. Next, how the data is collected for the experiment, and which methods are used for the analysis. Finally, the results of this experiment will be presented and an ending discussion regarding these results.

5.1 INTRODUCTION

Previous chapter discussed a case study examining if the current smartphone sensor quality is at all sufficient for collecting vibration and location data regarding the bicycle environment, and if the sensor quality is proportional between multiple devices. The results indicated that the current sensor technology embedded in smartphones should be sufficient for the intended use of assessing the bicycle pavement surface conditions.

This chapter presents a successive study in the form of a field experiment, which will put the smartphones into practice. It will examine if the assessment component of BIMS can rely on a smartphone-based vibration measurements to assess the pavement surface quality of a bicycle segment. As discussed in section 3.3, it will therefore use the dynamic comfort mapping method introduced by Bíl et al. (2015).

In addition, even though that the performance of dynamic comfort mapping method already has been justified in their study on a road network with varying types of pavement surfaces, it has to be re-examined on several aspects as one crucial condition in this study differs from their methodology. Namely that the data on bicycle vibrations is in fact collected via smartphones located in a cyclists' trousers, instead of an accelerometer mounted to the front fork of the bicycle. This entails that some additional aspects need to be taken into account towards the computation of the DCI. This experiment will examine these aspects in order to indicate how these should be handled regarding the method of dynamic comfort mapping for BIMS. The next sections will only briefly indicate the essence of each aspect as they are elaborately discussed in section 3.3.2 and 3.3.3, and in addition, how they are handled or will be examined in this study.

The first most important aspect is the adaptation of the original DCI formula used in the method of dynamic comfort mapping to objectively represent the measured bicycle vibrations. Normally, only the readings of the axis perpendicular to the road surface were included. However, since the orientation of the smartphone inside the trousers' pocket differs constantly per cyclist or even per trip, the readings of all three axes must be included to negate the position of the smartphone. Hence, an adaptation to the formula was necessary, which can be found in formula (3) of section 3.3.2 and is referred to as DCI_{sum}.

Secondly, the effect of cyclist's weight to the measured vibrations. The DCI is normally calculated out of data collected from an accelerometer mounted to the front fork of a bicycle. For BIMS, on the other hand, the DCI is calculated out of data collected form smartphones

located in cyclists' pockets. It is therefore likely that cyclist's weight will have a direct influence on the measured vibrations. This experiment will collect data from multiple test riders in order to give an indication how cyclist's weight influences the measurement, but also to illustrate how the DCI assessment method performs with data from multiple cyclists.

Thirdly, the effect of the bicycles used by cyclists. Originally, the vibrations were measured near the front fork, where the surface vibrations can be detected first and therefore bicycle characteristics could not significantly affect the measurement. However, this study measures the vibrations with a smartphone located in cyclists' trousers, which is near the saddle. It is therefore reasonable to assume that the bicycle frame will affect how the vibrations are transmitted and thus that the bicycle characteristics have an influence on the measurement. This aspect however is not examined in this field experiment, due to the limited time frame of this research and the assumption that these characteristics can be neglected if the data collection community is large enough.

Fourthly, the adaptation of calculating the DCI over distance intervals instead of time intervals. Normally, the DCI is calculated for every second of a recording, and is then linked to a location. This approach, however, is inconvenient for BIMS, as the data will be collected from multiple cyclists. Therefore, for BIMS, it is suggested to calculate the DCI over fixed distance-intervals. This approach will ensure that the index values are calculated consistently among cyclists, as the vibration data can be allocated to a specific interval based on the GPS data. In addition, it will be easier to refer to a specific section and its corresponding index value. Nevertheless, this experiment will examine multiple scales on which the DCI will be calculated to eventually select the most suitable scale-configuration for BIMS.

Fifth and last aspect concerns impact of cyclists' pedal movement on the vibration data, as the smartphone-based vibration measurement is conducted from cyclists' trousers while cycling. A variant towards the original formula was therefore suggested, which incorporated the difference in acceleration values of two consecutive points of each axis. This will reduce the acceleration-effect of the pedal movement, since it is a relatively slow acceleration. It will function as a sort of natural 'filter', filtering the pedal movement. Furthermore, a possible additional advantage of this variant is that it could represent local extremes more clearly, since if two consecutive points are located on the local maxima and minima than the data will represent the peak-to-peak value instead of two (smaller) peak values. The mathematical notation of the variant can be found in formulas (4) and (5) of section 3.3.3 and is referred to as DCI_{diff}. In This experiment will examine if the DCI_{diff} performs better than the DCI_{sum}.

5.2 Objectives

The main objective of this field experiment is to serve as a Proof-Of-Concept (POC) for the assessment component of BIMS. More specific, the experiment aims at demonstrating the feasibility of the using smartphone sensors for assessing the pavement surface condition of the bicycle environment. When put in context of the process flow diagram, the experiment mainly concerns topics regarding the main 'Process' of BIMS and some aspects regarding the 'Input', 'Pre-Process', as depicted in figure 5.1.

Furthermore, it will evaluate if the dynamic comfort mapping method introduced by Bíl et al. (2015) for computing the vibration data to a surface quality index is suitable to be adopted by BIMS. It will therefore examine if using this method, segments of different qualities, or of

different pavement types can be distinguished. Moreover, a first look will be provided towards the feasibility of using data from multiple cyclists by inspecting the similarities between these data sets. There will also be evaluated what the most suitable distance-interval configuration is for the DCI method, and if the proposed variant (DCI_{dif}) on the DCI method performs better than the DCI_{sum} approach.

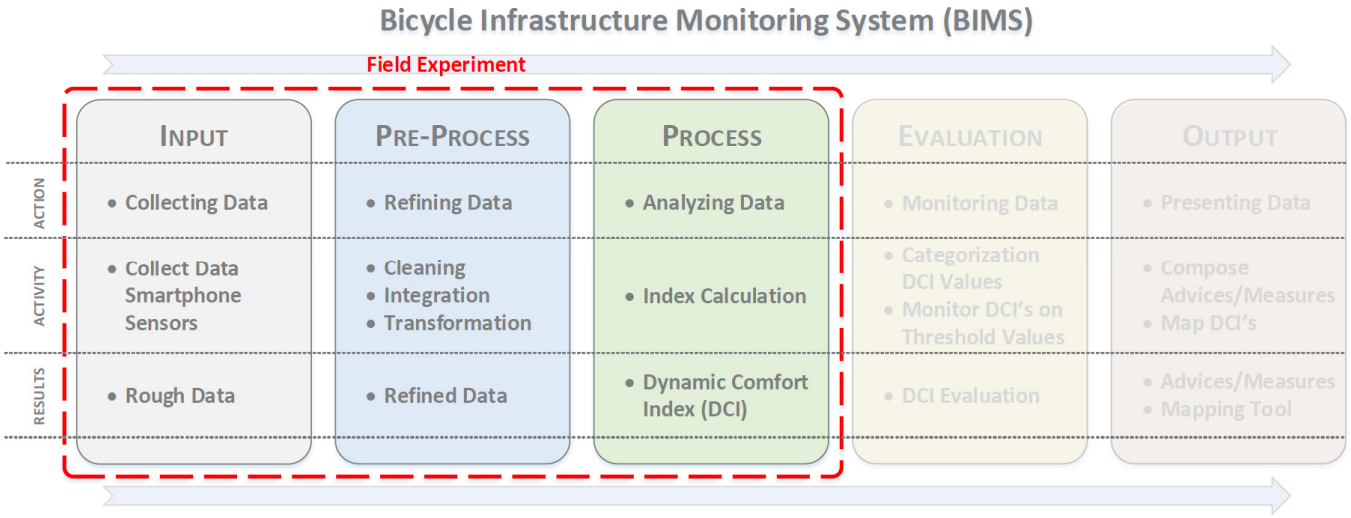

Figure 5.1: Field Experiment in context with BIMS process flow diagram

5.3 DATA COLLECTION

The field experiment applied the method of dynamic comfort mapping methodology inspired by Bíl et al. (2015) to four road segments in the city center of Eindhoven. The segments consisted of 2 asphalt segments of 200 meters and 2 cobblestone segments of 150 meters, where for both pavement types one is in good condition and one in bad condition. Figure 5.2 illustrates the locations of the segments in Eindhoven. Segment A and B are the asphalt segments, where segment A is in bad condition as it is worn and clearly shows signs of deterioration, and segment B in good condition as it has a smooth paved surface with no cracks or any other form of irregularities. Segment C and D are the cobblestone segments, where segment C is in bad condition as it has multiple places of sagging and on some places it even misses cobblestones, and segment D is in good condition as it retiled at the end of the summer of 2017. Appendix V depicts photos of the pavement surfaces of segments A to D in order to support the above assertions made about the conditions of the four segments.

In line with the characterization of pavement issues of Champoux et al. (2007) discussed in section 2.3.3 of the literature study, segments A can be characterized as a coarse road since it will transmit continuous random excitations to the bike due to a rough but uniform surface structure. Segment B is not characterized as it does not contain any form of pavement issues. Segment C can be characterized as both a cracked and coarse road, since it will also provide a series of successive impacts due to potholes and missing cobblestones. Segment D can also be characterized as a coarse road. Even though in principle it does not contain any pavement issues, the cobblestone surface will transmit continuous random excitations to the cyclist.

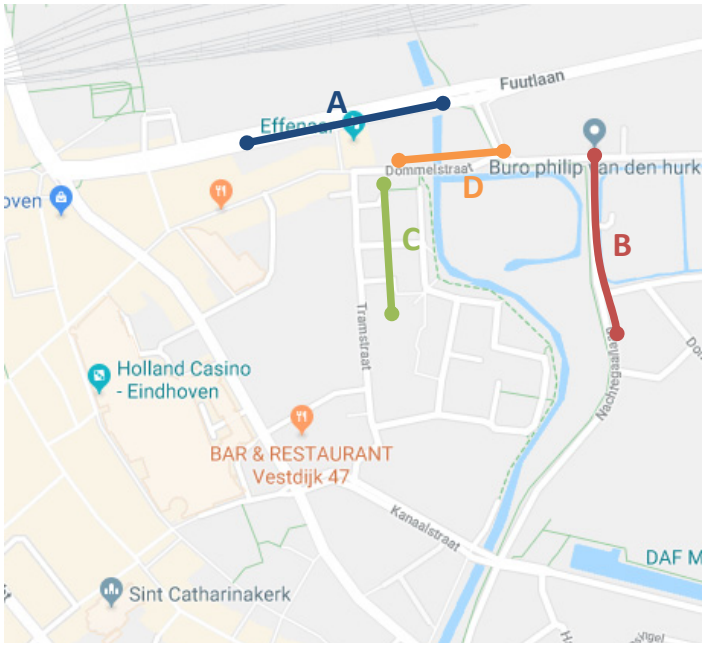

Figure 5.2: Location bicycle segments for data collection field experiment

Since BIMS relies on data to be collected from multiple cyclists, the segments were cycled by three test riders with varying weights for collecting the vibration data relevant for the assessment method. The weights of the test riders are listed in table 5.1. Based on the varying weights of the test riders, the field experiment aims to provide a first look of how the assessment method performs with data combined from multiple cyclists. In addition, this experiment will provide a general sense of how cyclist's weight affects the assessment outcome, since it is expected that their weights will affect the entity of the measured vibrations.

In order to properly analyze the data from the three test riders, is it important that the data is recorded consistently. The test riders therefore all rode the segments with the same bicycle maintaining a constant speed of 15 km/h. The 'OV-fiets' rental bicycle offered by the NS (Dutch Railway Agency) is used, as it represents an ordinary touring bike (figure 5.2). Each test rider cycled each segment three times with this bicycle, generating a total of 36 vibration data sets.

Table 5.1: Characteristics of test riders

# Rider	Weight (kg)
Test Rider 1	80
Test Rider 2	85
Test Rider 3	70

Figure 5.3: 'OV-fiets' rental bike of NS

This vibration data was measured by the OnePlus5 smartphone using the AndroSensor app with the same sampling frequency of 20 Hz as in the case study. This frequency should be sufficient as a higher frequency will lead to more excessive noise in the data and will require a lot of battery power, and lower frequencies for detailed information to get lost. As an indication, the smartphone will record a data point for approximately every 21 centimeters of road segment when cycling at a speed of 15 km/h (= 4.17 m/s) and a frequency of 20 Hz. Given that a data point is recorded every 21 centimeters, it seems that the chance of missing a crack is rather large. The vibration measurement however records the excitation experienced from both the front and rear wheel of the bicycle, as the measurement is executed from cyclists' trousers. If the recording misses the vibration caused by the crack with the front wheel, the rear wheel will most likely record this vibrations. Thus, the chance of missing a crack is considerably low.

In the study of Bíl et al. (2015) the same speed and sampling frequency was used enabling the results of this experiment to be compared to their results. Finally to ensure data consistency, the OnePlus5 was located in the left pocket of the test rider's trouser for each recording. An example of a recording is depicted in figure 5.4. Note that in this figure the resultant acceleration values are presented and not the DCI_{sum} values.

Furthermore, just like in test 4 and 5 of the case study, the GPS Trip recorder POI feature was used to indicate the exact start point of each recording, as the test riders had to build-up speed and the recordings were manually started preliminary to this event. A POI was created on the start point of each segment. The end points of the segments were determined based on the distance travelled indicated by the data.

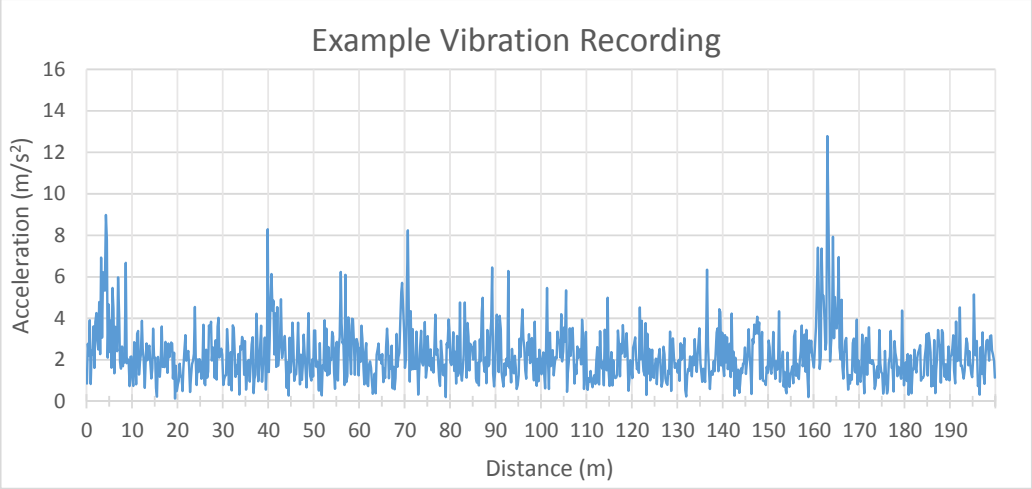

Figure 5.4: Example of a vibration recording segmented by distance. The data represents the resultant acceleration of the three axes of the smartphone

5.4 DATA PROCESSING

Since in the previous chapter the GPS accuracy of smartphones already is examined, this field experiment solely focus on analyzing the assessment of the pavement surface conditions of the segments depicted in figure 5.2 with the smartphone-based vibration data. Before the data can be analyzed, it first need to be processed to meaningful information, which in this case is the DCI_{sum} values. This section indicates how the vibration data collected in section 5.2 is processed for further analysis.

5.4.1 CALCULATION DCI_{SUM}

For the assessment of the segments depicted in figure 5.2, the DCI_{sum} (Dynamic Comfort Index) will be used to objectively represent the recorded bicycle vibrations with an index value, which is indirectly related to these vibrations. As discussed in section 3.3.2, this index value is similar to the index used in the methodology of Bíl et al. (2015), with the exception that this index formula includes the readings of all three axis to negate the orientation of the smartphone. Moreover, instead of calculating the index value over time-intervals, it will be calculated over distance-intervals, as it will be easier to combine the data from multiple cyclist. Since this experiment yet will evaluate the most optimal scale for the distance-interval, the DCI_{sum} is calculated for every 5 meters of data recording as a basis. This value corresponds most closely to the scale used in the DCI calculation of Bíl et al. (2015), as they calculated the index for every second at a cycling speed of 15 km/h, which is similar to approximately an DCI for every 4.17 meters. The exact computation of the DCI index can be found in formula (3) of section 3.3.2. The calculation of the DCI was conducted using MATLAB. The base of the developed MATLAB script can be found in appendix V.

5.4.2 COMBINING DATA SETS

For each data set corresponding to a particular road segment and test rider, the DCI_{sum}'s were calculated. Given that the base scale for the index is 5 meters, the data sets for the 200-meters-long asphalt and 150-meters-long cobblestone segments consisted of 40 and 30 index values respectively. Moreover, each index value is linked to a specific distance-interval. Next, the three data sets for each test rider for a specific segment are merged by averaging the index values of each distance-interval using MS Excel. This results in one set of average index values per test rider for each segment.

Note that for the calculation of the variant DCI_{diff}'s values the same procedure is followed with the only difference that in the formula of the index value the difference in acceleration values of adjacent data points is included. The MATLAB script for the DCI_{diff}'s calculation can be found in appendix VI.

5.5 DATA ANALYSIS & RESULTS

After the data is processed, it can be analyzed on the aspects mentioned in section 5.1. For each aspect there will be indicated how the data is analyzed and what the results are of this analysis. However, before the data sets are used for the analysis, an correlation analysis will be conducted in order to measure the strength of association between the data sets of the three test riders.

5.5.1 CORRELATION BETWEEN DATA SETS TEST RIDERS

A correlation analysis will be conducted in order to verify the assumption that for BIMS the data of multiple cyclist can be combined. The correlation coefficient derived from this analysis will indicate the extent to which the data sets of two test riders tend to change together. The correlation can range in value from -1 to +1 describing both the strength and direction of the relationship (Niven & Deutsch, 2012). Ideally, the data sets will have a correlation coefficient of +1 as it indicates that when an index value of one test rider increases over a specific section the values of the other test riders also increases by a consistent amount.

The two most widely used correlation statistic are the Pearson correlation and Spearman correlation. The Pearson correlation measures the degree of linear relationship between related variables, and the Spearman correlation the monotonic relationship (Bobko, 2001). Normally, the selection correlation statistics is assessed via scatter plots (Bobko, 2001). A matrix is depicted in figure 5.5 with the scatterplots of the total data sets from one test rider to another test rider. Note that for the scatterplots the data sets for each test rider distinctive to the four road segments are appended, resulting in one master data set for each test rider containing all the derived index values. Out of the scatterplots it seems that the relationships of the test riders' DCI values are linear and therefore the Pearson relationship should be used. The Pearson correlation however is based on the assumption that the data should be normally distributed, which appears not to be the case after a quick normality test.

Therefore, since it is not clear which of the two correlation statistics should be used, both will be measured to get a general sense of how the strength of association between the data sets. The correlation are measured over the master data sets containing the total 140 index values per test rider or so-called observations in statistics, and in addition, also for the data sets of each segment separately. The results of both the Pearson and Spearman correlation over the master data sets are listed in table 5.2 and table 5.3 respectively. The correlations coefficient for the segment data sets can be found in appendix VII.

From both the Pearson and Spearman correlation coefficient the data tends to strongly correlate, as correlation coefficients larger than 0.75 (or smaller than -0.75) indicates that the data strongly correlates (Bobko, 2001). Since both correlation statistics measure coefficients larger than 0.75 for all relationships with a significance of 0.01, there can be concluded that indeed the data among the test riders do correlate strongly, as expected.

However, when observing the correlation coefficient of the separate segment data sets listed in appendix VII, the data does not always seems to correlate. Note that this is solely the case for the data sets of segment B & D, which are the segments in good condition. Although these low correlation coefficients can be explained due to the low amount of variability in de data sets of segment B & D, often termed 'range restriction' or 'truncated range' (Goodwin & Leech, 2006). It is natural that on good surface less data spread is examined, since the data sets will contain no or less extreme values on which the correlation coefficient benefits.

This phenomenon can easily be identified by measuring the spread or range of the data sets. In table 5.4 the ranges for the data sets of each segment is presented. As one can see the average ranges of both segment B & D are lower than for the segments A & C respectively of the same pavement surface type. Note that the range of segment D does not much differ from segment C, however this is mainly caused by test rider 2 with the large range of 0.350.

Nevertheless, the assumption that data from multiple cyclist can be combined can be justified based on the derived correlation over the master data sets. Moreover, it can therefore be justified to combine the data sets of the test riders in further analysis.

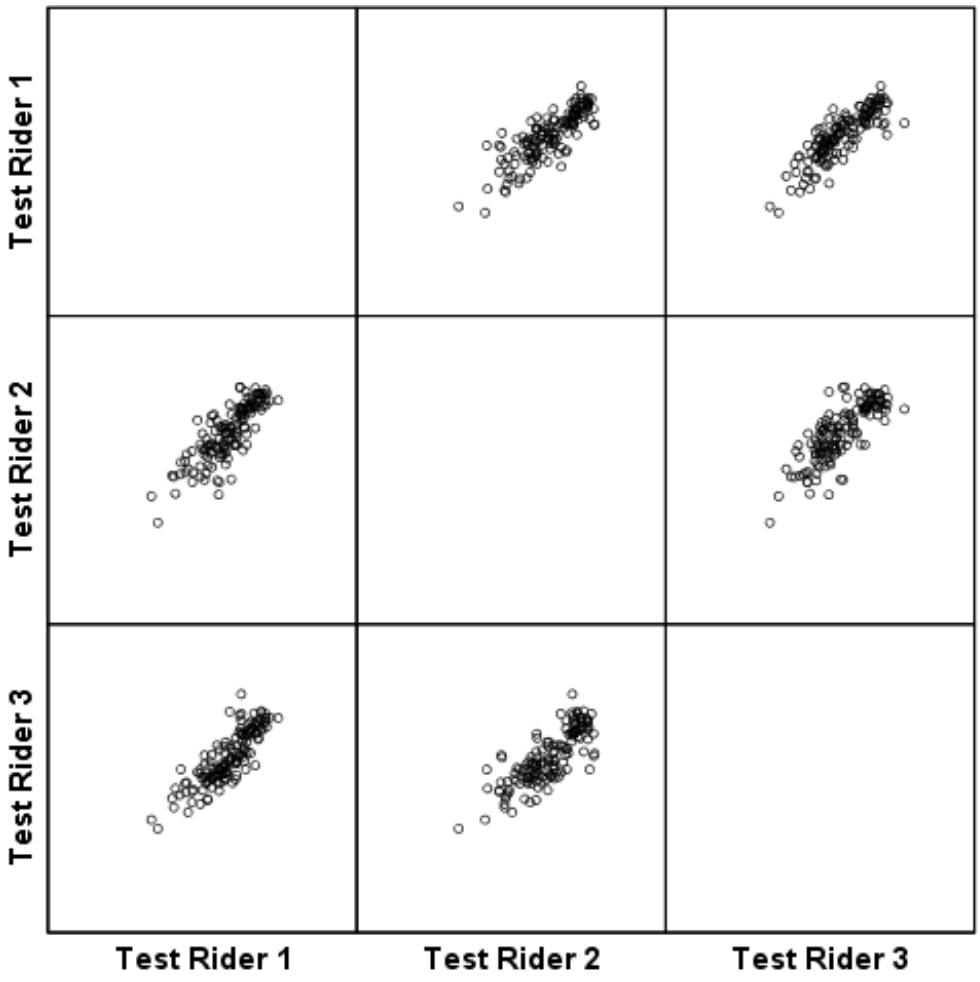

Figure 5.5: Scatterplot Matrix of the master data sets of the three test riders

Table 5.2: Pearson Correlation Coefficients of DCI_{sum} values between test riders

		Test Rider 1	Test Rider 2	Test Rider 3
Test Rider 1	Pearson Correlation	1	,827**	,848**
	Sig. (2-tailed)		,000	,000
	N	140	140	140
Test Rider 2	Pearson Correlation	,827**	1	,801**
	Sig. (2-tailed)	,000		,000
	N	140	140	140
Test Rider 3	Pearson Correlation	,848**	,801**	1
	Sig. (2-tailed)	,000	,000	
	N	140	140	140

**. Correlation is significant at the 0.01 level (2-tailed).

Table 5.3: Spearman correlation coefficient of DCI_{sum} values between test riders

		Test Rider 1	Test Rider 2	Test Rider 3
Test Rider 1	Spearman Correlation	1,000	,832**	,851**
	Sig. (2-tailed)		,000	,000
	N	140	140	140
Test Rider 2	Spearman Correlation	,832**	1,000	,801**
	Sig. (2-tailed)	,000		,000
	N	140	140	140
Test Rider 3	Spearman Correlation	,851**	,801**	1,000
	Sig. (2-tailed)	,000	,000	
	N	140	140	140

**. Correlation is significant at the 0.01 level (2-tailed).

Table 5.4: Range statistics of segment data sets

Segment		N	Range	Minimum	Maximum
Segment A	Test Rider 1	40	,336	,185	,521
	Test Rider 2	40	,339	,265	,604
	Test Rider 3	40	,281	,216	,497
	Average	**40**	**,319**	-	-
Segment B	Test Rider 1	40	,215	,381	,596
	Test Rider 2	40	,090	,526	,616
	Test Rider 3	40	,197	,426	,623
	Average	**40**	**,167**	-	-
Segment C	Test Rider 1	30	,250	,205	,455
	Test Rider 2	30	,287	,180	,467
	Test Rider 3	30	,217	,187	,404
	Average	**30**	**,251**	-	-
Segment D	Test Rider 1	30	,162	,334	,497
	Test Rider 2	30	,350	,270	,620
	Test Rider 3	30	,206	,353	,560
	Average	**30**	**,239**	-	-

5.5.2 DCI_{SUM} PERFORMANCE BASED ON VIBRATION DATA OBTAINED FROM SMARTPHONES

This experiment calculated the DCI_{sum} values of four segments based on the method of dynamic comfort mapping, as described in section 5.3. In order to properly evaluate the overall performance of the DCI_{sum}, it will be compared to the DCI methodology used in de study of Bíl et al. (2015), as both indexes still represent the basic principle of objectively representing the recorded bicycle vibrations. Ideally, the performance of the DCI_{sum} based on smartphone data would have been compared to the same values derived with the methodology of Bíl et al. (2015), namely with data retrieved from an accelerometer fixed to the bicycle's front fork. However, due to the lack of an professional accelerometer, this could not be accomplished and therefore the DCI_{sum} values will be compared to the DCI values derived in their study for segments of the city of Olomouc located in Czech Republic. Even though the bicycle infrastructure of the Czech Republic is not comparable to the Dutch cycling infrastructure, comparing the DCI values of this experiment with their study will provide a general sense of how well the method of dynamic comfort mapping performs with data collected from smartphones.

Figure 5.6 depicts a table from the study of Bíl et al. (2015) with the DCI values derived from 11 distinctive segments. The four road segments depicted in figure 5.2 will be compared to the segments with the most corresponding description described in the 'Surface Type' column of the table. Therefore, based on the conditions depicted in appendix V, the DCI_{sum} calculated for segment A will be compared to DCI value with 'Section ID' 4, segment B with number 11, and segment D with number 2 as they represent the index value of worn asphalt, 'normal' asphalt and new cobblestones respectively. For segment C there is no explicit comparative segment. Although, section ID's 7 has the most comparable surface type and is therefore used to compare the DCI_{sum} values derived for segment C. The comparative sections are also indicated in figure 5.6.

For the analysis, the data sets containing the combined DCI_{sum} values for each test rider of a particular segment will be merged to one, resulting in the data sets to represent the average derived index values for a specific segment. Next, the data sets will be compared by generating the same descriptive statistics as depicted in figure 5.6: minimum value, mean value, median value, maximum value and standard deviation. The descriptive statistics of segments A, B, C and D are presented in table 5.5.

Section ID	Length (m)	Surface type	DCI values					
			Minimum value	Mean value	Median value	Maximum value	Standard deviation	
1	208	Old small granite cobblestones	0.2454	0.3861	0.3753	0.5941	0.0809	
2	371	New cobblestones	0.4604	0.6922	0.7037	0.9206	0.0892	Segment D
3	333	Old large granite cobblestones	0.2015	0.3258	0.3203	0.4994	0.0655	
4	133	Worn asphalt	0.6057	0.7332	0.7441	0.8442	0.0634	Segment A
5	466	Uneven asphalt	0.3868	0.7945	0.8172	0.9026	0.0911	
6	212	Interlocking concrete pavement	0.5289	0.7108	0.7127	0.8119	0.0645	
7	185	Uneven interlocking concrete pavement	0.3172	0.6043	0.6152	0.7880	0.0869	Segment C
8	85	Unpaved path	0.4496	0.6452	0.6800	0.8131	0.0989	
9	170	Old large granite cobblestones	0.2083	0.3125	0.3016	0.4261	0.0611	
10	448	Old small granite cobblestones	0.2854	0.4631	0.4536	0.6677	0.0818	
11	626	Asphalt	0.6928	0.8132	0.8192	0.9100	0.0544	Segment B

Figure 5.6: Derived DCI values from study of Bíl et al. (2015)

It can be directly observed that in general the DCI_{sum} values are 0.2 to 0.3 lower than the DCI values derived in the study of Bíl et al. (2015), indicating that more severe vibrations are recorded from the cyclists' pocket than from the front fork of the bicycle. Typically, one would expect less vibrations as some vibrations are absorbed by the cyclists. This would however results in higher index values, as the index represent the inverse value of the measured accelerations. One possible explanation for this could be that the pedal movement of the cyclist has a more severe effect on the vibration-measurement than expected, as the pedal movement is a constant movement and the index values are consistently lower given the similar standard deviation.

However, the lower DCI values can rather be explained by the fact that in general more intense vibrations are recorded near the saddle than near the front fork of the bicycle, as the in the literature discussed study of Lépine et al. (2015) revealed. Near the saddle, the vibrations of both the front and rear wheel are measured, where in contrast to near the front fork, mainly the vibrations of the front wheel are measured. Another possible contributing factor is that including the acceleration values of all three axes, instead of only the axis perpendicular to the pavement surface, results in more vibrations to be recorded, since a crack most likely causes not only vertical bicycle vibrations but also horizontal vibrations.

Table 5.5: Descriptive statistics of DCI_{sum} values

Section	**Length (m)**	**Surface type**	**DCI values**				
			Minimum value	Mean value	Median value	Maximum value	Standard deviation
Segment A	200	Worn asphalt	0.2220	0.4039	0.4089	0.5161	0.0639
Segment B	200	Smooth asphalt	0.4445	0.5353	0.5353	0.5746	0.0245
Segment C	150	Uneven cobble stones	0.1908	0.3629	0.3763	0.4304	0.0520
Segment D	150	New (retiled) cobblestones	0.3506	0.4473	0.4482	0.5153	0.0419

Nonetheless, if solely is focused on table 5.5, there can be seen that the bad segments can be clearly distinguished from the good segments, as segment A is lower than segment B and segment C lower than segment D. Moreover, the asphalt segments can be distinguished from the cobblestone segments, when looking at the good and bad segments separately. Finally, interesting to note that segment A of worn asphalt on average scores lower than segment D of new cobblestones.

5.5.3 DCI_{SUM} SENSITIVITY TO CYCLIST'S WEIGHT

For BIMS the DCI is calculated with data collected from smartphones located in cyclist's trousers. It is therefore likely that the cyclist's weight will have a direct influence on the measured vibrations, as elaborately discussed in section 3.3.3. In section 5.3, the DCI_{sum}'s of the four segments were calculated with smartphone-based vibration data collected from three test riders. Since it is expected that cyclist's weight tends to affect the vibration data, this section will analyze the extent to which the DCI_{sum} values are sensitive to the weights of the test riders.

For the analysis, the test riders' data sets containing the index values will be analyzed by comparing the mean index values and standard deviation separately and combined for the segments. Moreover, it will also be analyzed visually by generating grouped boxplots of the index values for each segment and test rider separately. The boxplot is depicted in figure 5.7 and the average index values in table 5.6. Note that the columns indicated with 'N' represent the amount of index values for that particular segment, as for each 5 meters a DCI_{sum} is calculated. Thus, as discussed in section 5.4, the data sets of each test rider per segment contains 40 or 30 index values.

As can be seen in both the table and the boxplot, the raking from highest to lowest mean index values for the test rider is almost consistent over each segment. Test rider 2 always has the highest index values, followed by test rider 1 and test rider 3. Only over segment B the ranking is slightly different as test rider 1 has the lowest mean. Notice that when looking at table 5.1 of section 5.2, the same raking can be observed over the weights of the test riders, where test rider 2 is the heaviest and test rider 3 the lightest. Moreover, notice that all standard deviation are approximately equal for all test riders per segment. It therefore appears that weight indirectly affects the measured vibrations with a constant factor, as when the weight increases the measured vibrations decreases.

Furthermore, what is more noticeable in the boxplot than in the table is that for the cobblestone segments the spread between the mean index values of the test riders is much lower than for the asphalt segments. For the asphalt segments A and B the range is 0.0894 (=0.3604-0.4498) and 0.0536 (=0.5147-0.5683) respectively. For cobblestone segments the index values range is 0.0296 (=0.3479-0.3775) for segment C and 0.0381 (=0.4310-0.4691) for segment D. This could be explained by the fact that over cobblestone segments cyclists experience more consistent vibrations than over other pavement types, resulting in weight to play a lesser role.

Table 5.6: Summary index values per test rider for each segment

	Segment A			Segment B			Segment C			Segment D		
	N	Mean	Std. Dev.	N	Mean	Std. Dev.	N	Mean	Std. Dev.	N	Mean	Std. Dev.
Test Rider 1	40	0.4015	0.0737	40	0.5147	0.0395	30	0.3635	0.0611	30	0.4418	0.0423
Test Rider 2	40	0.4498	0.0712	40	0.5683	0.0234	30	0.3775	0.0600	30	0.4691	0.0783
Test Rider 3	40	0.3604	0.0618	40	0.5231	0.0332	30	0.3479	0.0490	30	0.4310	0.0435
Total	**120**	**0.4039**	**0.0777**	**120**	**0.5353**	**0.0401**	**90**	**0.3629**	**0.0576**	**90**	**0.4473**	**0.0588**

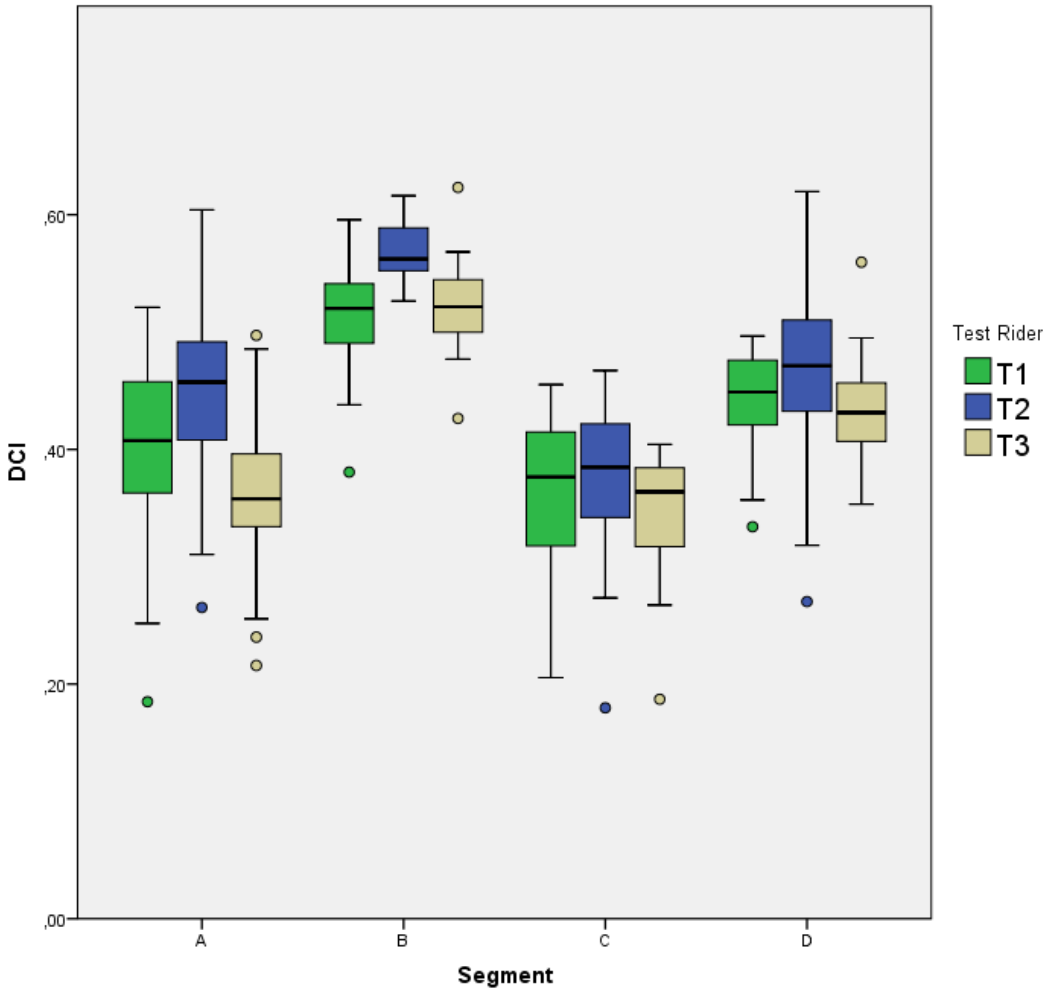

Figure 5.7: Boxplot of mean index values of the test riders clustered per segment

5.5.4 DCI_{SUM} DISTANCE-INTERVAL CONFIGURATION

In both section 3.3.3 and 5.1, the aspect involving the computation of the DCI over distance intervals was discussed. Normally, in de study of Bíl et al. (2015), the DCI was calculated for every second of a recording, and is then linked to a location. This approach, however, is inconvenient for BIMS, as the data will be collected from multiple cyclists. Therefore, for BIMS the data is linked to fixed distance sections. This approach will ensure that the DCI's are calculated more consistently among cyclists. In addition, it will be easier to refer to a specific

section and its corresponding DCI. As a basis the DCI_{sum} was calculated for every 5 meters of bicycle segment. In this section, multiple scales will be analyzed to propose the most suitable scale for BIMS.

Besides the 5-meter scale, the DCI_{sum}'s is calculated over distance-intervals of 10, 25 and 50 meters. For the calculation, the same procedure is followed as in section 5.4.1. The segments and the different distance-intervals are plotted in figure 5.8 to 5.11. Each figure plots a segment against distance with the corresponding DCI_{sum} values over different interval scales. Ideally, the base scale of 5 meters is used for BIMS, as it will identify more detailed information about the pavement surface. This will ensure that surface defects are more easily observed by extreme index values, as can be seen with segment A in figure 5.8 around 160 meters.

The GPS inaccuracy smartphones however makes this scale less optimal as BIMS relies on data to be collected from cyclists' smartphones. In the case study it was observed that these GPS receivers can be inaccurate up to approximately 15 meters. This inaccuracy can cause the DCI_{sum} to be calculated with data which originally corresponds to a different section. With small GPS inaccuracies this will not be a major issue, as it only causes some overlap of data included for the index calculation. However, inaccuracies of 15 meters can have greater impacts on the derived DCI values. The interval scales of 5 and 10 meters are therefore not optimal for BIMS. Note that the GPS inaccuracy is not an issue in this field experiment as the data was processed based on timestamps instead of GPS positioning.

Out of the two remaining options, it is proposed to select the 25-meter scale to divide the route segments, as the 50-meter scale can cause outliers to be leveled off by the rest of the data. This can be clearly observed in figure 5.8 of segments A, as around 20 and 160 meters the index value is leveled off when the scale is increased. On the other hand, outliers can also cause data to be leveled off in such way that the whole segment is indicated as bad. This can be observed in figure 5.10 of segments C around 40 meters. This however is more preferred since the section's index will indicate that there is a problem. Thus, the most optimal seems to calculate the DCI_{sum} over sections of 25 meters, considering the discussed aspects.

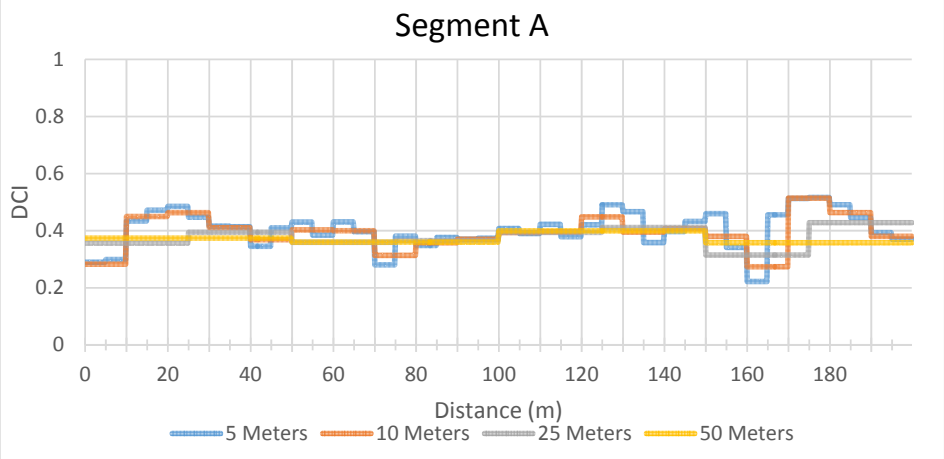

Figure 5.8: Segment A index values over different interval scales

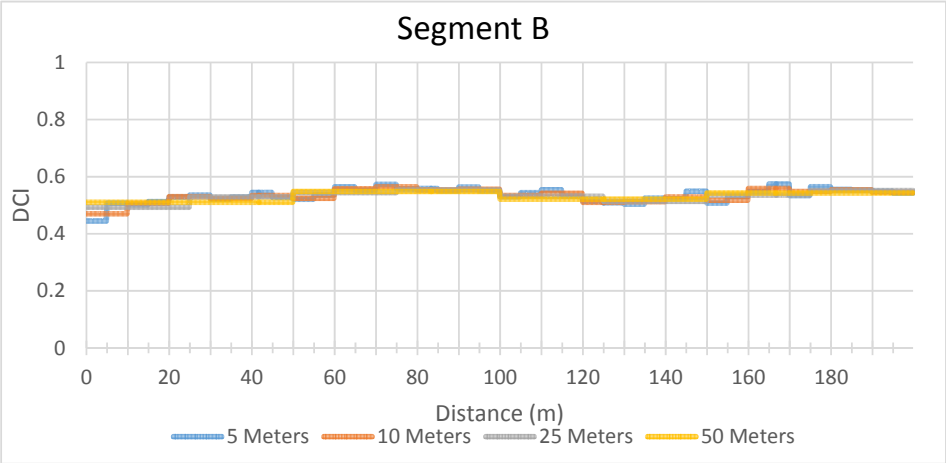

Figure 5.9: Segment B index values over different scales

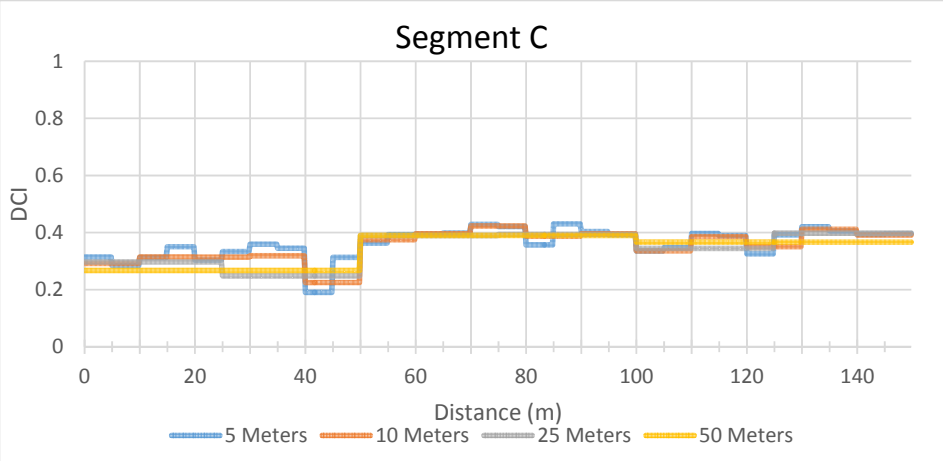

Figure 5.10: Segment C index values over different scales

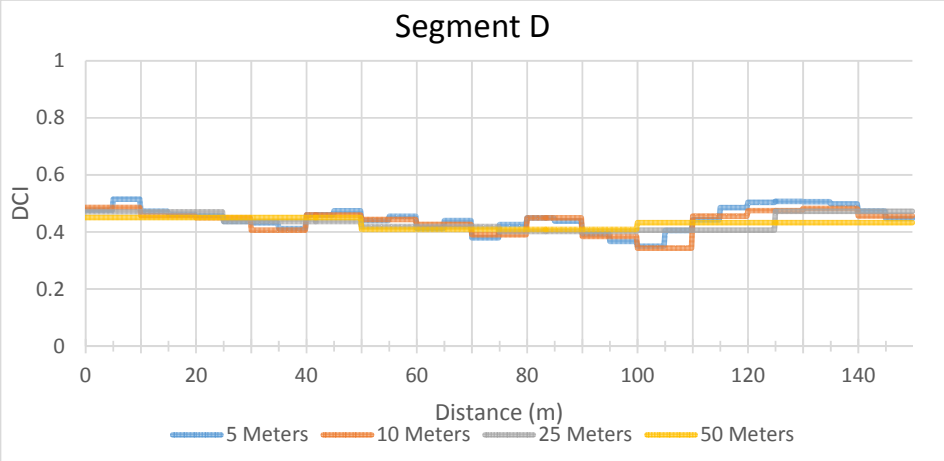

Figure 5.11: Segment D index values over different scales

5.5.5 DCI PERFORMANCE BASED ON DIFFERENCES IN ACCELERATION DATA

In section 3.3.3 the aspect concerning the pedal movement of the cyclist was discussed, as it was expected to influence the outcome of the DCI assessment methodology. A variant towards the DCI_{sum} formula was therefore suggested, which incorporated the difference in acceleration values of two consecutive points of each axis in order to reduce the effect of the pedal movement. Moreover, an additional expected benefit of the variant was that it will better identify extreme values. The variant is referred to as DCI_{diff} and its formula and more information can be found in section 3.3.3 of this study. This section will analyze if the variant DCI_{diff} performs better than the DCI_{sum} by comparing the values calculated with the DCI_{sum} and DCI_{diff}.

Based on the reasoning that the DCI_{diff} formula should reduce or naturally 'filter' the effect of the pedal movement and identify extremes more clearly, the DCI_{diff} values should on average be higher for the segments in good condition and lower for the ones in bad condition than the index values derived with the DCI_{sum} formula. Thus, the DCI_{diff} values for segment B and D should be higher than the DCI_{sum} values, and for segment B and D they should be lower. This section will analyze if these statements can be confirmed.

Even though in the previous section it was concluded that the index should be calculated over sections of 25 meters, the two approaches will be compared on the 5-meter scale in order to compare them in more detail. Thus, the DCI_{diff} is also calculated over 5-meter sections. By generating the same descriptive statistics for the DCI_{diff} as for the DCI_{sum} listed in table 5.5, the two approaches will be compared. Besides these statistics, also graphs of each segment with both derived DCI values will be plotted in order to demonstrate if indeed the DCI_{diff} better identifies extremes, and it also better provides a quick graphical display of the difference between the two indexes. The descriptive statistics of DCI_{diff} are listed in table 5.7 and the graphs are depicted in figure 5.12 to 5.15.

From the graphs, it can be seen that in general DCI_{diff} performs similarly to the DCI_{sum}, as it follows the same trend line. This observation can be supported by the descriptive statistics of table 5.7, as similar standard deviation for the segments are observed for the calculated DCI_{diff} values as for the DCI_{sum} values (presented in table 5.5), with the exception for segment B. Proportionally, for segment B a twice as big standard deviation is found. The larger spread of index values can also be observed in the graph of segment B depicted in figure 5.13, only it seems that in general it follows the same line. In order to quickly check this last assumption, the degree of relationship between the two index values derived for segment B is determined with both Pearson's and Spearman's correlation. The Pearson's and Spearman's correlation coefficient are 0.891 and 0.845 respectively, and are significant at the 0.01 level, indicating that indeed the DCI_{diff} and DCI_{sum} values of segment B tend to change together.

Furthermore, as expected, the DCI_{diff} indeed provides higher values for the segments in good condition and lower for the ones in bad condition, with the exception for segment D. The latter could be explained by the fact that the DCI_{diff} variant is based on changes in acceleration (or vibrations) and the cobblestone segments continuously transmit small vibrations to the cyclist due to its rough surface, as was indicated in section 5.3. When cycling on an asphalt segment a cyclist does not experience these kind of small continuous vibrations due to the surface, and therefore results in a better DCI.

Moreover, it was expected that the DCI_{diff} values better identified extreme values in the data. From the graphs, one can see that every time a local minimum is identified by the DCI_{sum}, the DCI_{diff} indicates a more extreme minimum. For example at distance section 160-165 of segment A, where for DCI_{sum} a value of approximately 0.22 is calculated and for DCI_{diff} a value of 0.17. Another example can be observed at distance section 40-45 of segment C.

Even though the new variant appears to perform as expected, the new variant performs in general much worse than the values derived with the DCI_{sum} formula, and therefore also regarding the DCI values derived in the study of Bíl et al. (2015). Segment B is the only one which is evaluated better based on the new approach and even its average index value is not even close to which segment B was originally compared in section 5.5.2.

Table 5.7: Descriptive statistics of DCI_{diff} values

Section	DCI values				
	Minimum value	Mean value	Median value	Maximum value	Standard deviation
Segment A	0.1698	0.3349	0.3343	0.5173	0.0785
Segment B	0.3757	0.6082	0.6133	0.7126	0.0592
Segment C	0.1304	0.2968	0.3047	0.3771	0.0506
Segment D	0.3228	0.4027	0.4045	0.4924	0.0363

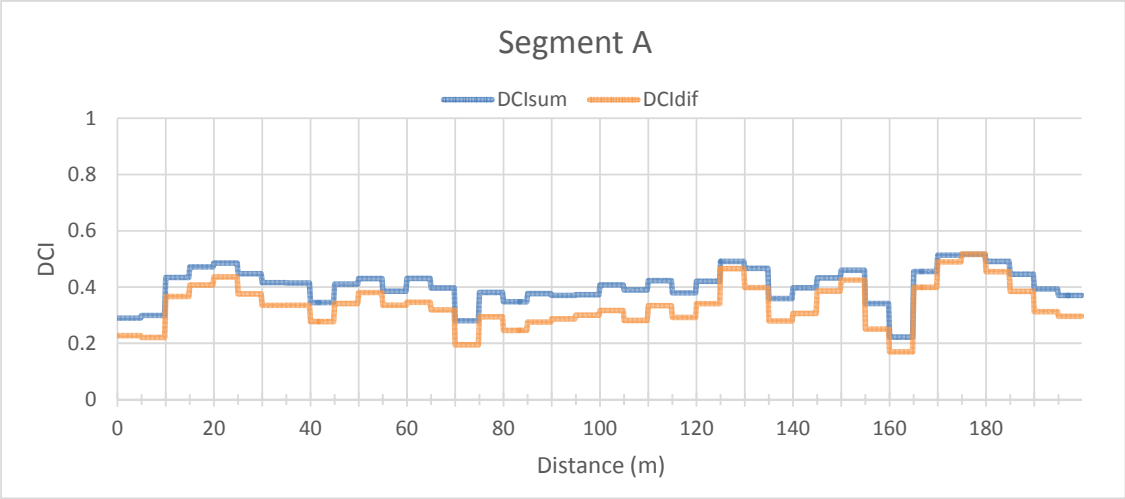

Figure 5.12: DCI_{sum} and DCI_{diff} values over segment A

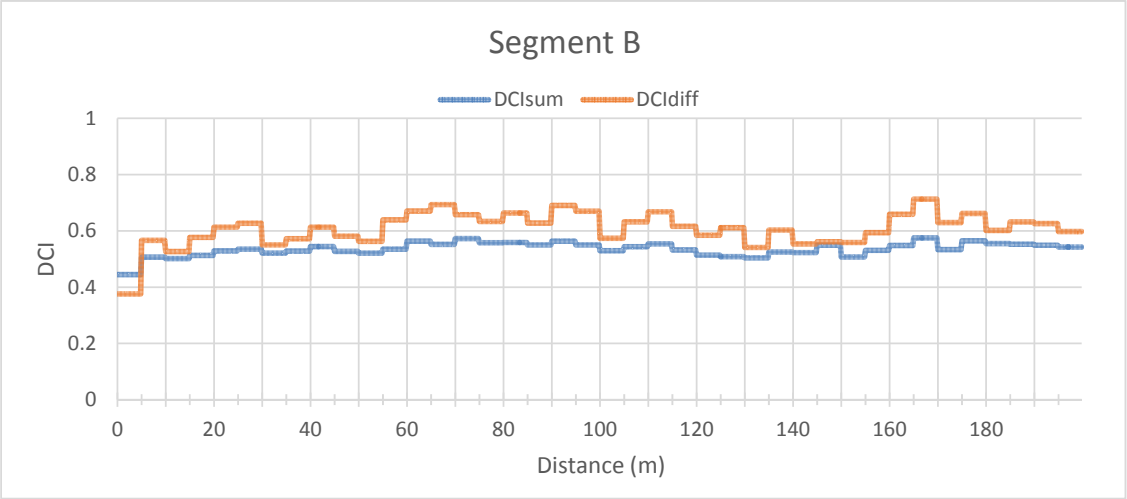

Figure 5.13: DCI_{sum} and DCI_{diff} values over segment B

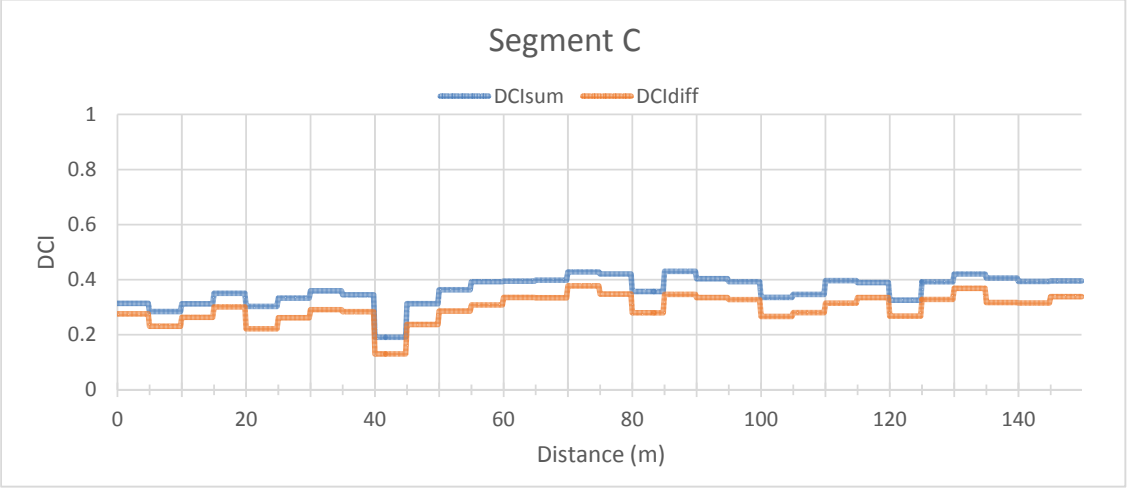

Figure 5.14: DCI_{sum} and DCI_{diff} values over segment C

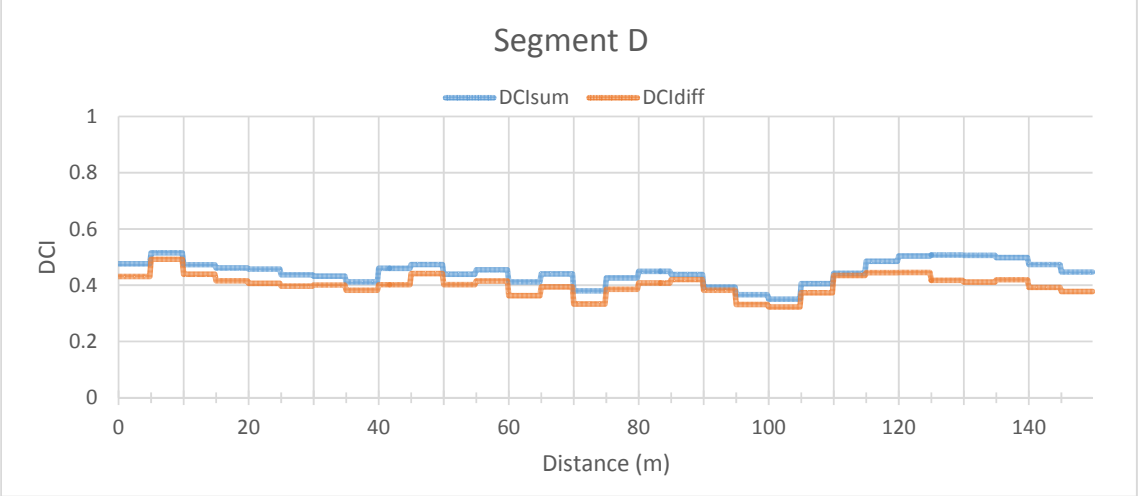

Figure 5.15: DCI_{sum} and DCI_{diff} values over segment D

5.6 Discussion & conclusion

The goal of this field experiment was to demonstrate the feasibility of the assessment component of BIMS, discussed in section 3.3. More specific, the method of assessing the pavement surface condition of the bicycle environment based on the dynamic comfort mapping method introduced by Bíl et al. (2015). Overall it can be concluded that the field experiment achieved to demonstrate the feasibility of the assessment component of BIMS, as clear distinctions were observed between the good segments and bad segments based on the DCI_{sum} values calculated with vibration data collected from smartphones. In addition, based on the strong correlations found between the data sets of the test riders, the experiment achieved to illustrate the workability of combining data gathered from multiple cyclists. Based on the literature findings, and the results and experience gained from the field experiment, the sixth and seventh sub-research question can be answered.

Another goal of the experiment was to re-examine the method on four aspects, due to the principal difference of using smartphones in this study for the vibration measurement instead of an separate accelerometer, as discussed in section 3.3.2 and 3.3.3. These aspects were examined in order to evaluate if and how the method should be adjusted before it is adopted for BIMS.

First and foremost, the original formula was altered so it would include the readings of all three axes of the smartphones in order to negate the smartphone orientation, as originally the orientation of the measuring device stayed fixed during the recordings and only acceleration outputs perpendicular to the road surface needed to be included, while for BIMS the smartphone position is basically unknown. The new formula is referred to as DCI_{sum}. The field experiment tested the altered method over 4 road segments in city-center of Eindhoven to evaluate the appropriateness as well as the performance of the method for BIMS. The performance was evaluated by using some outcomes of the study of Bíl et al. (2015) as benchmark to which the DCI_{sum} values of the four road segments were compared. The DCI_{sum} values were calculated from vibration data collected from three cyclists with varying characteristics, as BIMS will rely on data to be collected from all day cyclists. Overall it was observed that the altered method performed significantly worse in contrast to the method of Bíl et al. (2015), as the DCI_{sum} values were considerably lower than the DCI values of the selected matched segments, indicating that more intense acceleration are recorded in the field experiment. This was explained by the fact that more intense vibrations are experienced near the saddle than the front fork. Even though the DCI_{sum} performed badly, the experiment was able to clearly distinguish the segments of different quality and of different pavement types.

Secondly, based on the literature of chapter two, it was expected that the cyclist's weight will have an direct influence on the entity of the recorded vibrations, as the smartphone-based vibration-measurement is conducted from cyclist's trousers. The experiment therefore analyzed the index values calculated from data of three cyclists with varying weights. Out of the analysis, it was concluded that in general weight dampens the vibrations, as improving index values were observed with increasing weights. This will however be of less interest for the total BIMS, as it is expected that if the community collecting the data is large enough, the noise effect of cyclist's weight on the index values will automatically be averaged out. This latter statement however requires further inquiry in order to be certain on this matter.

Thirdly, it was suggested to calculate the DCI_{sum} over distance-intervals instead of time-intervals, as it will be easier to allocate the data from multiple cyclists. The experiment examined the ideal distance configuration over which the DCI will be calculated. Eventually, it was concluded that distance sections of 25 meters were the most suitable for BIMS, as with larger distances the index value will level off extreme values too much and with smaller distance the GPS inaccuracy of smartphones will become an issue of concern.

Fourthly, as the literature review of chapter 2 showed that the pedal movement of cyclists could have an influence on the recorded vibrations, an alteration to the DCI_{sum} was suggested, which was intended to naturally 'filter' the pedal movement. The field experiment examined if the DCI_{diff} formula would better represent the segments pavement surface conditions. The contrary was observed as the DCI_{diff} formula provided worse index values for those segments on which continuous vibrations are experienced due to their coarse characteristics. It therefore seems that the DCI_{diff} variant mainly weighs vibrations heavier, and in addition, does not filter the pedal movement. The latter however cannot be stated with certainty as it was not researched in this experiment. It could for instance also indicate the contrary, namely that the pedal movement does not has a severe effect on the recorded vibrations. Further inquiry is required in order to get a definitive answer.

5.7 LIMITATIONS

The literature review in chapter 2 revealed that besides the characteristics of the cyclist and condition of the road, also the bicycle characteristics could be of influence on the vibrations experienced as a cyclist. The study of Bíl et al. (2015) however showed the contrary as no significant difference between bicycle types was observed. It would therefore have been interesting to investigate the effect of different bicycle types on the experienced vibrations, though since more factors also had to be taken into account, the experiment would become too large. Although it is advised to re-investigate the influence of bicycle type on the DCI outcome in order to be definite on the matter.

Another factor which appeared to affect the entity of the vibrations, was the speed of the cyclist at which the data was recorded. The literature indicated that with increasing speeds more severe vibrations were experienced. This was confirmed by the study of Bíl et al. (2015). Since the results of this study were intended to be compared to the results of the study of Bíl et al. (2015), the same data recording conditions were maintained. The relation between speed and the DCI_{sum} however should be researched, as BIMS collects data from multiple cyclist and they will not all maintain cycling speeds of 15 km/h while collecting data.

Finally, this field experiment was restricted to only conduct the vibration measurement with a smartphone located in cyclist's trousers to measure the vibrations. In reality, not every cyclist will have his/her smartphone located in their trousers, as they might also be located inside a cyclist's backpack or purse for instance. This will most likely affect the vibration measurement in how severe the vibration are measured. It is therefore advised to also research the effect of the smartphone location on the vibration measurement. This can imply some limitations to BIMS, as for instance the method's reliability only can be assured if the smartphone is located in a trouser.

6 CONCLUSIONS

6.1 GENERAL CONCLUSION

The objective of this research was to provide a strong foundation for a 'Bicycle Infrastructure Monitoring System' (BIMS) capable of continuously collecting, analyzing and monitoring asset condition data regarding the bicycle pavement surfaces. Furthermore, to provide a first look towards the feasibility of the assessment component of this BIMS, which includes the assessment of the bicycle pavement surfaces based on vibration data collected through cyclists' smartphones located in their trousers. The main research question in order to satisfy this study's objective was therefore as follow:

"Can the pavement quality be indicated with a set of individual vibration measurements using internal smartphone sensors, and is it possible to convert these measurements into a surface quality index, for the benefit of collecting asset condition data regarding the bicycle pavement quality?"

First the sub-research questions are answered as they were defined in order to support the main research question.

- *How is pavement and its condition related to cyclists' level of comfort and safety according to current literature?*

In order to provide an answer to this question, the results of an extensive literature review have been presented in chapter 2. Many articles were reviewed to find out how pavement is related to cycling comfort and safety. Remarkable is that many researchers often combine the terms safety and comfort, but do not substantiate how they are interrelated. An own interpretation was therefore made regarding the relation between comfort and safety based on the reviewed articles in order to better indicate how pavement is related to the two. The relation was defined as cyclists' level of comfort not only being related to the ease of cycling, but also to cyclists' subjective levels of safety, and that cyclists' level of safety itself represented the objective levels of safety. Hence, it was stated in section 2.5 that when referring to cyclists' level of comfort in this study, the relation to the ease of cycling is meant.

Based on this terminology, the literature showed that most research relates pavement to cyclists' level of comfort, as bicycle vibrations are for cyclists the most important cause of discomfort and uneven pavement is the main reason for these vibrations to occur. As the bicycle vibrations increases, comfort decreases. Cyclists perceive the pavement condition by means of vibrations the surface transmits to them, hence why researchers attempt to indicate the pavement conditions based on its vibration properties. Moreover, the comfort issues related to pavement also affect route-choice behavior of cyclists, as cyclists are prepared to make a detour to a certain level if more route-comfort is assured. Furthermore, only few researchers also relate pavement issues to cyclists' level of safety. Although these articles are more related to severe cases of pavement issues or damages where cyclist's safety undoubtedly is compromised.

- *Which factors influence the vibrations transmitted from the pavement surface to the cyclist?*

As already discussed in the previous question, the most common factor for the vibrations experienced as a cyclist is the condition of pavement itself. Basically, two different types of vibrations can be identified from the literature, namely the vibrations directly associated with a particular pavement surface structure and the vibrations associated with pavement issues. The vibrations due to pavement issues can then be further divided into vibrations as a series of successive impacts due to a cracks or other surface defects and as a continuous random excitation due to a coarse road.

Other factors which were defined to influence the vibrations transmitted to the cyclist were weights of the cyclists and the bicycle. The first was also observed in the field experiment, as vibrations were damped when cyclist's weight increased. The latter refers to characteristics such as the mass, tire pressure, and stiffness of the frame. Logically the suspension will also have an effect on how the vibrations are transmitted if present.

- *What is the current practice for assessing the bicycle environments' pavement surface condition?*

Since the literature was short of information regarding the current practice for the assessment of bicycle environment's pavement conditions, three interviews were conducted with experts in the field of road management. This in order to gain more knowledge on the subject and to provide a more adequate answer for this question. Thus, out of the proceedings of both the literature and the expert interviews it was learned that currently the pavement condition is assessed through visual inspections. The expert interviews provided more specific knowledge on the matter by indicating that these inspections are mostly conducted by car driving at crawl speed or foot, and sometimes by high definition video footage in order to minimize the obstruction of traffic. Moreover, during these inspections all the sections of the roads are inspected simultaneously. It is advised to inspect closed pavements once a year and open pavements once every two or three years. The higher frequency of closed pavements is because of the risks of higher associated costs due to negligence.

These inspections, however, are not the triggering factor on the decision if maintenance is conducted. A road manager makes the final call with a 'measurement assessment' in which he/she assesses if maintenance is necessary and if he/she deems it to be executed. Unfortunately, because governmental authorities overall have limited funds for road management, the road manager must make priorities in which roads they deem to be maintained. The prioritizations can differ from authority to authority.

- *What are state-of-the art bicycle monitoring technologies for collecting asset condition data regarding the bicycle environments?*

This answer will be limited to only the technologies that have been proven in the field. Basically two distinctive state-of-the art bicycle monitoring can be identified out of the literature, namely the IPB's (Instrumented Probe Bicycles) and crowdsource-based monitoring technologies. The IPB technology uses simple bicycles equipped with high-performance sensors capable of measuring, gathering and recording data about the environments in which

the sensors find themselves in order to generate and provide reliable objective data regarding the bicycle environment. Mostly, IPB's are equipped with simple sensors like accelerometers and GPS receivers to measure bicycle position and vibrations, just like this study in order to assess the pavement conditions.

The crowdsourcing monitoring technologies on the other hand, use public platforms to outsource work to open communities in order to gather asset condition data about the environment. Mostly in the form of a smartphone-app, which is an excellent technique for distributing the platform as almost everyone in the world is in possession of a smartphone. The amount of effort an user has to commit to provide asset condition data varies per technology, which also logically affects the amount of data the technology acquires. The more effort, the more data it can acquire. Additionally, the amount of effort also affect the response rates of users. The more effort, the lower the response should be expected.

- *How reliable is the smartphone as a data collection tool for BIMS?*

In order to provide an answer to this question, a case study was conducted, as the literature only indicated that current sensor technology is progressive and contains no further information regarding the actual reliability. As for BIMS only vibration and location data needs to be collected, the case study only tested smartphones' motion and location sensors based on five test. Based on the results of the motion tests, it can overall be concluded that smartphones are capable of measuring accelerations with high level of precision, as for the motion sensors considerable low sensitivities and accuracies were observed with high consistencies. The results of the location sensors provided relatively sound results, as it is generally known and accepted that GPS data can be inaccurate to a specific level. Although the three tested smartphones provided an overall impression of the reliability of smartphones, it should be noted that it cannot entirely be assured that similar reliabilities are acquired with all smartphones.

- *What are the benefits and drawbacks of the smartphone-based vibration measurement for determining the pavement surface condition compared to the current practices?*

For this answer the smartphone-based vibration measurement is compared to both the current practice of assessing the bicycle environment on pavement surface conditions and the state-of-the-art bicycle monitoring technologies dealt with in the previous questions' answers. First and foremost, compared to the current practice of visual inspections, the smartphone-based vibration measurement is a much more resource efficient manner of assessing the pavement conditions as the smartphone-based assessment is conducted while cycling instead of on foot or by car driving at crawl speed. This makes it less labor-intensive and more efficient, as no designated inspector is needed, and the assessment is conducted at a higher speeds enabling to cover more surface in less time. Secondly, the smartphone-based vibration measurement will most probably provide more reliable assessments, as it is an objective method in contrast to the subjective visual assessments. Thirdly, the current quality of the bicycle environments' pavement will be better maintained or even improved based on the intended crowdsourced data collection model, as it will continuously monitor the pavement conditions. This results in hazardous and poor segments, and defects to be spotted faster, enabling road managers to act faster keeping the maintenance measure costs low, since for some damages the costs can rise considerably if not acted quickly. Meanwhile, the visual

inspection is only conducted once every 1-3 years depending on the type of pavement. Fourthly, the method can provide more valuable data in addition to data about the pavement conditions, as the location data of the vibration measurement can be used to evaluate bicycle movements and bottlenecks. Finally, this data can also easily be transferred to be used by other applications, such as traffic models.

The drawbacks of the vibration measurement on the other hand are that first the vibration measurement depends on cyclist's lateral position and given that, the state of a cycle path can vary laterally, the vibration measurements can fail to record certain surface defects, as cyclists usually avoid defects if possible. Although, since for the assessments the acceleration recordings of all axes of the smartphone are included, sudden lateral movements will be recorded. Secondly, no distinction can be made between damages based on the data, which is the case for the visual inspections, and in addition, out of the visual inspection directly follows what kind of maintenance measure is advised regarding the perceived surface defects. The latter however can be nullified as the road manager performs a second inspection in the form of a 'measurement assessment' on the segments in need of maintenance followed out of the visual inspections. The second round could be employed to define the surface defects and the associated advised maintenance measures.

Thus, the smartphone-based vibration measurement is overall in contrast to the current visual inspection mostly beneficial, as most drawbacks can be overruled. However, it should be noted that all the established benefits will only apply if the development of the sophisticated assessment method is completed, as it currently is not ready to be applied in the field.

Furthermore, in contrast to the recent bicycle monitoring technologies the smartphone-based vibration measurement combines the beneficial aspects of both the IPB as well as the crowdsourcing techniques. Firstly, the crowdsourcing technique of using smartphones was already discussed to be an excellent approach for collecting the measurements' data, as almost everyone is in possession of a smartphone. The only challenge however is convincing people to participate, in order to be able to collect data from them. Secondly, the current crowdsourcing technologies rely on users to take effort to mark and/or describe unsafe or unsatisfying bicycle-related traffic situations. For the vibration measurement, users will have to make much less effort to provide the data, as the smartphone records the data for them. In addition, the measurement is objective, where the crowdsourcing technologies rely on users' subjective opinions just like the visual inspection. Fourthly, in contrast to the IPB's the smartphone-based measurement is more widely applicable and easily transferable, as it used the current most common device to gather the data, namely the smartphone. Fifthly, the IPB's rely on one or maybe a hand full of people to generate the data, where the vibration measurement intends to use a larger community of every-day cyclists, which also leads to more continuous data.

The smartphone-based vibration measurement also has in contrary to these technologies several disadvantages. First, as discussed the vibration measurement depends on the lateral position of cyclists and since the state of a bicycle path can vary laterally, it could fail to record certain defects, which most likely will be less the case with the subjective assessments of the crowdsourcing techniques. Although, this can be simply overcome if for the intended BIMS smartphone app an additional feature is developed enabling cyclists to also add subjective opinion to their cycled routes. Secondly, in contrast to IPB, the vibration measurement is

limited in the amount of data it can obtain. The IPB's are equipped with more sensors like camera's enabling them to assess the bicycle environment on more aspects concerning cyclists' safety and comfort levels. However most of these aspects stay unchanged for quite some time until the area is restructured. These aspects can therefore also be obtained in a different manner, like for instance HD video footage. Thirdly, in contrast to the IPB's, the smartphone-based vibration measurement needs more calibration, as more factors should be taken into account that influence the measurement outcome, like the pedal movement of the cyclist and bicycle type.

- *How can the results of this research be implemented in operations and maintenance plans of road managers?*

The direct results of these study are unfortunately not sophisticated enough to be directly implemented in the operation and management plans of road managers. Although it does provide a strong foundation for a BIMS capable to continuously monitor the bicycle environment on pavement surfaces conditions, providing road managers with valuable data regarding the bicycle asset condition data. As discussed in the previous question, BIMS can replace the current visual inspections, making it very beneficial for road managers, as this system will enable them to plan in a more resource efficient manner the operations and maintenance of the bicycle pavement surfaces, by using the data provided by the system as input. However, if BIMS ought to replace the visual inspections, the second round assessment specified as the 'measurement assessment' should become more sophisticated, since BIMS data does not distinct different surface defects and in addition does not assess the severity and dimensions of the defects.

Furthermore, road managers can use the data of BIMS in two forms for their operations and maintenance. First, the data allows road manager to spot local extremes which in most cases identifies hazardous locations. This will enable them to act more quickly on these locations, keeping the maintenance cost low, as costs can significantly rise if not acted at the right moment. Second, the aggregated values the data provides linked to cycling tracks can be a good representation of the aggregate condition of a bicycle path. These condition values can be useful to evaluate if the current quality is above or below established standards. The scale over which these values are calculated can even be extended, since the local extremes are spotted separately it will not be an issue if these extremes are leveled off by the rest of the segment. When the method is completely sophisticated, the data could also be used for predicting the lifespans of pavement, since the system continuously collects data enabling to build prediction models to be build based on the data.

Finally, based on the answers of the sub-research questions, an answer can be formulated for the main research question: *"Can the pavement quality be indicated with a set of individual vibration measurements using internal smartphone sensors, and is it possible to convert these measurements into a surface quality index, for the benefit of collecting asset condition data regarding the bicycle pavement quality?".*

Basically, this question could be answered with a simple yes or no, however when considering all the findings of this report the answer is not so simplistic. In order to provide a solid answer to the above stated question this study proposed, investigated and tested an assessment method in which the data collected from a smartphone-based vibration measurement was

converted to a DCI_{sum} (Dynamic Comfort Index) value, which objectively represents the recorded bicycle vibrations. This surface quality index was derived from an already existing method introduced by Bíl et al. (2015) called 'dynamic comfort mapping', which was already proven to be a sound objective manner to indicate pavement surface conditions of cycle paths as it was already applied. However, since the assessment method of this research differed in using smartphones located in cyclist's trousers instead of an accelerometer mounted to the front fork of a bicycle to record the bicycle vibrations, the method was altered and therefore needed to be re-validated.

Based on the results of the field experiment the smartphone-based method appears not to perform similar the original method, as more severe vibrations were measured during the field experiment, which most likely is due to difference in where the vibrations were recorded. However, even though the smartphone-based method performed worse in comparison with the original method, the field experiment shows that it is possible, on the basis of the calculated DCI_{sum}'s, to distinguish different pavement surfaces of different qualities. Moreover, repeatability is fairly good, as strong correlations were found between measurements of different individuals. Therefore, the main question can generally be answered with 'yes', however more extensive research and calibration is needed before this method can be applied in the field or by BIMS.

6.2 General discussion & recommendations

The literature is acknowledging the opportunities that arise of what can be achieved with recent advancements of sensor technologies, though research concerning new innovative manners of collecting asset condition data regarding the bicycle environment based on these recent sensor technologies is scarce. Moreover, given the growing interest of using the bicycle as a transportation mode and that many cities are coping with severe problems emerging from the high dependency on motorized traffic, such manners will become more of interest to maintain and improve the bicycle environment in order to stimulate cycling behavior. The purpose of this study was to contribute to the development of such an objective method, by providing a strong basis for a monitoring system named BIMS, which intends to use every-day cyclists and their smartphone to collect asset condition data regarding the bicycle environment's pavement surfaces. This valuable information will ensure more efficient use of limited resources of road managers in relation to operation and maintenance, renewal and auditing of the bicycle environment. As a basis, this report presented a comprehensive case study researching the capabilities of smartphones' motion and location sensors and a field experiment examining an existing assessment method, in order to prove that smartphones are capable of collecting reliable asset condition data and in addition of what can be achieved with this data. This section will provide recommendations specifically for further research and development of BIMS assessment method based on smartphone data, as well as for BIMS in general. However, first there will be discussed which users other than road managers can benefit from the outcomes of a system such as BIMS.

6.2.1 Potential users

Road managers are not the only users that will benefit from the objective assessment of a system such as BIMS. Firstly, cyclist themselves can use the information regarding the vibrations to plan their cycling routes. For instance, leisure cyclists using racing bikes usually seek the most comfortable (or fewest vibrations) routes in order to achieve the best

performance. The data resulting out of the assessment can therefore for instance be placed on a web-application where it is accessible for all people. This will also make it more attractive for people to contribute to the system. Secondly, which has already been mentioned, are researchers and other people working with traffic models and simulations. In literature, it was stated that route comfort affects cyclist route-choice behavior and that one of the attributes which strongly contributed to the route comfort was the pavement conditions. The data can therefore be used by researchers to generate better prediction models and by modellers as input in order to improve the performance and correctness of their traffic models and simulations. Third and finally, following on the previous users, researchers studying cyclist route-choice behavior can use this data.

6.2.2 SMARTPHONE APP

The first recommendation regarding assessment component of BIMS is the development of a smartphone application. Due to the lack of expertise in developing apps, this study used the AndroSensor-app for collecting the raw sensor data of smartphones. For this study, the use of such a simple application was sufficient enough as it involves a relatively small amount of data. For BIMS on the other hand such a simple application will not be adequate, and therefore a more sophisticated app is recommended in order to automatically process the large entailed data sets. Moreover, the app can also be used to audit if certain condition regarding the data collection are met. If certain conditions are not met, no data is recorded.

Ideally, the app will be a stand-alone app collecting the data relevant to BIMS (vibration and location data) from each cyclist. However, developing an app is one thing, distributing the app by convincing people to install this app is another challenge. As smartphones are linked to specific people and the app intends to collect location data, one should for instance keep into account cyclists' privacy. The literature study already provided some examples of how distributing the application can successfully be achieved. Thus, besides the recommendation of developing a smartphone-app, it is also recommended to research how it is going to be distributed and the challenges associated with it. One option is for instance to use the platform from an already existing application and run the vibration measurement on the background.

6.2.3 BIMS ASSESSMENT METHOD

It is observed in the field experiment that based on smartphone data it is possible to distinguish pavement surfaces of different qualities. However the method used in this study did not perform according to the original method of Bíl et al (2015), as overall much lower index values were observed, which indicated that more severe vibrations were recorded. This was explained to be mainly due to where the vibrations were recorded. The original method recorded directly at the front fork of a bicycle, leading to mainly record the vibrations of the front wheel. In the case of the field experiment on the other hand the vibrations are measured near the saddle, including the vibrations of both the front and rear wheel. This statement however is due to the limited time frame of this research restricted to findings in literature and experience gained over the time period of this research. It is therefore recommended to further research this statement in order to validate it. Especially if the dynamic comfort mapping method is still intended to be employed by BIMS, which is advised since the DCI is based on a relatively simple method, and it provides a sound and objective representation of the recorded vibrations. In addition, it is expected that the DCI only needs to be re-calibrated

to a different scale, since it was observed in the field experiment that the average index values of each segment were with a constant level lower compared to their benchmark values, hence the statement that more vibrations are recorded near the saddle.

The aspect of including the acceleration values of all three axes, instead of only the axis perpendicular to the pavement surface, was also expected to contribute to more vibrations to be recorded, as cracks or other surface defects are most likely to cause horizontal vibrations apart from the vertical vibrations. An alternative approach for calculating the DCI_{sum} could be to not weigh all three axes equally, but to weigh the axis perpendicular to the road surface heavier than the other acceleration values, or to only include the axis perpendicular to the road surface. This approach could better fit the computation of the acceleration values to the DCI values. This requires a complex procedure in which the smartphone coordinate system needs to be re-oriented to the Earth's coordinate system during or after the measurements. This re-orientation can be achieved by including an algorithm that uses the data from the accelerometer, linear acceleration, magnetometer, and gyroscope to re-orient the smartphone, as has been done in the studies of Ferreira et al. (2017) and Vittorio et al. (2014). This alternative approach however will not record the lateral evasive maneuvers of cyclists towards extreme surface defects as clearly as when the values of all three axes was included, resulting in surface defects to be missed. Although this could be overcome by including a feature in the intended BIMS app (discussed in section 6.2.1) where cyclist can subjectively report surface defects, as with the ORcycle platform of Figliozzi (2015) discussed in section 2.4.2 of the literature.

Furthermore, from the field experiment followed two aspects which are recommended to be further researched, as currently these aspects impose several specific conditions towards how the smartphone-based vibrations measurement should be conducted to provide reliable outcomes, limiting the applicability of the dynamic comfort mapping methodology. The first aspects concerns the speed of the cyclists. In both this study as in the study of Bíl et al (2015) a cycling speed of 15 km/h was maintained and since cycling speed appears to affect the recorded bicycle vibrations, the reliability of the DCI's outcome can currently only by assured if the same speed of 15 km/h is maintained. It is however very unlikely that all cyclists will maintain cycling speeds of 15 km/h while the data is recorded for BIMS. Therefore, the relation between cycling speed and bicycle vibrations should be established. Based on this relation, the recorded vibrations could be corrected on the basis of cyclists' speed, as with the study of Yamaguchi et al. (2015) discussed in section 2.4.3 of the literature review. The second aspects concerns to the location of the smartphone for the vibration measurement. This study was limited to only research the vibration measurement to be conducted from cyclist's trousers, more specifically cyclists' left pocket. In reality, cyclists will not always have their smartphones located inside their trousers. It should therefore be researched how the location of the smartphone affect the measurements. If the effect is minor, it may be corrected as with the cycling speed. However if the effect is major, it will imply that BIMS should exclude the data that is collected on a different manner.

A third aspect followed from the field experiment revealed which should be further researched, as it was shown to affect the recorded vibrations, namely the bicycle itself. This aspect however does not impose certain conditions towards how the vibrations measurement should be conducted, as it was expected that if BIMS data is collected by a large population, the noise effect of the bicycle will be automatically averaged out. However even though this

is expected, it is still recommended to research the effect of the bicycle type on the measured vibrations. This in order to analyze if certain bicycle types appear to influence the recorded vibrations too much. Then, It can be decided to for instance exclude the cyclists riding these specific bicycle types for BIMS data collection.

6.2.4 PRACTICAL IMPLEMENTATION BIMS

As already stated, for BIMS the dynamic comfort mapping method can basically be used in two ways. First, it can be used to indicate the aggregate condition of a particular segment, and secondly to spot local extremes. The first form of providing reliable aggregate condition data is achievable with smartphone data, however it requires more extensive research regarding topics discussed in previous section. In addition, another important research topic should be the verification if indeed it can be assumed that based on a large community the noise effect of cyclist's weight and their bicycle on the vibration measurement can be neglected for the method as the large community will automatically average out the method's outcomes. This could for instance be researched by performing a pilot with a large group.

The second form of spotting local extremes, on the other hand, can be confirmed to be achievable with smartphone data, as for this form the factors which were identified to affect the data are overall less of interest. In every situation when a cyclist hits a surface defect, like a pothole or a tree root, an extreme will be recorded. This can also be observed in the field experiment, as for all three test riders extremes were detected at approximately the same locations on the driven segments. The exact value of this extreme can of course still vary due to the factors like weight and bicycle type, but the data will identify an anomaly. Moreover, since the factors affecting the bicycle vibrations are of less interest for spotting local extremes, the community does not has to be of considerable size in order to provide reliable data.

Thus, since it is reasonable to assume that in the early stages when BIMS is implemented in the field the community will not be large enough to assure reliable aggregate values regarding the bicycle pavement conditions, it is recommended to first use BIMS for spotting local extremes. This until the community of BIMS has increased to a considerable size so reliable data can be assured. Note that for spotting local extremes the scale of the distance-interval discussed in section 5.5.4 should be adjusted to 5 meters in order to spot these extremes more clearly. Even though the GPS inaccuracy will cause for these extremes to be spotted on slightly different locations, they will provide an indication were severe surface defects are.

An alternative approach for BIMS to provide and collect reliable asset condition data about the bicycle pavement surface conditions could be by equipping common bicycles with simple sensors for collecting the data. For instance, by equipping the identical bicycles of bicycle sharing systems. Using these bicycles will considerably reduce the amount of factors that affect the vibration measurement, especially if the motion sensor is mounted to the front fork of the bicycle, like in de study of Bíl et al (2015). Exiting from the latter, the pedal movement can for instance directly be neglected. Moreover, the original method of dynamic comfort mapping can most likely directly be transferred, as it was stated that the outcome of the method is not affected by the bicycle type. Acquiring the motion and location sensors to equip these bicycles with does not has to be a large investment, as the case study of this research revealed what can be achieved with the relatively simple sensors of smartphones. Overall using a bicycle equipped with simple sensors will considerably improve the data reliability as less factors influence the measurement.

6.2.5 FUTURE RESEARCH AND DEVELOPMENT

This study specifically focused on the assessment component of BIMS and provided a basis for the components concerning the evaluation and implementation of the results following out of the assessments, discussed briefly in the process flow diagram of section 3.2. These components need to be further elaborated as they also are essential for how the system will function. For instance, it should be researched how the DCI values will be categorized into different levels of quality for the 'Evaluation' process of BIMS. Basically, the DCI value already represents the surface pavement conditions of a bike segment with a value between 0 and 1, where 0 is very poor and 1 perfectly smooth. The DCI however is not yet categorized into different levels of quality. Therefore a comfort perception study should be conducted to draw opinions of cyclists, and use this study to categorize the index values and create a quality rating system. This rating scale should also be balanced with the quality standards defined by governments for road managers. This quality rating scale should then be established for each pavement type separately, as the study of Calvey et al. (2015) showed that cyclists differently evaluate the same level of vibrations on different types of pavement. For instance, the same level of vibration on an asphalt is most likely to be evaluated less comfortable than on cobblestones, since cyclists expect less comfort on cobblestones. Furthermore, it is essential to conduct a validity study towards the results in order to check if the system achieves the same or better results than the current practice of visual inspections.

BIBLIOGRAPHY

Accenture. (2014). Low-Carbon Mobility Report: As part of the Transform Program, 33. Retrieved from http://urbantransform.eu/wp-content/uploads/sites/2/2015/07/20141002-low-carbon-mobility-low-res.pdf

Akhavian, R., & Behzadan, A. H. (2016). Smartphone-based construction workers' activity recognition and classificatio. *Automation in Construction*, *71*(Part 2), 198–209. https://doi.org/10.1016/j.autcon.2016.08.015

Allmendinger, R. W., Siron, C. R., & Scott, C. P. (2017). Structural data collection with mobile devices: Accuracy, redundancy, and best practices. *Journal of Structural Geology*, *102*, 98–112. https://doi.org/10.1016/j.jsg.2017.07.011

Amick, R., Patterson, J., & Jorgensen, M. (2013). Sensitivity of Tri-Axial Accelerometers within Mobile Consumer Electronic Devices: A Pilot Study. *International Journal of Applied Science and Technology*, *3*(2), 97–100. https://doi.org/10.13140/2.1.1568.8324

Android Developers. (2017a). Introduction to Android. Retrieved December 7, 2017, from https://developer.android.com/guide/index.html

Android Developers. (2017b). Sensors Overview. Retrieved December 1, 2017, from https://developer.android.com/guide/topics/sensors/sensors_overview.html#sensors-configs

Ayachi, F. S., Dorey, J., & Guastavino, C. (2015). Identifying factors of bicycle comfort: An online survey withenthusiast cyclists. *Applied Ergonomics*, *46*(PA), 124–136. https://doi.org/10.1016/j.apergo.2014.07.010

Azzoug, A., & Kaewunruen, S. (2017). RideComfort: A Development of Crowdsourcing Smartphones in Measuring Train Ride Quality. *Frontiers in Built Environment*, *3*(3), 1–12. https://doi.org/10.3389/fbuil.2017.00003

Bauer, C. (2013). On the (In-) Accuracy of GPS Measures of Smartphones : A Study of Running Tracking Applications. *International Conference on Advances in Mobile Computing & Multimedia*, (April), 335–340. https://doi.org/10.1145/2536853.2536893

Bayat, A., Pomplun, M., & Tran, D. A. (2014). A study on human activity recognition using accelerometer data from smartphones. *Procedia Computer Science*, *34*(C), 450–457. https://doi.org/10.1016/j.procs.2014.07.009

Bicycle Network. (2017). Surface Smoothness. Retrieved June 28, 2017, from https://www.bicyclenetwork.com.au/general/for-government-and-business/2833/

Bike Citizens, & Mobiel 21. (2017). PING if you care – changing Brussels at the push of a button. Retrieved July 10, 2017, from http://pingifyoucare.brussels/en/ping-if-you-care/

Bíl, M., Andrášik, R., & Kubeček, J. (2015). How comfortable are your cycling tracks? A new method for objective bicycle vibration measurement. *Transportation Research Part C: Emerging Technologies*, *56*, 415–425. https://doi.org/10.1016/j.trc.2015.05.007

Blanc, B., & Figliozzi, M. (2017). Safety perceptions , roadway characteristics and cyclists ' demographics : a study of the of crowdsourced smartphone bicycle safety data. *96th Annual Meeting of the Transportation Research Board*, (July 2016), 20.

Blauw. (2016). *Recreatief fietsen in Utrecht*. Rotterdam.

Bobko, P. (2001). *Correlation and regression : applications for industrial organizational psychology and management* (2nd editio). Thousand Oaks, California: SAGE Publications, Inc.

Botzheim, J., Tang, D., Yusuf, B., Obo, T., Kubota, N., & Yamaguchi, T. (2013). Extraction of daily life log measured by smart phone sensors using neural computing. *Procedia Computer Science*, *22*, 883–892. https://doi.org/10.1016/j.procs.2013.09.171

Brabham, D. C. (2013). *Crowdsourcing*. Cambridge, MA: MIT Press.

Calvey, J. C., Shackleton, J. P., Taylor, M. D., & Llewellyn, R. (2015). Engineering condition assessment of cycling infrastructure: Cyclists' perceptions of satisfaction and comfort. *Transportation Research Part A: Policy and Practice*, *78*, 134–143. https://doi.org/10.1016/j.tra.2015.04.031

Cesario, E., Comito, C., & Talia, D. (2017). An approach for the discovery and validation of urban mobility patterns. *Pervasive and Mobile Computing*, *42*, 77–92. https://doi.org/10.1016/j.pmcj.2017.09.006

Champoux, Y., & Drouet, J. (2012). Technique to Measure the Dynamic Behavior of Road Bike Wheels. *Topics Modal Anal II*, *6*, 465–470. https://doi.org/10.1007/978-1-4614-2419-2

Champoux, Y., Richard, S., & Drouet, J. M. (2007). Bicycle Structural Dynamics. *Sound and Vibration*, 16–22.

Clifford, M. (2006). *Detecting Freefall with Low-G Accelerometers*. *Freescale Semiconductor*. Retrieved from http://cache.nxp.com/files/sensors/doc/app_note/AN3151.pdf?fsrch=1&sr=1&pageNum=1

De Silva, C. W. (2007). *Vibration Monitoring, Testing, and Instrumentation*. *CRC Press* (1st Editio). Boca Raton: CRC Press.

DiGioia, J., Watkins, K. E., Xu, Y., Rodgers, M., & Guensler, R. (2017). Safety impacts of bicycle infrastructure: A critical review. *Journal of Safety Research*, *61*, 105–119. https://doi.org/10.1016/j.jsr.2017.02.015

Docherty, I. (2003). Transport and the urban renaissance agenda. *Journal of Transport Geography*, *11*(3), 241. https://doi.org/10.1016/S0966-6923(03)00034-6

Douangphachanh, V., Oneyama, H., & Engineering, E. (2013). A Study on the Use of Smartphones for Road Roughness Condition Estimation. *Proceedings of the Eastern Asia Society for Transportation Studies*, *9*(2007), 14. https://doi.org/10.1186/1687-1499-2014-114

European Commision. (2017). Clean transport, Urban transport: Cycling. Retrieved May 22, 2017, from https://ec.europa.eu/transport/themes/urban/cycling_en

Feldbusch, A., Sadegh-Azar, H., & Agne, P. (2017). Vibration analysis using mobile devices (smartphones or tablets). *Procedia Engineering*, *199*, 2790–2795. https://doi.org/10.1016/j.proeng.2017.09.543

Fernee, H., Sonck, N., & Scherpenzeel, A. (2012). Data collection with smartphones : experiences in a time use survey. *New Techniques and Technologies for Statistics Conference 2013*, 8. Retrieved from https://ec.europa.eu/eurostat/cros/content/data-collection-smartphones-experiences-time-use-survey-henk-fernee-et-al_en

Ferreira, J., Carvalho, E., Ferreira, B. V., de Souza, C., Suhara, Y., Pentland, A., & Pessin, G. (2017). Driver behavior profiling: An investigation with different smartphone sensors and machine learning. *PLOS ONE*, *12*(4), 16. https://doi.org/10.1371/journal.pone.0174959

Figliozzi, M. (2015). Crowdsourcing Cycling Safety and Route Data with the "ORcycle" Smartphone App. In *TREC Friday Seminar Series* (p. 33). Portland: Portland State University.

Figliozzi, M., & Blanc, B. (2015). *Evaluating the Use of Crowdsourcing as a Data Collection Method for Bicycle Performance Measures and Identification of Facility Improvement Needs*. Portland. Retrieved from http://pdxscholar.library.pdx.edu/cengin_fac%5Cnhttp://pdxscholar.library.pdx.edu/cgi/viewcontent.cgi?article=1327&context=cengin_fac

Fishman, E. (2016). Cycling as transport. *Transport Reviews*, *36*(1), 1–8. https://doi.org/10.1080/01441647.2015.1114271

Fitchard, K. (2015). 8 Crowdsourcing apps (besides OpenSignal) we love. Retrieved July 13, 2017, from https://opensignal.com/blog/2015/07/09/8-crowdsourcing-apps-besides-opensignals-love/

Galbis, A., & Maestre, M. (2012). *Vector Analysis Versus Vector Calculus*. *Vector Analysis Versus Vector Calculus*. Boston, MA: Springer US. https://doi.org/10.1007/978-1-4614-2200-6

Giubilato, F., & Petrone, N. (2012). A method for evaluating the vibrational response of racing bicycles wheels under road roughness excitation. *Procedia Engineering*, *34*, 409–414. https://doi.org/10.1016/j.proeng.2012.04.070

Goodwin, L. D., & Leech, N. L. (2006). Understanding correlation: Factors that affect the size of r. *Journal of Experimental Education*, *74*(3), 249–266. https://doi.org/10.3200/JEXE.74.3.249-266

Gössling, S. (2016). Urban transport justice. *Journal of Transport Geography*, *54*, 1–9. https://doi.org/10.1016/j.jtrangeo.2016.05.002

Hanly, S. (2016). *Shock & Vibration - Overview* (Vol. 2). Medford: Mide Technology. Retrieved

from https://info.mide.com/data-loggers/shock-vibration-testing-overview-ebook

Heinen, E., Wee, B. Van, Maat, K., Heinen, E. V. A., Wee, B. V. A. N., & Maat, K. (2010). Commuting by Bicycle: An Overview of the Literature. *Transport Reviews*, *30*(1), 59–96. https://doi.org/10.1080/01441640903187001

Hess, B., Farahani, A. Z., Tschirschnitz, F., & von Reischach, F. (2012). Evaluation of fine-granular GPS tracking on smartphones. In *Proceedings of the First ACM SIGSPATIAL International Workshop on Mobile Geographic Information Systems - MobiGIS '12* (p. 33). New York, New York, USA: ACM Press. https://doi.org/10.1145/2442810.2442817

Hölzel, C., Höchtl, F., & Senner, V. (2012). Cycling comfort on different road surfaces. *Procedia Engineering*, *34*, 479–484. https://doi.org/10.1016/j.proeng.2012.04.082

Howe, J. (2006). The rise of crowdsourcing. *Wired Magazine*, *14*(6), 1–4.

Hull, A., & O'Holleran, C. (2014). Bicycle infrastructure: can good design encourage cycling? *Urban, Planning and Transport Research*, *2*(1), 369–406. https://doi.org/10.1080/21650020.2014.955210

Informatica. (2017). What is Data Monitoring? Retrieved November 20, 2017, from https://www.informatica.com/services-and-training/glossary-of-terms/data-monitoring-definition.html#fbid=mx40FpPb1bT

Johnston, S., & Robinson, J. (2015). Mobile Sensor Networks: Creating a Social Laboratory. Retrieved July 13, 2017, from https://opensignal.com/reports/2015/01/mobile-sensor-networks/

Joo, S., & Oh, C. (2013). A novel method to monitor bicycling environments. *Transportation Research Part A: Policy and Practice*, *54*, 1–13. https://doi.org/10.1016/j.tra.2013.07.001

Kang, L., & Fricker, J. D. (2013). Bicyclist commuters' choice of on-street versus off-street route segments. *Transportation*, *40*, 887–902. https://doi.org/10.1007/s11116-013-9453-x

Khoo Chee Han, C., Shanmugam, R. AL, & Choon Siew Kit, D. (2014). Accuracy, Consistency, and Reproducibility of the Triaxial Accelerometer in the iPod Touch: A Pilot Study. *JMIR mHealth and uHealth*, *2*(4), e39. https://doi.org/10.2196/mhealth.3008

KOAC WMD. (2002). *Verhardingskeuze voor fietsverbindingen : asfalt , beton of tegels?*

Kobana, Y., Takahashi, J., Kitsunezaki, N., Tobe, Y., & Lopez, G. (2014). Detection of Road Damage using Signals of Smartphone-Embedded Accelerometer while Cycling. In *Proceedings of the 2014 International Workshop on Web Intelligence and Smart Sensing - IWWISS '14* (pp. 1–2). New York, New York, USA: ACM Press. https://doi.org/10.1145/2637064.2637107

Korpilo, S., Virtanen, T., & Lehvävirta, S. (2017). Smartphone GPS tracking—Inexpensive and efficient data collection on recreational movement. *Landscape and Urban Planning*, *157*, 608–617. https://doi.org/10.1016/j.landurbplan.2016.08.005

Landis, B. W. (1994). Bicycle Interaction Hazard Score: a Theoretical Model. *Transportation Research Record*, (1438), 3–8. Retrieved from http://onlinepubs.trb.org/Onlinepubs/trr/1994/1438/1438-001.pdf%5Cnhttps://scholar.google.com/scholar_lookup?title=BICYCLE+INTERACTION+HAZARD+SCORE:+A+THEORETICAL+MODEL&author=B.+Landis&publication_year=1994%5Cnhttps://trid.trb.org/view/413761%5Cnhttp://w

Landis, B. W., Vattikuti, V., & Brannick, M. (1997). Real-Time Human Perceptions: Toward a Bicycle Level of Service. *Transportation Research Record*, *1578*, 119–126. https://doi.org/10.3141/1578-15

Lépine, J., Champoux, Y., & Drouet, J.-M. (2014). Road bike comfort: on the measurement of vibrations induced to cyclist. *Sports Engineering*, *17*(2), 113–122. https://doi.org/10.1007/s12283-013-0145-8

Lépine, J., Champoux, Y., & Drouet, J. M. (2015). The relative contribution of road bicycle components on vibration induced to the cyclist. *Sports Engineering*, *18*(2), 79–91. https://doi.org/10.1007/s12283-014-0168-9

Lyons, G. (2016). Getting smart about urban mobility – Aligning the paradigms of smart and sustainable. *Transportation Research Part A: Policy and Practice*, 1–11. https://doi.org/10.1016/j.tra.2016.12.001

Matarazzo, T., Vazifeh, M., Pakzad, S., Santi, P., & Ratti, C. (2017). Smartphone data streams for bridge health monitoring. *Procedia Engineering*, *199*, 966–971. https://doi.org/10.1016/j.proeng.2017.09.203

Mednis, A., Strazdins, G., Zviedris, R., Kanonirs, G., & Selavo, L. (2011). Real time pothole detection using Android smartphones with accelerometers. *2011 International Conference on Distributed Computing in Sensor Systems and Workshops, DCOSS'11*, (June). https://doi.org/10.1109/DCOSS.2011.5982206

Ministry of Infrastructure and the Environment. (2016). *Overstappen naar 2040 - Flexibel en slim OV*. The Hague. Retrieved from https://epublicatie.minienm.nl/toekomstbeeld-ov#/slide_overstappen-naar-2040

Mohan, P., Padmanabhan, V. N., & Ramjee, R. (2008). Nericell: Rich Monitoring of Road and Traffic Conditions using Mobile Smartphones. *Proceedings of the 6th ACM Conference on Embedded Network Sensor Systems - SenSys '08*, 323. https://doi.org/10.1145/1460412.1460444

Mohanty, S., Lee, A., Carvalho, T., Dias, L., & Lovegrove, G. (2014). A Global Review of Current Instrumented Probe Bicycle (IPB) Technology and Research. *Procedia Engineering*, *72*, 392–397.

Nehls, K. (2015). Crowdsourcing. *Learning, Media and Technology*, *40*(1), 123–126. https://doi.org/10.1080/17439884.2014.929144

Neirotti, P., De Marco, A., Cagliano, A. C., Mangano, G., & Scorrano, F. (2014). Current trends

in smart city initiatives: Some stylised facts. *Cities*, *38*, 25–36. https://doi.org/10.1016/j.cities.2013.12.010

Niska, A., & Sjögren, L. (2014). *Using a smartphone to measure irregularities on cycle paths. A study of the possibilities*. Linköping, Sweden.

Niven, E. B., & Deutsch, C. V. (2012). Calculating a robust correlation coefficient and quantifying its uncertainty. *Computers and Geosciences*, *40*, 1–9. https://doi.org/10.1016/j.cageo.2011.06.021

Noury-Desvaux, B., Abraham, P., Mahé, G., Sauvaget, T., Leftheriotis, G., & Le Faucheur, A. (2011). The Accuracy of a Simple, Low-Cost GPS Data Logger/Receiver to Study Outdoor Human Walking in View of Health and Clinical Studies. *PLoS ONE*, *6*(9), 8. https://doi.org/10.1371/journal.pone.0023027

Novakova, L., & Pavlis, T. L. (2017). Assessment of the precision of smart phones and tablets for measurement of planar orientations: A case study. *Journal of Structural Geology*, *97*, 93–103. https://doi.org/10.1016/j.jsg.2017.02.015

Olieman, M., Marin-Perianu, R., & Marin-Perianu, M. (2012). Measurement of dynamic comfort in cycling using wireless acceleration sensors. *Procedia Engineering*, *34*, 568–573. https://doi.org/10.1016/j.proeng.2012.04.097

Parkin, J., Wardman, Æ. M., & Page, Æ. M. (2008). Estimation of the determinants of bicycle mode share for the journey to work using census data. *Transportation*, *35*, 93–109. https://doi.org/10.1007/s11116-007-9137-5

Pearson, D. (2012). *Deteriotation and Maintenance of Pavements*. London: ICE Publishing.

Pelland-Leblanc, J.-P., Lépine, J., Champoux, Y., & Drouet, J.-M. (2014). Using Power as a Metric to Quantify Vibration Transmitted to the Cyclist. *Procedia Engineering*, *72*(October), 392–397. https://doi.org/10.1016/j.proeng.2014.06.067

Pucher, J., Dill, J., & Handy, S. (2010). Infrastructure, programs, and policies to increase bicycling: An international review. *Preventive Medicine*, *50*(SUPPL.), S106–S125. https://doi.org/10.1016/j.ypmed.2009.07.028

Ranacher, P., Brunauer, R., Trutschnig, W., Van der Spek, S., & Reich, S. (2016). Why GPS makes distances bigger than they are. *International Journal of Geographical Information Science*, *30*(2), 316–333. https://doi.org/10.1080/13658816.2015.1086924

Ritchie, D. A. (2007). *Factors That Affect the Global Positioning System and Global Navigation Satellite System in an Urban and Forested Environment.* Retrieved from http://dc.etsu.edu/etd/2089

Schaap, N., Harms, H., Kansen, M., & Wust, H. (2015). *Fietsen en lopen : de smeerolie van onze mobiliteit*. The Hague.

Scheper, W., Van Zundert, S., De Jong, N., Valkema, J., & Valenta, S. (2016). Het geheim van de Fiets Telweek: bevestiging van vermoedens. Retrieved July 7, 2017, from

http://www.verkeerskunde.nl/internetartikelen/vakartikelen/het-geheim-van-de-fiets-telweek-bevestiging-van.44160.lynkx

Schepers, P. (2008). *De rol van infrastructuur bij enkelvoudige fietsongevallen*. The Hague.

Schepers, P., Twisk, D., Fishman, E., Fyhri, A., & Jensen, A. (2017). The Dutch road to a high level of cycling safety. *Safety Science*, *92*, 264–273. https://doi.org/10.1016/j.ssci.2015.06.005

Schirmer, M., & Höpfner, H. (2013). Smartphone Hardware Sensors. *Mobile Media Group*, 14. Retrieved from https://www.uni-weimar.de/medien/wiki/images/Zeitmaschinen-smartphonesensors.pdf

Segadilha, A. B. P., & Sanches, S. da P. (2014). Identification of Factors that Influence Cyclistś Route Choice. *Procedia - Social and Behavioral Sciences*, *160*(Cit), 372–380. https://doi.org/10.1016/j.sbspro.2014.12.149

ST Microelectronics Technical Manual. (2008). *LIS331DL MEMS motion sensor*. *STMicroelectronics*.

Stinson, M. A., & Bhat, C. R. (2003). An Analysis of Commuter Bicyclist Route Choice Using a Stated Preference Survey. *Transportation Research Record*, *1828*, 107–115.

Telgarsky, R. (2013). Dominant Frequency Extraction. Retrieved from http://arxiv.org/abs/1306.0103

Transport for London. (2008). *CYCLING IN LONDON*.

Van den Berg, N., & Groenendijk, J. (2009). Eisen aan vlakheid en fietscomfort. *Asfalt*, *1*(0), 26–30.

Van Overdijk, R. P. J. (2016). *The Influence of Comfort Aspects on Route- and Mode-Choice decisions of Cyclists in the Netherlands*. Eindhoven University of Technology, Eindhoven.

Van Overdijk, R. P. J., Van der Waerden, P., & Borgers, A. (2017). *The Influence of Comfort and Travel Time on Cyclists ' Route Choice Decisions Rens van Overdijk*. Eindhoven.

Vanwalleghem, J., Mortier, F., De Baere, I., Loccufier, M., & Van Paepegem, W. (2012). Design of an instrumented bicycle for the evaluation of bicycle dynamics and its relation with the cyclist's comfort. *Procedia Engineering*, *34*, 485–490. https://doi.org/10.1016/j.proeng.2012.04.083

Vieyra, R., Vieyra, C., Jeanjacquot, P., Marti, A., & Monteiro, M. (2015). Turn Your Smartphone into a Science Laboratory: Five Challenges That Use Mobile Devices to Collect and Analyze Data in Physics. *The Science Teacher*, *82*(9), 32–40.

Vittorio, A., Rosolino, V., Teresa, I., Vittoria, C. M., Vincenzo, P. G., & Francesco, D. M. (2014). Automated Sensing System for Monitoring of Road Surface Quality by Mobile Devices. *Procedia - Social and Behavioral Sciences*, *111*, 242–251. https://doi.org/10.1016/j.sbspro.2014.01.057

Wang, M. L., & Birken, R. (2014). Sensing solutions for assessing and monitoring roads. In *Sensor Technologies for Civil Infrastructures : Volume 2: Applications in Structural Health Monitoring* (pp. 461–496). Woodhead Publishing Limited. https://doi.org/10.1533/9781782422433.2.461

Wang, M. L., Lynch, J. P., & Sohn, H. (2014). Introduction to sensing for structural performance assessment and health monitoring. In *Sensor Technologies for Civil Infrastructures: Volume 1: Sensing Hardware and Data Collection Methods for Performance Assessment* (pp. 1–22). Woodhead Publishing Limited. https://doi.org/10.1533/9780857099136.1

Wefering, F., Rupprecht, S., Burhmann, S., & Bohler-Baedecker, S. (2013). *Guidelines - Developing and implementing a sustainable urban mobility plan*. *ELTISplus*. Brussels. Retrieved from http://www.eltis.org/sites/eltis/files/sump_guidelines_en.pdf

Wegman, F., Zhang, F., & Dijkstra, A. (2012). How to make more cycling good for road safety? *Accident Analysis and Prevention*, *44*(1), 19–29. https://doi.org/10.1016/j.aap.2010.11.010

Wijlhuizen, G. J., Dijkstra, A., & Petegem, J. W. H. van. (2014). *Safe Cycling Network Ontwikkeling van een systeem ter beoordeling van de veiligheid van fietsinfrastructuur*. The Hague. Retrieved from https://www.swov.nl/publicatie/safe-cycling-network

Winters, M., Davidson, G., Kao, D., & Teschke, K. (2011). Motivators and deterrents of bicycling : comparing influences on decisions to ride, 153–168. https://doi.org/10.1007/s11116-010-9284-y

Wojtowicki, J., Champoux, Y., & Thibault, J. (2001). MODAL PROPERTIES OF ROAD BIKES VS RIDE COMFORT. *Proceedings of IMAC-XIX*, *1*, 648–652.

Yamaguchi, T., Nagayama, T., & Su, D. (2015). Simple Estimation of Bicycle Lane Condition by Using the Dynamic Response of a Bicycle. Tokyo: University of Tokyo. Retrieved from http://sstl.cee.illinois.edu/papers/aeseancrisst15/152_Yamaguchi_Simple.pdf

APPENDICES

APPENDIX I SEMI-STRUCTURED INTERVIEW

At the beginning of the interview I will introduce myself. After the introduction the interviewee will be provided with a context for the interview by a briefing. In this briefing the situation for the interviewee is defined, the purpose of this interview is explained, and the use of a tape recorder is mentioned. Before starting the interview, the interviewee is asked if he has any questions before starting. After the interview, further and more detailed explanations about the research topic will be discussed (if subject is interested) to prevent biased answer on the interview questions.

GENERAL

1.What is the core business of your organization is?

2. What is your role in the organization, and with what organizations do you often cooperate?
    - Only relevant organizations are noted

OPERATIONS AND MAINTENANCE OF BICYCLE INFRASTRUCTURE

3. How is your organization related to O&M of bicycle infrastructure?
    a. How are you (the expert) related to O&M of bicycle infrastructure?

4. What kind of policy is maintained regarding the O&M of bicycle infrastructure?
    a. What is current decision-making procedure of planning O&M?
    b. What is the assessment procedure for deciding whether or not maintenance is necessary?
    c. Do you think that the current approach for O&M of bicycle infrastructure is efficient?
        - *If yes, why?*
        - *If no, where do you see improvement possibilities?*

VISUAL INSPECTIONS

5. Do you have experience with visual inspections for (bicycle) infrastructure?
    a. if yes, what is the current practice for visual inspections?
        - *what is the procedure?*
        - *who executes these inspections?*
        - *who evaluates these inspections?*
        - *how are these inspections evaluated?*
        - *how frequent are these inspections executed*
        - *Is this practice similar for all pavement types (asphalt, concrete, tiles, cobblestones)*

BICYCLE MONITORING TECHNIQUES

6. Do you know recent bicycle monitoring techniques used for the benefit of operation and maintenance of bicycle infrastructure?
    a. if yes, what is this technique(s) and where did you heard of it?
        - *What is the objective of this technique?*
        - *Is it already tested or applied in the field?*

7. Do you see potential in using smartphones and crowdsourcing techniques for monitoring bicycle infrastructures for the benefit of cyclists safety and comfort?
    a. ….. for the benefit of road managers

APPENDIX II EVALUATION MATRIX SMARTPHONE APPLICATIONS

Table 8.1: Matrix requirements smartphone apps

Smartphone Application - Developer	General		Sensors				Recording			Exporting			Additional features			
	Available in Playstore	Costs Application	Accelero-meter	Linear Accelerati on	GPS position	Date-Time	Multi-record	Adjust recording Frequency	Format as csv- or txt-file	Save locally	Export to e-mail or Google Drive	Manually Configure filename	Keep-screen-on function	Configure recording time	Device Sensor Info
AndroSensor - Fiv Asim	✓	€ 0,99 (Optional)	✓	✓	✓	✓	✓	✓	✓	✓	✓	✗	✓	✗	✓
FietsComfort - SGS Intron	✗	Free	✓	✓	✓	✓	✓	✗	✓	✓	✓	✓	✗	✗	✗
Physics Toolbox Suite - Vieyra Software	✓	€ 3,39 (Optional)	✓	✓	✓	✓	✓	✓	✓	✓	✓	✓	✓	✗	✓
Raw Sensor Data - AJB Tech	✓	Free	✓	✓	✓	✓	✗	✗	✗	✗	✗	✗	✗	✗	✓
Sensor Data - Vipul Lugade	✓	€ 5,49 (Optional)	✓	✓	✗	✓	✓	✓	✓	✓	✓	✓	✗	✓	✓
Sensor Record (a)- Martin Golpashin	✓	Free	✓	✓	✓	✓	✓	✓	✓	✓	✓	✗	✗	✗	✗
Sensors Record (b)- mrwojtek	✓	Free	✓	✓	✓	✓	✓	✓	✓	✓	✓	✗	✗	✗	✓
Sensor Tracker - Bicasoft Technologies	✓	Free	✓	✗	✓	✓	✓	✓	✓	✓	✓	✗	✓	✗	✗
Sensors toolbox - EXA Tools	✓	€ 0,69 (Optional)	✓	✓	✓	✓	✗	✗	✗	✗	✗	✗	✓	✗	✓
Sensors Multitool - Wered Software	✓	Free	✓	✓	✓	✗	✗	✗	✗	✗	✗	✗	✓	✗	✓
Sensors Toolbox - Galaxy Developers	✓	Free	✓	✓	✓	✓	✗	✗	✗	✗	✗	✗	✗	✗	✓

APPENDIX III COMPREHENSIVE RESULTS CASE STUDY

TEST 1

Table 8.2: Results test 1

#	Measure	Oneplus 5		Google Nexus		HTC M9	
		Mean (g)	Std dev.	Mean (g)	Std dev.	Mean (g)	Std dev.
Trial 1	Screen Up	1,0006	0,0104	1,0099	0,0058	1,0053	0,0022
	Screen Down	1,0149	0,0099	1,0102	0,0054	0,9925	0,0022
	Sensitivity	0,0143	0,0101	0,0003	0,0056	0,0128	0,0022
Trial 2	Screen Up	0,9999	0,0102	1,0101	0,0057	1,0048	0,0022
	Screen Down	1,0151	0,0060	1,0104	0,0055	0,9925	0,0022
	Sensitivity	0,0153	0,0081	0,0004	0,0056	0,0124	0,0022
Trial 3	Screen Up	0,9995	0,0098	1,0095	0,0058	1,0045	0,0022
	Screen Down	1,0151	0,0061	1,0105	0,0053	0,9922	0,0022
	Sensitivity	0,0156	0,0080	0,0009	0,0055	0,0123	0,0022
Total		0,0151	0,0087	0,0005	0,0005	0,0056	0,0125

TEST 2

Table 8.3: Results test 2. All units are in g's

#	Measure	Oneplus 5			Google Nexus			HTC M9		
		X-axis	Y-axis	Z-axis	X-axis	Y-axis	Z-axis	X-axis	Y-axis	Z-axis
Trial 1	a_1	0,4647	0,1397	9,8385	0,2227	0,1126	9,9465	0,19	0,15	9,98
	a_2	0,3325	-0,0285	-0,0484	0,0647	-0,0263	0,1030	0,01	-0,30	0,19
	dynamic sensitivity	1,0084			1,0040			0,9995		
Trial 2	a_1	0,5036	0,1415	9,884	0,2658	0,0599	9,8914	0,26	0,24	9,91
	a_2	0,3019	-0,1135	-0,0268	0,0407	-0,0527	0,0742	0,00	-0,31	0,18
	dynamic sensitivity	1,0112			1,0014			0,9941		
Trial 3	a_1	0,5114	0,1649	9,8229	0,4838	-0,2395	9,9058	0,26	0,17	9,91
	a_2	0,2558	-0,0171	-0,022	-0,024	-0,0048	0,1772	0,01	-0,30	0,22
	dynamic sensitivity	1,0044			0,9937			0,9896		
Trial 4	a_1	0,5198	0,1409	9,8151	0,1605	0,0096	9,9872	0,25	0,19	9,97
	a_2	0,2900	-0,0249	-0,0184	0,1461	-0,0862	0,1245	0,01	-0,33	0,17
	dynamic sensitivity	1,0032			1,0058			1,0010		
Trial 5	a_1	0,5120	0,1481	9,8139	0,2874	0,0192	9,9298	0,27	0,21	9,94
	a_2	0,3109	-0,0931	0,0157	0,0982	-0,0862	0,2108	0,01	-0,27	0,18
	dynamic sensitivity	0,9997			0,9913			0,9968		
Total		1,0054			0,9992			0,9962		

TEST 3

Table 8.4: Results estimated Frequencies test 3

Condition	Input Frequency (Hz)	Sequence Number	OnePlus 5			Google Nexus			HTC M9		
			Frequency (Hz)	Error		Frequency (Hz)	Error		Frequency (Hz)	Error	
A-05	5,0261	1	5,0352	0,0091	0,18%	5,0359	0,0098	0,19%	5,0353	0,0092	0,18%
A-05	5,0261	2	5,0357	0,0096	0,19%	5,0360	0,0099	0,20%	5,0359	0,0098	0,19%
A-05	5,0261	3	5,0353	0,0092	0,18%	5,0364	0,0103	0,20%	5,0355	0,0094	0,19%
B-05	5,0269	1	5,0353	0,0084	0,17%	5,0362	0,0093	0,18%	5,0355	0,0086	0,17%
B-05	5,0269	2	5,0357	0,0088	0,17%	5,0362	0,0093	0,18%	5,0357	0,0088	0,17%
B-05	5,0269	3	5,0355	0,0086	0,17%	5,0360	0,0091	0,18%	5,0355	0,0086	0,17%
C-05	5,0261	1	5,0357	0,0096	0,19%	5,0362	0,0101	0,20%	5,0357	0,0096	0,19%
C-05	5,0261	2	5,0353	0,0092	0,18%	5,0362	0,0101	0,20%	5,0357	0,0096	0,00%
C-05	5,0261	3	5,0348	0,0087	0,17%	5,0364	0,0103	0,20%	5,0359	0,0098	0,19%
D-05	5,0234	1	5,0353	0,0119	0,24%	5,0362	0,0128	0,25%	5,0359	0,0125	0,25%
D-05	5,0234	2	5,0353	0,0119	0,24%	5,0362	0,0128	0,25%	5,0350	0,0116	0,23%
D-05	5,0234	3	5,0355	0,0121	0,24%	5,0362	0,0128	0,25%	5,0360	0,0126	0,25%
E-05	5,0206	1	5,0347	0,0141	0,28%	5,0362	0,0156	0,31%	5,0353	0,0147	0,29%
E-05	5,0206	2	5,0355	0,0149	0,30%	5,0362	0,0156	0,31%	5,0357	0,0151	0,30%
E-05	5,0206	3	5,0353	0,0147	0,29%	5,0362	0,0156	0,31%	5,0355	0,0149	0,30%
A-10	10,0494	1	10,0380	0,0114	0,11%	10,0720	0,0226	0,23%	10,0714	0,0220	0,22%
A-10	10,0494	2	10,0707	0,0213	0,21%	10,0720	0,0226	0,23%	10,0700	0,0206	0,21%
A-10	10,0494	3	10,0707	0,0213	0,21%	10,0720	0,0226	0,23%	10,0710	0,0216	0,22%
B-10	10,0259	1	10,0373	0,0114	0,11%	10,0390	0,0131	0,13%	10,0384	0,0125	0,12%
B-10	10,0259	2	10,0377	0,0118	0,12%	10,0380	0,0121	0,12%	10,0380	0,0121	0,12%
B-10	10,0259	3	10,0367	0,0108	0,11%	10,0390	0,0131	0,13%	10,0377	0,0118	0,12%
C-10	10,0458	1	10,0370	0,0088	0,09%	10,0390	0,0068	0,07%	10,0384	0,0074	0,07%
C-10	10,0458	2	10,0377	0,0081	0,08%	10,0387	0,0071	0,07%	10,0380	0,0078	0,08%
C-10	10,0458	3	10,0373	0,0085	0,08%	10,0380	0,0078	0,08%	10,0380	0,0078	0,08%
D-10	10,0477	1	10,0377	0,0100	0,10%	10,0390	0,0087	0,09%	10,0380	0,0097	0,10%
D-10	10,0477	2	10,0377	0,0100	0,10%	10,0390	0,0087	0,09%	10,0387	0,0090	0,09%
D-10	10,0477	3	10,0357	0,0120	0,12%	10,0390	0,0087	0,09%	10,0380	0,0097	0,10%
E-10	10,0204	1	10,0377	0,0173	0,17%	10,0390	0,0186	0,19%	10,0387	0,0183	0,18%
E-10	10,0204	2	10,0380	0,0176	0,18%	10,0387	0,0183	0,18%	10,0380	0,0176	0,18%
E-10	10,0204	3	10,0370	0,0166	0,17%	10,0387	0,0183	0,18%	10,0380	0,0176	0,18%
Total				**0,0119**	**0,17%**		**0,013**	**0,18%**		**0,012**	**0,17%**

Table 8.5: Results estimated amplitudes test 3

Condition	Input Amplitude (g)	Sequence Number	OnePlus 5			Google Nexus			HTC M9		
			Amplitude (g)	Error		Amplitude (Hz)	Error		Amplitude (Hz)	Error	
A-05	0,20	1	0,206	0,006	2,89%	0,224	0,024	11,79%	0,210	0,010	5,12%
A-05	0,20	2	0,206	0,006	2,79%	0,221	0,021	10,58%	0,210	0,010	5,16%
A-05	0,20	3	0,205	0,005	2,66%	0,221	0,021	10,64%	0,210	0,010	5,07%
B-05	0,40	1	0,412	0,012	3,10%	0,419	0,019	4,78%	0,421	0,021	5,26%
B-05	0,40	2	0,412	0,012	3,01%	0,421	0,021	5,26%	0,421	0,021	5,22%
B-05	0,40	3	0,412	0,012	3,12%	0,422	0,022	5,52%	0,423	0,023	5,63%
C-05	0,60	1	0,616	0,016	2,63%	0,618	0,018	2,93%	0,631	0,031	5,20%
C-05	0,60	2	0,616	0,016	2,59%	0,624	0,024	4,01%	0,636	0,036	6,04%
C-05	0,60	3	0,616	0,016	2,59%	0,623	0,023	3,91%	0,635	0,035	5,88%
D-05	0,80	1	0,823	0,023	2,85%	0,826	0,026	3,25%	0,856	0,056	6,94%
D-05	0,80	2	0,825	0,025	3,14%	0,821	0,021	2,69%	0,842	0,042	5,29%
D-05	0,80	3	0,820	0,020	2,55%	0,819	0,019	2,37%	0,848	0,048	5,98%
E-05	1,00	1	1,023	0,023	2,31%	1,049	0,049	4,88%	1,067	0,067	6,74%
E-05	1,00	2	1,020	0,020	2,00%	1,041	0,041	4,11%	1,051	0,051	5,15%
E-05	1,00	3	1,024	0,024	2,40%	1,030	0,030	2,98%	1,056	0,056	5,61%
A-10	0,20	1	0,207	0,007	3,39%	0,220	0,020	9,91%	0,212	0,012	5,75%
A-10	0,20	2	0,207	0,007	3,26%	0,220	0,020	9,94%	0,210	0,010	4,95%
A-10	0,20	3	0,206	0,006	3,16%	0,220	0,020	10,17%	0,212	0,012	5,88%
B-10	0,40	1	0,408	0,008	2,06%	0,420	0,020	5,01%	0,426	0,026	6,50%
B-10	0,40	2	0,409	0,009	2,26%	0,418	0,018	4,61%	0,419	0,019	4,67%
B-10	0,40	3	0,409	0,009	2,25%	0,423	0,023	5,70%	0,425	0,025	6,28%
C-10	0,60	1	0,611	0,011	1,91%	0,620	0,020	3,38%	0,632	0,032	5,40%
C-10	0,60	2	0,610	0,010	1,61%	0,617	0,017	2,81%	0,632	0,032	5,31%
C-10	0,60	3	0,611	0,011	1,85%	0,622	0,022	3,74%	0,623	0,023	3,86%
D-10	0,80	1	0,812	0,012	1,52%	0,814	0,014	1,76%	0,838	0,038	4,73%
D-10	0,80	2	0,813	0,013	1,62%	0,816	0,016	2,02%	0,844	0,044	5,56%
D-10	0,80	3	0,810	0,010	1,29%	0,815	0,015	1,91%	0,843	0,043	5,38%
E-10	1,00	1	1,003	0,003	0,33%	1,013	0,013	1,35%	1,061	0,061	6,08%
E-10	1,00	2	1,001	0,001	0,06%	1,011	0,011	1,13%	1,032	0,032	3,20%
E-10	1,00	3	1,000	0,000	0,05%	1,011	0,011	1,05%	1,057	0,057	5,66%
Total				**0,0119**		**0,012**	**2,24%**	**0,022**	**0,021**	**4,81%**	**0,035**

TEST 4

Table 8.6: Comprehensive results test 4

Route Segment	Trial	OnePlus 5			Google Nexus			HTC M9		
		Accuracy (m)	Connected Satellites	Available Satellites	Accuracy (m)	Connected Satellites	Available Satellites	Accuracy (m)	Connected Satellites	Available Satellites
Segment A	1	10,95	16,62	31,00	13,57	8,83	24,97	18,36	0,00	21,97
	2	11,92	14,52	30,98	13,54	7,83	24,00	18,70	7,88	20,92
	3	12,21	14,09	32,00	14,99	7,98	24,00	17,60	9,44	20,96
	4	14,76	10,83	32,97	15,55	6,88	24,96	19,67	11,26	21,97
	5	11,57	13,59	33,00	21,90	7,51	25,97	19,40	12,45	21,98
	Total	**12,28**	**13,93**	**31,99**	**15,91**	**7,81**	**24,78**	**18,75**	**8,21**	**21,56**
Segment B	1	10,77	17,99	31,61	10,40	8,93	24,99	11,02	0,28	22,00
	2	10,87	18,00	31,61	10,34	8,97	23,99	12,83	7,95	20,86
	3	10,94	16,82	31,97	11,11	8,91	23,97	15,03	9,97	20,99
	4	14,34	13,73	32,96	15,11	8,87	24,96	14,98	12,94	20,99
	5	11,37	18,09	32,26	15,16	7,94	25,03	15,18	14,00	21,05
	Total	**11,66**	**16,93**	**32,08**	**12,42**	**8,72**	**24,59**	**13,81**	**9,03**	**21,18**
Segment C	1	11,99	15,34	30,97	17,44	8,82	24,97	9,44	2,69	22,00
	2	14,09	15,42	31,98	16,56	8,63	23,96	19,48	7,86	20,98
	3	13,49	14,25	32,98	19,65	8,80	24,98	12,37	9,79	21,92
	4	13,94	12,65	33,11	29,01	6,48	24,95	16,10	12,96	20,98
	5	12,39	15,29	32,00	28,89	6,95	24,95	17,82	14,00	21,22
	Total	**13,18**	**14,59**	**32,21**	**22,31**	**7,94**	**24,76**	**15,04**	**9,46**	**21,42**
Total		**12,37**	**15,15**	**32,09**	**16,88**	**8,16**	**24,71**	**15,86**	**8,90**	**21,39**

Figure 8.2: GPS data plots of each device for Segment X

Figure 8.1: GPS data plots of each device for Segment Y

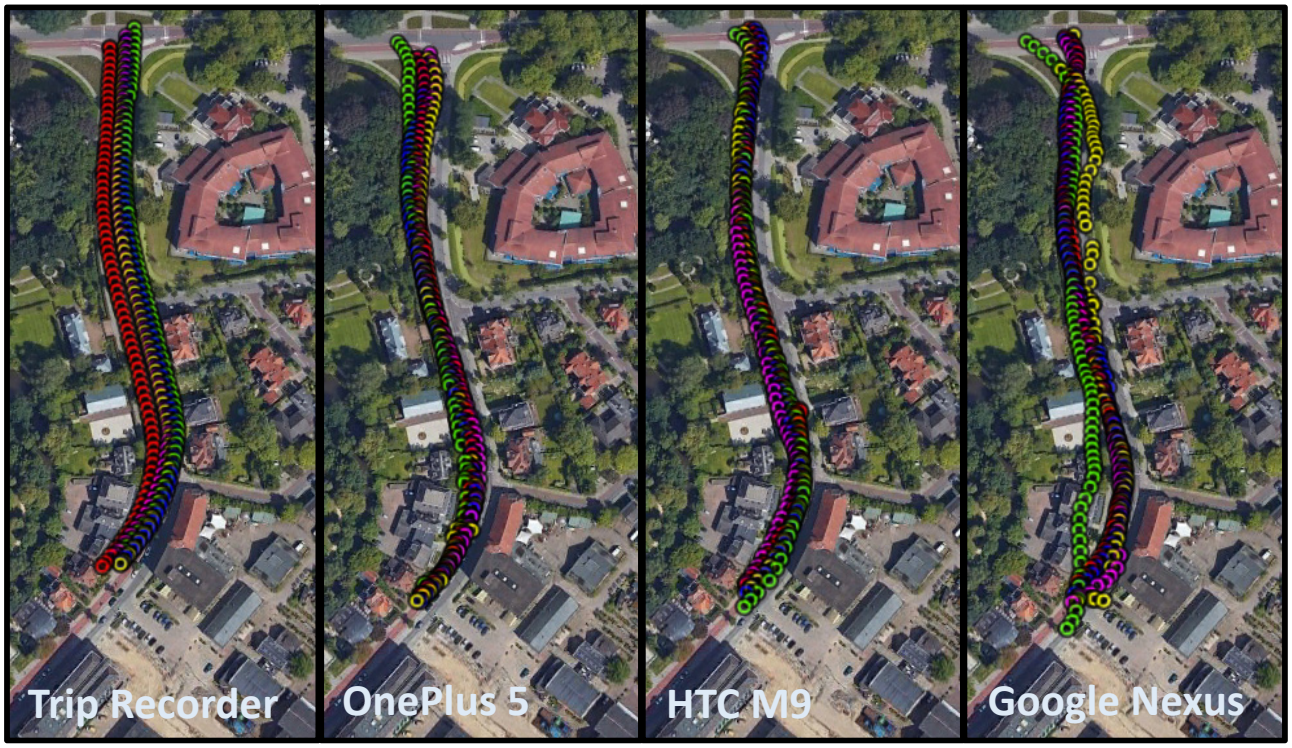

Figure 8.3: GPS data plots of each device for Segment Z

TEST 5

Table 8.7: Comprehensive results test 5

#	Exact distance (km)	Trip Recorder		OnePlus 5		Google Nexus		HTC M9	
		Distance GPS (km)	Error	Distance GPS (km)	Error	Distance GPS (km)	Error	Distance GPS (km)	Error
Trial 1	1,88	1,81	3,55%	1,83	2,74%	1,95	3,49%	1,87	0,70%
Trial 2	1,88	1,81	3,54%	1,87	0,50%	1,91	1,53%	1,87	0,45%
Trial 3	1,88	1,82	3,36%	1,84	2,28%	2,20	16,89%	1,84	1,87%
Trial 4	1,88	1,83	2,41%	1,97	4,94%	1,94	3,36%	1,88	0,09%
Trial 5	1,88	1,80	4,24%	1,96	4,05%	2,00	6,49%	1,94	3,05%
Total	**1,88**	**1,82**	**3,42%**	**1,89**	**2,90%**	**2,00**	**6,35%**	**1,88**	**1,23%**

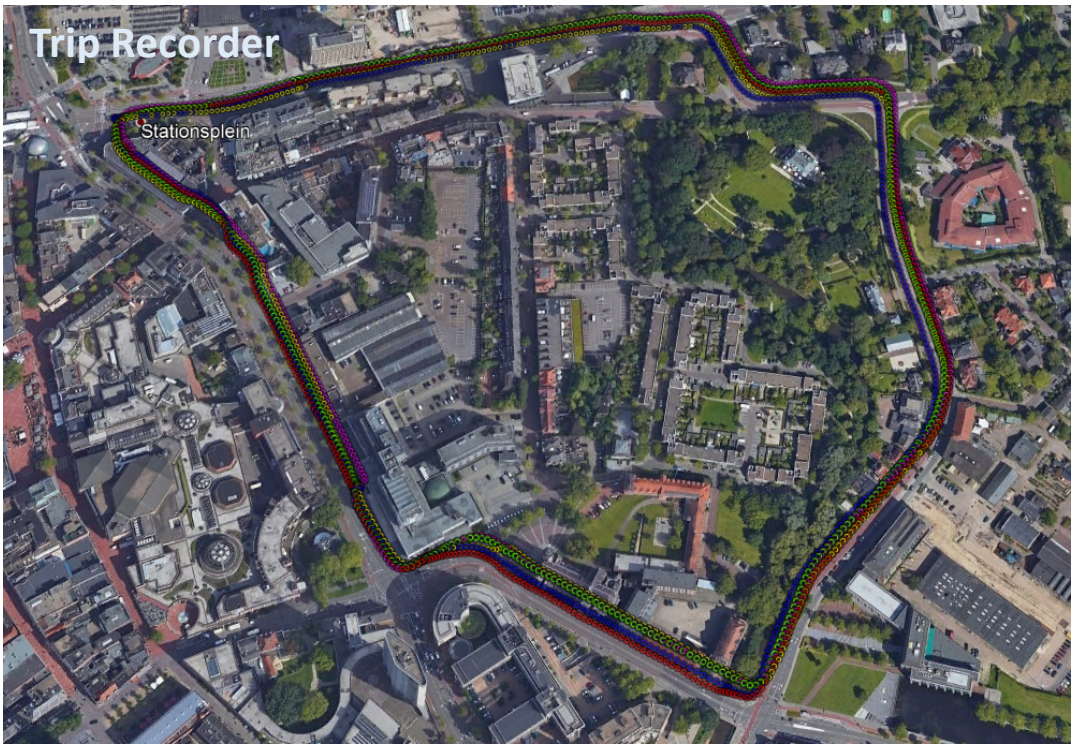

Figure 8.4: GPS data plots of the Trip Recorder

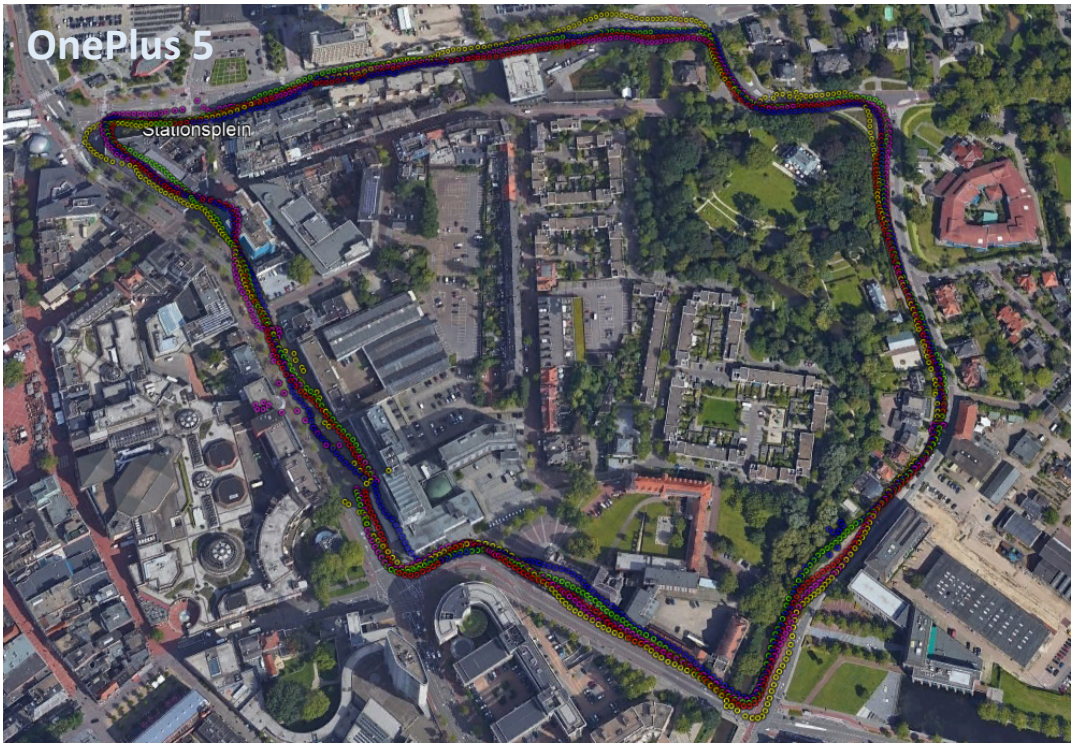

Figure 8.5: GPS data plots of the OnePlus 5

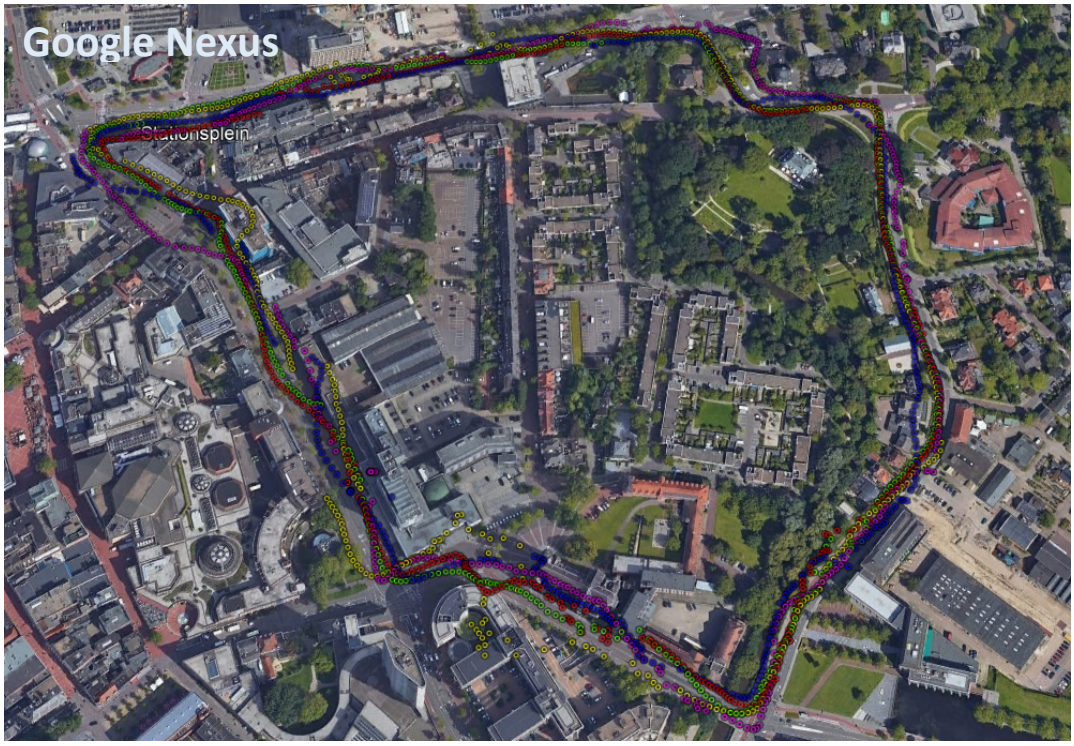

Figure 8.6: GPS data plots of Google Nexus

Figure 8.7: GPS data plots of HTC M9

APPENDIX IV MATLAB SCRIPT FOR FFT TRANSFORMATION

```
%% Import data from spreadsheet (Excel)
%  read Excel document xlsread('NameDocument','NameTable','xlRange')
%  xlRange = 'A2 or B2:Dmax or Emax'

[~, ~, raw] = xlsread('T3_ASOP_10.xlsx','T3_ASOP_10E3','G2:H1501');

%% Create output variable
data = reshape([raw{:}],size(raw));

%% Create table
T3_ASOP_10E3 = table;

%% Allocate imported array to column variable names
T3_ASOP_10E3.Time = data(:,2)/1000;
T3_ASOP_10E3.LIN_ACC_Z = data(:,1)/9.80665 ;


%% Clear temporary variables
clearvars data raw;

%% Determine variables for FFT-analysis
Ns = height(T3_ASOP_10E3);                          % Number of samples

Fs = height(T3_ASOP_10E3) / max(T3_ASOP_10E3.Time);% Sampling
frequency,Hertz

%% Clear temporary variables
clearvars data raw;

%% Fast Fourrier Transform
Y   = fft(T3_ASOP_10E3.LIN_ACC_Z);  % Fourrier transformation signal

P2  = abs(Y/Ns);                    % Two-sided spectrum P2
P1  = P2(1:Ns/2+1);                 % Single-sided spectrum P1
P1 (2:end-1)= 2*P1(2:end-1);        % Even-valued signal length L

f = Fs * (0:(Ns/2))/Ns;             % Define frequency domain f

%% Plot graph in frequency domain
plot(f,P1)                          % Plot single-sided amplitude spectrum
P1
title ('T3-ASOP-10E3')
xlabel('Frequency(Hz)')
ylabel('Magnitude');

%% Frequency
[peak_Magnitude, PeakFreqIdx] = findpeaks(P1, 'minpeakheight', 0.1,
'NPeaks', 1);
Frequency(end+1,:) = f(PeakFreqIdx);
```

APPENDIX V BICYCLE PAVEMENT CONDITIONS OF ROUTE SEGMENTS FIELD EXPERIMENT

Figure 8.8: Bicycle pavement conditions Segment A

Figure 8.9: Bicycle pavement conditions Segment B


Figure 8.10: Bicycle pavement conditions Segment C


Figure 8.11: Bicycle pavement conditions Segment D

APPENDIX VI MATLAB SCRIPT FOR CALCULATE DCI OVER MULTIPLE DISTANCE

```
%% Import data from spreadsheet
% Script for importing data from the following spreadsheet:
%
%    Workbook: C:\Users\s115933\Dropbox\Graduation Project\Thesis\Proof of
Concept\Cycle data\DCI_T#OP_A.xlsx
%    Worksheet: DCI_T1OP_A1A
%
% To extend the code for use with different selected data or a different
% spreadsheet, generate a function instead of a script.

% Auto-generated by MATLAB on 2017/10/27 11:34:10

%% Import the data
[~, ~, raw] = xlsread('C:\Users\s115933\Dropbox\Graduation
Project\Thesis\5. Field Experiment\Cycle
data\T#OP_A.xlsx','T1OP_A3','A2:I961');
stringVectors = string(raw(:,1));
stringVectors(ismissing(stringVectors)) = '';
raw = raw(:,[2,3,4,5,6,7,8,9]);

%% Create output variable
data = reshape([raw{:}],size(raw));

%% Create table
T1OP_A3 = table;

%% Allocate imported array to column variable names
T1OP_A3.Date = stringVectors(:,1);
T1OP_A3.Time = (data(:,1)-min(data(:,1)))/1000;
T1OP_A3.X = data(:,2);
T1OP_A3.Y = data(:,3);
T1OP_A3.Z = data(:,4);
T1OP_A3.SUMXYZ = sqrt(data(:,2).^2 + data(:,3).^2 + data(:,4).^2);
T1OP_A3.Lat = data(:,5);
T1OP_A3.Lon = data(:,6);
T1OP_A3.Speed = data(:,7);
T1OP_A3.Accuracy = data(:,8);

%% Clear temporary variables
clearvars data raw stringVectors;

%% Transform  table to temporary array for calculations

A = table2array(T1OP_A3(:,[2,3,4,5,6,7]));

%% DCI values per # meters for segment A
Am = height(T1OP_A3)/40;          % per 5 meter
Bm = height(T1OP_A3)/20;          % per 10 meter
Cm = height(T1OP_A3)/8;          % per 25 meter
Dm = height(T1OP_A3)/4;          % per 50 meter



%% Calculation of DCI value per 5 meter

% Calculate square values of SUMXYZ
```

```
A(:,5) = A(:,5).^2;

% Determine mean values of SUMXYZ per 5 meter
z=zeros(size(A,1)/Am);          % Create array with zeros
for i =0:Am:size(A,1)-1         % Create for loop with increments  of Fs
    a = i/Am+1;
    z(a)=mean(A(i+1:i+Am,5));    % Mean SUMXYZ per second
end

% Repeat copies of array elements and calculate DCI value by calculating
square root and inverse of mean values SUMXYZ
B(:,1) = repelem(z(:,1),Am);           % Repeat copies of array elements
B(:,1) = sqrt(B(:,1));
B(:,1)= B(:,1).^-1;

% Allocate DCI values based on SUMXYZ to table
T1OP_A3.SUM_DCI_5m = B(:,1);

%% Calculation of DCI value per 10 meter


% Determine mean values of SUMXYZ per 10 meter
z=zeros(size(A,1)/Bm);          % Create array with zeros
for i =0:Bm:size(A,1)-1         % Create for loop with increments  of Fs
    a = i/Bm+1;
    z(a)=mean(A(i+1:i+Bm,5));    % Mean SUMXYZ per second
end

% Repeat copies of array elements and calculate DCI value by calculating
square root and inverse of mean values SUMXYZ
B(:,2) = repelem(z(:,1),Bm);           % Repeat copies of array elements
B(:,2) = sqrt(B(:,2));
B(:,2)= B(:,2).^-1;

% Allocate DCI values based on SUMXYZ to table
T1OP_A3.SUM_DCI_10m = B(:,2);

%% Calculation of DCI value per 25 meter


% Determine mean values of SUMXYZ per 25 meter
z=zeros(size(A,1)/Cm);          % Create array with zeros
for i =0:Cm:size(A,1)-1         % Create for loop with increments  of Fs
    a = i/Cm+1;
    z(a)=mean(A(i+1:i+Cm,5));    % Mean SUMXYZ per second
end

% Repeat copies of array elements and calculate DCI value by calculating
square root and inverse of mean values SUMXYZ
B(:,3) = repelem(z(:,1),Cm);           % Repeat copies of array elements
B(:,3) = sqrt(B(:,3));
B(:,3)= B(:,3).^-1;

% Allocate DCI values based on SUMXYZ to table
T1OP_A3.SUM_DCI_25m = B(:,3);

%% Calculation of DCI value per 50 meter
```

```
% Determine mean values of SUMXYZ per 50 meter
z=zeros(size(A,1)/Dm);          % Create array with zeros
for i =0:Dm:size(A,1)-1         % Create for loop with increments  of Fs
    a = i/Dm+1;
    z(a)=mean(A(i+1:i+Dm,5));    % Mean SUMXYZ per second
end

% Repeat copies of array elements and calculate DCI value by calculating
square root and inverse of mean values SUMXYZ
B(:,4) = repelem(z(:,1),Dm);           % Repeat copies of array elements
B(:,4) = sqrt(B(:,4));
B(:,4)= B(:,4).^-1;

% Allocate DCI values based on SUMXYZ to table
T1OP_A3.SUM_DCI_50m = B(:,4);

%% Export Data to Excelfile

filename = 'DCI_TOP_Av2.xlsx';
writetable(T1OP_A3,filename,'Sheet',3,'Range','A1')

clear a A B C DIF Fs i z;
```

APPENDIX VII MATLAB SCRIPT FOR CALCULATING DCI_{DIF}

```
%% Import data from spreadsheet
% Script for importing data from the following spreadsheet:
%
%    Workbook: C:\Users\s115933\Dropbox\Graduation Project\Thesis\Proof of
Concept\Cycle data\DCI_T#OP_A.xlsx
%    Worksheet: DCI_T1OP_A1A
%
% To extend the code for use with different selected data or a different
% spreadsheet, generate a function instead of a script.

% Auto-generated by MATLAB on 2017/10/27 11:34:10

%% Import the data
[~, ~, raw] = xlsread('C:\Users\s115933\Dropbox\Graduation
Project\Thesis\5. Field Experiment\Cycle
data\T#OP_A.xlsx','T1OP_A3','A2:I961');
stringVectors = string(raw(:,1));
stringVectors(ismissing(stringVectors)) = '';
raw = raw(:,[2,3,4,5,6,7,8,9]);

%% Create output variable
data = reshape([raw{:}],size(raw));

%% Create table
T1OP_A3 = table;

%% Allocate imported array to column variable names
T1OP_A3.Date = stringVectors(:,1);
T1OP_A3.Time = (data(:,1)-min(data(:,1)))/1000;
T1OP_A3.X = data(:,2);
T1OP_A3.Y = data(:,3);
T1OP_A3.Z = data(:,4);
T1OP_A3.SUMXYZ = sqrt(data(:,2).^2 + data(:,3).^2 + data(:,4).^2);
T1OP_A3.DIFXYZ = zeros(height(T1OP_A3),1);
T1OP_A3.Lat = data(:,5);
T1OP_A3.Lon = data(:,6);
T1OP_A3.Speed = data(:,7);
T1OP_A3.Accuracy = data(:,8);

%% Clear temporary variables
clearvars data raw stringVectors;

%% Determine Sampling Frequency

Fs = height(T1OP_A3) / max((T1OP_A3.Time));      % Sampling frequency,
Hertz
Fs = round(Fs);

%% Transform  table to temporary array for calculations

A = table2array(T1OP_A3(:,[2,3,4,5,6,7]));

%% Calculate consective difference of X,Y and Z acceleration values
DIF = zeros(size(A,1)-1,4);                              % Create array with
4 columns of zeros
```

```
DIF(:,1) = diff(A(:,2));                                % Calculate of
consective difference of X
DIF(:,2) = diff(A(:,3));                                % Calculate of
consective difference of Y
DIF(:,3) = diff(A(:,4));                                % Calculate of
consective difference of Z

% Calculate total acceleration DIFXYZ
DIF(:,4) = sqrt(DIF(:,1).^2+DIF(:,2).^2+DIF(:,3).^2);   % Calculate total
acceleration

% Add values to temporary array
A(2:end,6) = DIF(:,4);
A(1,6) =  DIF(1,4);

% Allocate DIFXYZ values to table
T1OP_A3.DIFXYZ = A(:,6);

%% DCI values per # meters for segment A
Am = height(T1OP_A3)/40;          % per 5 meter

%% Calculation DCI values DIFXYZ

% Calculate square values of DIFXYZDCI
A(:,6) = A(:,6).^2;

%% Calculation of DCI values based on DIFXYZ per 5 meter
z=zeros(size(A,1)/Am);          % Create array with zeros
for i =0:Am:size(A,1)-1         % Create for loop with increments  of Fs
    a = i/Am+1;
    z(a)=mean(A(i+1:i+Am,6));    % Mean SUMXYZ per second
end

% Repeat copies of array elements and calculate DCI value by calculating
square root and inverse of mean values SUMXYZ
C(:,1) = repelem(z(:,1),Am);           % Repeat copies of array elements
C(:,1) = sqrt(C(:,1));
C(:,1)= C(:,1).^-1;

T1OP_A3.DIF_DCI_5m = C(:,1);


%% Export Data to Excelfile

filename = 'DCI_TOP_Av2.xlsx';
writetable(T1OP_A3,filename,'Sheet',3,'Range','A1')

clear a A B C DIF Fs i z;
```

APPENDIX VIII PEARSON & SPEARMAN CORRELATION FOR DATA SETS

Table 8.8: Pearson Correlations of data sets test riders segment A

Segment A

		Test Rider 1	Test Rider 2	Test Rider 3
Test Rider 1	Pearson Correlation	1	,786**	,783**
	Sig. (2-tailed)		,000	,000
	N	40	40	40
Test Rider 2	Pearson Correlation	,786**	1	,795**
	Sig. (2-tailed)	,000		,000
	N	40	40	40
Test Rider 3	Pearson Correlation	,783**	,795**	1
	Sig. (2-tailed)	,000	,000	
	N	40	40	40

**. Correlation is significant at the 0.01 level (2-tailed).

Table 8.9: Spearman Correlations of data sets test riders Segment A

Segment A

			Test Rider 1	Test Rider 2	Test Rider 3
Spearman's rho	Test Rider 1	Correlation Coefficient	1,000	,725**	,723**
		Sig. (2-tailed)	.	,000	,000
		N	40	40	40
	Test Rider 2	Correlation Coefficient	,725**	1,000	,787**
		Sig. (2-tailed)	,000	.	,000
		N	40	40	40
	Test Rider 3	Correlation Coefficient	,723**	,787**	1,000
		Sig. (2-tailed)	,000	,000	.
		N	40	40	40

**. Correlation is significant at the 0.01 level (2-tailed).

Table 8.10: Pearson Correlations of data sets test riders Segment B

Segment B

		Test Rider 1	Test Rider 2	Test Rider 3
Test Rider 1	Pearson Correlation	1	,649**	,318*
	Sig. (2-tailed)		,000	,046
	N	40	40	40
Test Rider 2	Pearson Correlation	,649**	1	,122
	Sig. (2-tailed)	,000		,454
	N	40	40	40
Test Rider 3	Pearson Correlation	,318*	,122	1
	Sig. (2-tailed)	,046	,454	
	N	40	40	40

**. Correlation is significant at the 0.01 level (2-tailed).

*. Correlation is significant at the 0.05 level (2-tailed).

Table 8.11:1 Spearman Correlations of data sets test riders Segment B

Segment B

			Test Rider 1	Test Rider 2	Test Rider 3
Spearman's rho	Test Rider 1	Correlation Coefficient	1,000	,672**	,304
		Sig. (2-tailed)	.	,000	,057
		N	40	40	40
	Test Rider 2	Correlation Coefficient	,672**	1,000	,136
		Sig. (2-tailed)	,000	.	,402
		N	40	40	40
	Test Rider 3	Correlation Coefficient	,304	,136	1,000
		Sig. (2-tailed)	,057	,402	.
		N	40	40	40

**. Correlation is significant at the 0.01 level (2-tailed).

Table 8.12:2 Pearson Correlations of data sets test riders Segment C

Segment C

		Test Rider 1	Test Rider 2	Test Rider 3
Test Rider 1	Pearson Correlation	1	,755**	,745**
	Sig. (2-tailed)		,000	,000
	N	30	30	30
Test Rider 2	Pearson Correlation	,755**	1	,780**
	Sig. (2-tailed)	,000		,000
	N	30	30	30
Test Rider 3	Pearson Correlation	,745**	,780**	1
	Sig. (2-tailed)	,000	,000	
	N	30	30	30

**. Correlation is significant at the 0.01 level (2-tailed).

Table 8.13: Spearman Correlations of data sets test riders Segment C

Segment C

			Test Rider 1	Test Rider 2	Test Rider 3
Spearman's rho	Test Rider 1	Correlation Coefficient	1,000	,679**	,675**
		Sig. (2-tailed)	.	,000	,000
		N	30	30	30
	Test Rider 2	Correlation Coefficient	,679**	1,000	,704**
		Sig. (2-tailed)	,000	.	,000
		N	30	30	30
	Test Rider 3	Correlation Coefficient	,675**	,704**	1,000
		Sig. (2-tailed)	,000	,000	.
		N	30	30	30

**. Correlation is significant at the 0.01 level (2-tailed).

Table 8.14:3 Pearson Correlations of data sets test riders Segment D

Segment D

		Test Rider 1	Test Rider 2	Test Rider 3
Test Rider 1	Pearson Correlation	1	,365*	,573**
	Sig. (2-tailed)		,047	,001
	N	30	30	30
Test Rider 2	Pearson Correlation	,365*	1	,212
	Sig. (2-tailed)	,047		,260
	N	30	30	30
Test Rider 3	Pearson Correlation	,573**	,212	1
	Sig. (2-tailed)	,001	,260	
	N	30	30	30

*. Correlation is significant at the 0.05 level (2-tailed).

**. Correlation is significant at the 0.01 level (2-tailed).

Table 8.15: Spearman Correlations of data sets test riders Segment D

Segment D

			Test Rider 1	Test Rider 2	Test Rider 3
Spearman's rho	Test Rider 1	Correlation Coefficient	1,000	,307	,518**
		Sig. (2-tailed)	.	,099	,003
		N	30	30	30
	Test Rider 2	Correlation Coefficient	,307	1,000	,235
		Sig. (2-tailed)	,099	.	,211
		N	30	30	30
	Test Rider 3	Correlation Coefficient	,518**	,235	1,000
		Sig. (2-tailed)	,003	,211	.
		N	30	30	30

**. Correlation is significant at the 0.01 level (2-tailed).